A

VIBRATIONAL CIRCULAR DICHROISM AND ITS APPLICATIONS TO STRUCTURAL STUDIES OF PEPTIDES

By

Ping Xie

A dissertation submitted to the Graduate Faculty in Chemistry in partial fulfillment of the requirement for the degree of Doctor of Philosophy, The City University of New York.

1995

This manuscript has been read and accepted for the Graduate Faculty in Chemistry in satisfaction of dissertation requirement for the degree of Doctor of Philosophy.

4/27/95
Date

Max Tieman
Chair of Examining Committee

4/27/95
Date

Executive Officer

Thomas C. Strekas

Supervisory Committee

The City University of New York

ABSTRACT

VIBRATIONAL CIRCULAR DICHROISM AND ITS APPLICATIONS TO STRUCTURAL STUDIES IN PEPTIDES

By

Ping Xie

Adviser: Professor Max Diem

This dissertation reportes recent progress in vibrational circular dichroism (CD) and its application to the measurement of secondary structure of peptide. It is focused on two aspects: elimination of artifact in VCD measurement and structural studies of small peptides.

System artifact has limited application of biomolecule structural studies, because its small amplitude of ΔA in vibrational CD. Such an artifact can arise from both hardware and software. The new method of data acquisition and processing proposed can largely reduce such an artifact. Results from new method shows a same pattern of poly-L-lysine in DMSO at low concentration (0.05 absorbance unit) as it in high concentration.

Conformational changes of several small peptides with various chemical environment are monitored by VCD. Such environment variations can be polarity and hydrogen-bond ability of solvent as well as size and charge of cation. The variety of solvent properties can be as a probe, which can help us to understand the

driving force in peptide folding. The frequency strategy of VCD is employed in interpreting such structural changes. Structures from such an analysis consist with that from other techniques. The computed spectra based on COM model further confirmed structures from observed VCD.

To my wife, Dr. Xue Li (Lisha)

Her encouragement made the completion of this work possible.

And to my father, Yinian Xie and mother, Lanfang Li as well as my father in law,

Jingtang Li

And to my sisters and brother

for their encouraging words and help.

Acknowledgments

I wish to express my appreciation to Professor Max Diem, my mentor, for his guidance throughout the entire work I did, and for his invaluable time and his patience in the preparation of this manuscript. Everything he did for me will definitely be remembered.

I would like to express my respect here to Dr. Qicong Ying, my former boss in Institute of Chemistry, Chinese National Academia of Science. Under her leadership and friendship, I obtained the basic training to being a scientist in academic area. She also introduced me to come U.S.A. for further education.

I also like to thank my colleagues Drs. David Zakim, Sheryl Birk, Ou Lee and Mr. Qinwei Zhou and Luis Chiriboga.

Finally, I am very grateful for the financial support given to me by Chemistry Department of Brooklyn college and Hunter college, CUNY in form of teaching assistantship, university fellowship, and by NIH in form of research assistantship.

PREFACE

The ultimate goal of molecular biology is to understand biological processes in terms of chemistry and physics of macromolecules that participate in them. One of essential differences between chemistry of living and nonliving systems is the greater structural complexity of biological macromolecules. We shall not unravel chemistry of life in molecular detail without knowing the structure of biological macromolecules, especially the proteins at atomic resolution.

The importance of molecular structure for understanding its function is best exemplified, of course, by DNA. The simple and beautiful double-helical, base-paired structure of DNA immediately made genetics intelligible in chemical terms. Genes, the previously mysterious factor that controlled inheritance of particular traits, were segments of the DNA molecules that could be spooled out of solution at the end of a rotating glass rod, like cotton candy on stick.

By contrast, determining the structure of protein, e.g. myoglobin and hemoglobin, has not yielded a simple and all-embracing explanation of the relation between protein structure and function. We know the three-dimensional structure of some 300 different proteins, yet we are still unable to formulate a set of general rules that predict three-dimensional structure from amino acid sequence of its polypeptide chains. It is perhaps not surprising that protein structures are so much more complex than those of DNA. Proteins are built up from twenty different amino acids compared with the four nucleotides of DNA. Moreover, proteins

fulfill a much wider range of biological functions than DNA, and functional diversity dictates structural diversity.

By comparison with molecular genetics, progress in research on protein structure has been painfully slow, not only because of the great diversity that protein structures have, but also because of the simple technical problem of obtaining protein crystals. Until now there has been no technique that is perfect for structural studies of peptides and proteins. The best way to do that is by using multi-technique.

The varieties of bioactivities of proteins or peptides is due mostly to the varieties of their conformations in different environments. these conformations exhibit chirality, which may be monitored by measurement of VOA. Natural optical activity is one of the most structurally sensitive molecular properties available for spectroscopic probing, and, as such its measurement has been exploited extensively in stereochemical analyses. Most spectroscopic techniques (for example, infrared and Raman spectroscopies) sense detailed aspects of molecular geometry only via perturbation of energy levels and selection rules. However, molecular optical activity originates as a direct consequence of the geometrical arrangement and interaction of atoms in a molecule. In other words, the observable optical activity can be considered to have a **first-order dependence on the molecular geometry**. In recent years, the standard technique for assessing optical activity has been circular dichroism(CD) spectroscopy, or measurement of the differential absorption of left and right circular polarized light ($\Delta\varepsilon = \varepsilon_L - \varepsilon_R$). Circular dichroism is related to the previously used measurement of optical rotatory dispersion (ORD).

Conventional CD is a study of transitions to excited electronic states only a few of which, such as the $\pi^* \leftarrow \pi$ and $\pi^* \leftarrow$ n of aromatics and carbonyls, are accessible for UV-CD in proteins and nucleic acids. These transitions usually also

involve overlapping, broad, featureless spectral bands that consequently have interfering CD signals. This interference has compromised the results, for example, in cases where aromatic side chains provide a significant contribution to the spectrum.

In the vibrational region of the spectrum, infrared and Raman transitions are typically much better resolved and are more straightforward to assign and interpret than are electronic transitions. The nature and polarization of various characteristic vibrations have been established firmly in many cases. Extensive infrared and Raman studies have demonstrated that certain spectral features are characteristic in frequency or intensity for expected structural aspects of either proteins or nucleic acids. However, in ordinary infrared and Raman spectroscopies, the spectral differences between related structures are quite small; so, even though a great amount of spectral detail is available, sensitivity to conformational changes is limited.

Vibrational circular dichroism studies combine the advantages of each of these techniques by providing the detail of infrared data with the added conformational sensitivity of CD.

The extension of measurements of circular dichroism into the infrared region has been a long-sought goal for many scientists. It utilizes the combination of the sensitivity of CD and the specificity of infrared spectroscopy to solve a variety of problems in molecular stereochemistry. Technical obstacles made the goal impractical until the early 1970's. The infrared circular dichrograph became reality, thanks to technical advances on several fronts, such as highly sensitive IR detectors, personal computers and, especially, photoelastic modulators in the IR region.

The aim of the research project in this dissertation has evolved, under general objectives of the laboratory research group, from optimization of the VCD

instrumentation to series studies of the conformations of small peptides to demonstrate the advantage of VCD, in comparison with results from other techniques, such as NMR, IR, Raman and CD.

The scope of this thesis incorporates seven chapters. Chapter one briefly reviews the basic concept about structures of peptides and proteins, including peptide linkage and primary, secondary and tertiary structure of peptides and protein. The second part of chapter one presents an overview of the available, physical techniques that are used to measure secondary structure of peptides and proteins. In chapter two, we focus on the theoretical background of optical activity and computation models of circular dichroism. In the quantum chemical description of optical activity, we discuss in detail the basic concepts of dipole strength and rotatory strength. The computation of CD is a broad topic. We concentrate on the "Coupled Oscillator Model", which is successful in computing conformations of some peptides and DNA. In Chapter three, we concentrate exclusively on the instrumental aspect of vibrational circular dichroism (VCD). This chapter contains the discussion of circular polarized light, photoelastic modulator and the measurement of CD. In chapter four, we discusses the recent progress of VCD in our laboratory, which focuses on how to overcome the artifact of VCD. The result shows that artifacts in VCD can be from either hardware or data treatment method used. A new method proposed demonstrates much better results under the same measurement condition. Most of system artifacts can be canceled out, and therefore, sample concentration range can be lowered below 10-15mM.

In chapter five, six and seven we deal exclusively with the applications of conformational studies of peptides, especially with that of small peptides. Several typical examples show that VCD is significantly sensitive to conformations and their changes when peptides are in different chemical environments. The VCD is

an enormously sensitive tool for monitoring the conformation of peptides and proteins.

REFERENCES

I. Applequest, (1987) *J., American Scientist*, 75, 58.

II. Stinson, S.C., (1985) *Chemical & Eng. News*, Nov. 11, 21.

III. Max Diem,(1993) " Introduction Modern Virbrational Spectroscopy" John Wiley and Son,-interscience; NY.

TABLE OF CONTENTS

Chapter Two: Optical Activity of Molecules

(Theoretical Background of Optical Activity and Computation of VCD)

Chapter Three: Instrumentation and Measurement of Vibrational Circular Dichroism

Chapter Four: Artifact and Optimization of Dispersive VCD

Abbreviations

AC- alternating current

CD - cricular dichroism

COM - coupled oscillator model.

CPL - circularly polarized light.

DC - direct current.

FT - Fourier transform.

IR - infrared spectroscopy.

LD - linear dichroism.

PEM - photoelastic modulator.

PLL - poly-L -lysine.

VCD - vibrational circular dichroism.

Symbols

$A(\nu)$ - absorbance of sample.

$A_+(\nu)$ - absorbance of sample toward right CPL.

$A_-(\nu)$ - absorbance of sample toward left CPL.

C - concentration, in mole/ L.

D - dipole strength or dipole moment.

g - anisotropy, or dissymetric factor.

$I(\nu)$ - light intensity.

$J_n(x)$ - n th order Bessel function.

k - light wave vector, $k = (2\pi\nu/c)\varepsilon_K$

l - sample cell pathlength.

m - magnetic dipole operator.

m_j - mass of particale j.

p_j - momentum of particale j.

Q - nuclear coordiates.

q - electron coordinates.

R - rotational strength.

r_j - position of particle j.

$V(\nu)$ - signal output of detector.

$V_{DC}(\nu)$ - transmission signal which is not modulated by PEM.

$V_{AC}(\nu)$ - signal modulated by PEM.

$\varepsilon(\nu)$ - molar extinction coefficient, L. $mole^{-1}.cm^{-1}$.

ε_U - unit vector in direction U.

λ- light wavelength.

ν- light frequency, c / λ in Hz.

μ- electric dipole operator.

θ - initial phase of light.

Θ- quadrupole transition moment.

Ψ - molecular wavefunction.

List of Tables

List of Figures

CHAPTER ONE

INTRODUCTION

1.1. STRUCTURE OF POLYPEPTIDES AND PROTEINS

Nucleic acids, a class of biopolymers, can store and transmit the genetic information of the cell. This information is subsequently expressed into another class of biopolymers, the proteins.

Proteins play a large variety of roles: Some carry out the transport and storage of small molecules; others make up a large part of the structural framework of cells and tissues. In keeping with the multiplicity of their functions, proteins are extremely complex molecules. The fundamental reason why the multi-functional capacity of proteins or peptides remains unsolved lies in the fact that there are 20 different α-amino acids, from which proteins are composed . There is a vast number of ways in which similar structural domains can be generated in proteins by different amino acid sequences. By contrast, the structure of DNA, made up of only four different nucleotide building blocks that occur in two pairs, is relatively simple, regular, and predictable.

1.1.1. Primary Structure of Proteins

Peptides and proteins are composed of 20 α-amino acids. All of them have in common a central α-carbon atom (Cα) to which is attached a hydrogen

atom, an amino group (NH_2), and a carboxyl group (COOH). What distinguishes one α-amino acid from another is the side chain attached to the Cα through its fourth valence. There are 20 different side chain groups specified by the genetic code; (Figure 1-1) others occur, in rare cases, as the products of enzymatic modifications after translation.

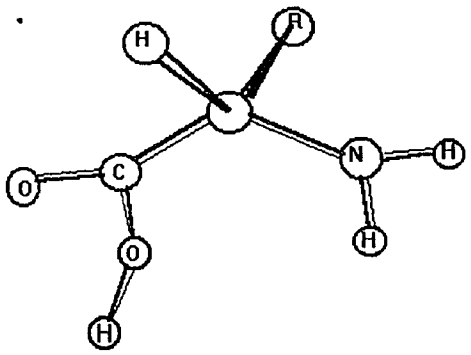

Figure 1-1. The structure of amino acid with various side-chain R

Depending on the chemical nature of the side chain, the amino acids are divided into three or four different classes. The first class comprises those with strictly hydrophobic side chains A, V, L, F, P, I, C and M. The four charged residues D, E, K and R form the second class or polar group. The third class comprises those with polar side chains S, T, N, Q, Y, H and W. (Table 1-1.) The amino acid glycine (G), which only has a hydrogen atom as a side chain and so is the simplest of the 20 amino acids, it has special properties and is usually considered to form a fourth class or to belong to the first class.

Table 1-1. Structure of side-chain of normal amino acids

Side chain group	Side -chains of amino acids
hydrophobic group	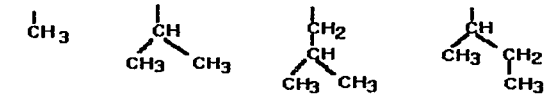 Alanine Ala (A) Valine Val. (V) Leucine Leu (L) Isoleucine Ile (I) 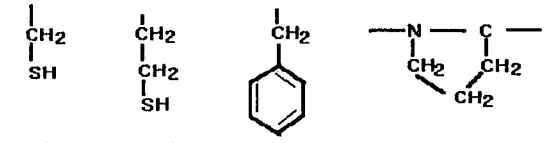 Cysteine Cys (C) Methionine Met (M) Phenolalanine Phe (F) Proline Pro (P)
Charged group	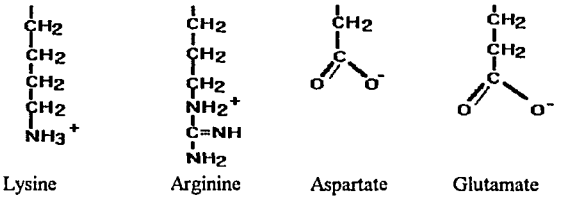 Lysine Lys (L) Arginine Arg (R) Aspartate Asp (D) Glutamate Glu (E)
Polar group	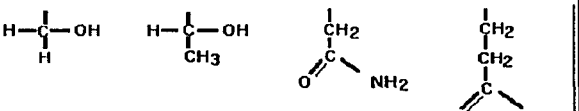 Serine Ser (S) Threonine Thr (T) Asparagin Asn (N) Glutamine Gln (Q) 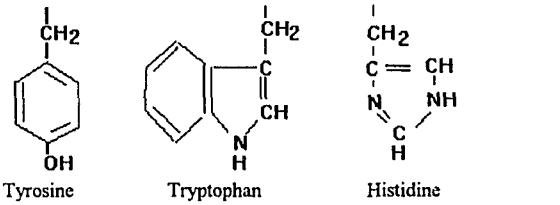 Tyrosine Try (Y) Tryptophan Trp (W) Histidine His (H)

Since four groups attached to the Cα atom are chemically different, all amino acids except glycine are thus chiral molecules. They can exist in two different forms with handeness, or charility, the levo (*l*) - or dextro (*d*)-form.

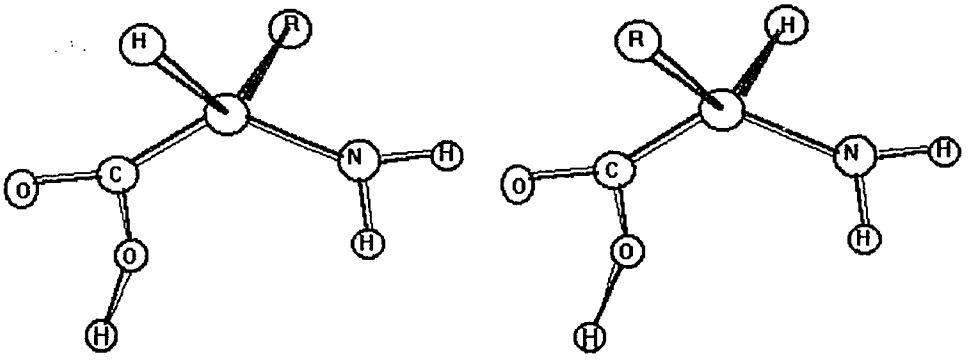

L-form D-form

Figure 1-2. Enantimers of amino acid.

Biological systems depend on detailed recognition of molecules involving differentiation between chiral forms. The translation machinery for protein synthesis has evolved to utilize only one of the chiral forms of amino acids, the L-form. All amino acids that occur in proteins therefore have the L-form. There is, however, no obvious reason why the L-form was chosen during evolution over the D-form.

Proteins and peptides, as well as nucleic acids, exist as unbranched polymers. The complete covalent structure is called the primary structure. It must specify the configuration of all asymmetric centers, both in the polymer chain backbone and on side chains of each of the monomer residues.

1.1.2. Secondary Structure of Protein

(Peptide units are building blocks of protein structures)

1.1.2.1. Peptide Units

Amino acids are joined end to end during protein synthesis by the formation of peptide bonds. The carboxyl group of the first amino acid condenses with the amino group of the next to eliminate water and yield a peptide bond. This process is repeated as the chain elongates.

Each Cα atom except the first and last one in the chain conects with two peptide units, by which the two amino acid are linked together. The reason for dividing the chain in this way is that all atoms in such a unit of peptide linkage are fixed in a plane with given bond lengths and bond angles, which are very nearly the same in all units in all proteins. Note that the peptide units of the main chain do not involve the different side chains. (Figure 1-3)

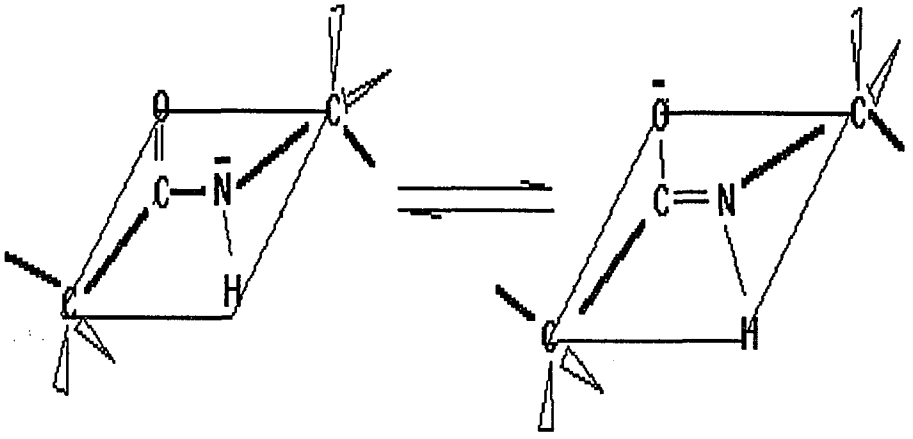

Figure 1-3. Peptide linkage forms a rigid plane.

Since the peptide units are effectively rigid groups that are linked into a chain by covalent bonds at the Cα atoms, the only degrees of freedom they have are rotations around two bonds: the N-Cα and the Cα-C' bonds. A convention has been adopted to call the angle of rotation around the N-Cα bond phi(ϕ) and angle around Cα-C' bond from the same Cα atom psi(φ). In this way each amino acid residue is associated with two conformational angles ϕ and φ. Thus, the conformation of the whole polypeptide chain is known completely determined when the ϕ and φ angles for each amino acid are defined.

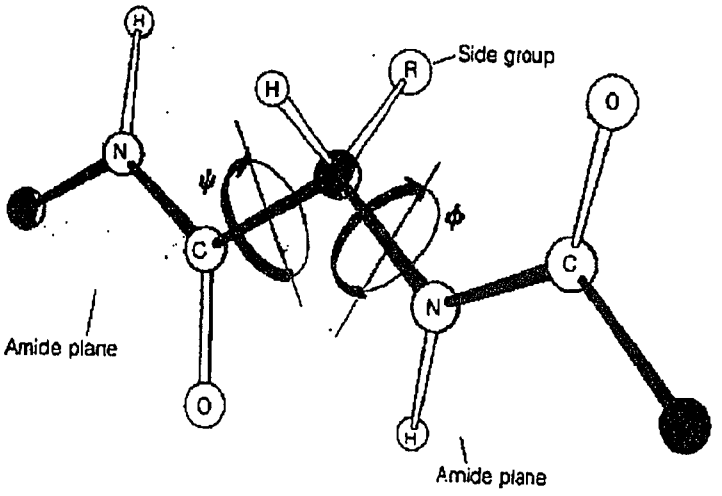

Figure 1-4. The tertiary angles (ϕ and φ) of the peptide chain, which determines the conformation of a peptide, ϕ and φ shown here as 180°.

To make the definition more meaningful, one must specify the positive direction of rotation and the zero angle conformation of each. The direction of both oxygen of C=O and hydrogen of N-H rotating toward Hα of Cα in clockwise is positive direction of rotation and the conformation shown in Figure 1-4 is 180° for both angles. Therefore any backbone of particular residue in protein can be described by point on map with coordinates ϕ and φ. The potential energy of residue, plotted against ϕ and φ are called a Ramachandran plots (Figure 1-5). One of the most useful features of Ramachandran maps is that they allow us to describe simply which structures are sterically possible and which are not.

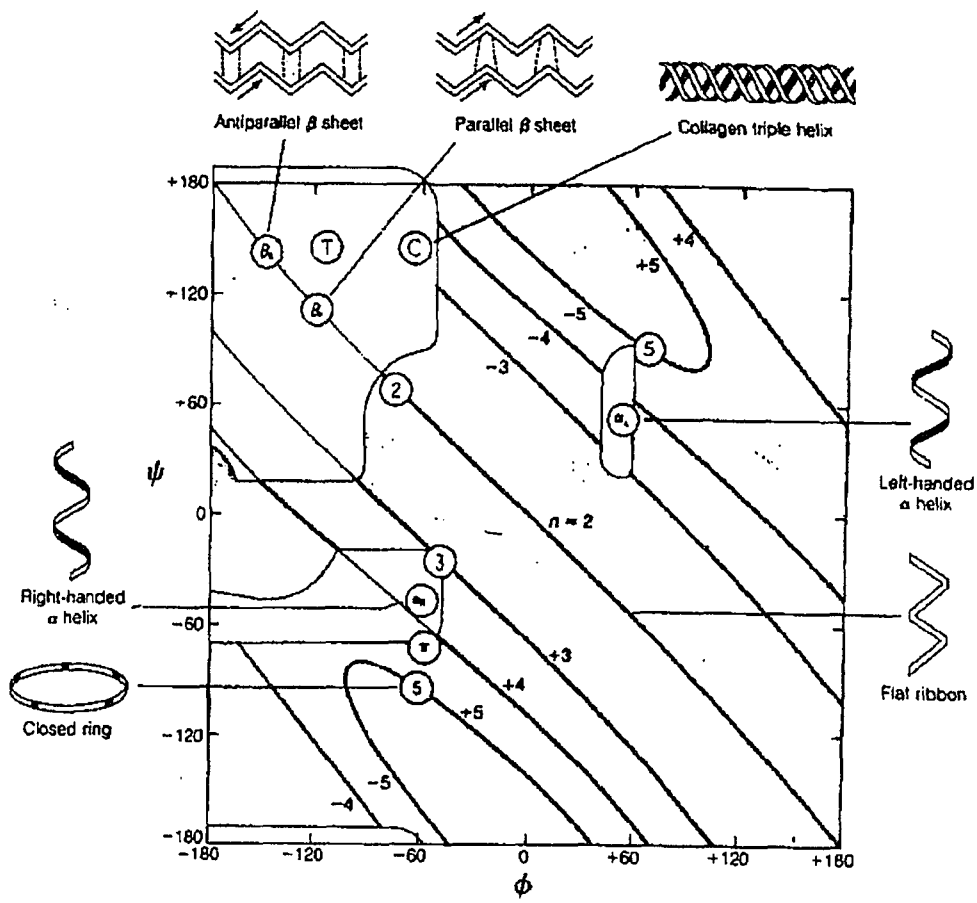

Figure 1-5. The Ramachandran diagram. The coordinates are ϕ and φ angles defined as in Figure 1-4. The areas correspond to various conformation which are indicated outside of plot.

1.1.2.2. The Motivation of protein folding

(The interior of proteins is hydrophobic)

Many biopolymer chains can form locally ordered, three-dimensional structures. For individual, linear, head to tail polymers, with asymmetric monomer units, the most common symmetric three-dimensional ordered structure possible is a helix. A good example for motivation of protein folding is noticed by the subsequent high-resolution studies of myoglobin that the amino acids in the interior of the protein had almost excessively hydrophobic side chains long time ago. This was one of the first important general principles that emerged from studies of protein structures. The driving force for folding water-soluble globular protein molecules is to pack hydrophobic side chain into the interior of the molecule, thus creating a hydrophobic core and hydrophilic surface (Figure 1-6). There is a major problem, however, in creating such a hydrophobic core from a protein chain. In order for the side chains to be in the core, the main chain must also fold into the interior. The main chain is highly polar and therefore hydrophilic, with one hydrogen bond donor, NH, and one hydrogen bond acceptor, C=O, for each peptide unit. These polar groups in main chain must be neutralized by hydrogen bond formation in a hydrophobic environment. This problem is solved in an elegant way by the formation of regular secondary structures within the interior of the protein molecule. That secondary structure are either alpha helices or beta sheets.

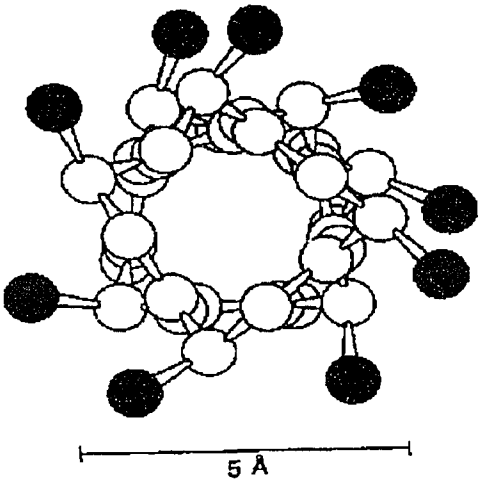

Figure 1-6. Hydrophobic core inside of α-helix.

The most famous polypeptide secondary structure is the right handed α-helix, which was first proposed as a possible conformation of the polypeptide chain by Pauling and his collaborators[1-1a]. The basic features of the α-helix are 3.6 residues per turn and translation along the helix axis of 1.5Å per residue. This leads to a pitch of 3.6 x 1.5= 5.4 Å. The dihedral angles are ϕ =–57.4° and φ = – 47.5°. The diameter, neglecting side chains, is about 5Å. Neglecting end effects, every peptide carbonyl in the α helix serves as a hydrogen bond acceptor for the peptide N-H donor four residues away.(see Figure 1-7a)

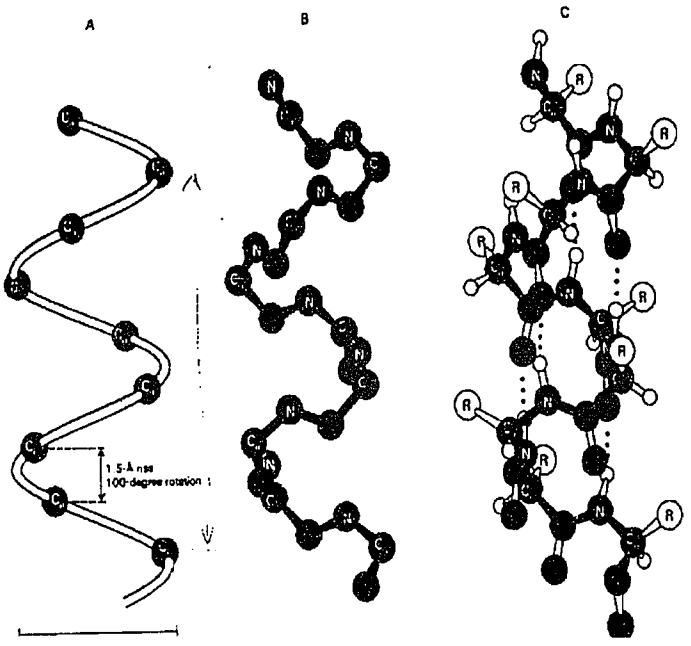

Figure 1-7. Secondary structure of peptide : α-helix.

The β-sheet is another common secondary structure of peptides. Apparently, the right-handed α-helix nicely meets all the criteria used by Pauling and Corey. A similar-looking left-handed α-helix was also postulated, and so were two β-sheet forms. Each single strand in β-sheet is a 2-fold helix, a pleated structure. All peptide units participate in hydrogen bonding, but these bonds are interstrand rather than intrastrand. The geometry of the peptide backbone in the β-sheet approaches the most extended chain conformation allowed by normal bond lengths and angles; this displacement along the helix axis is about 3.47Å per residue. In many proteins, parallel and antiparallel β chains combine to produce a large structural core.

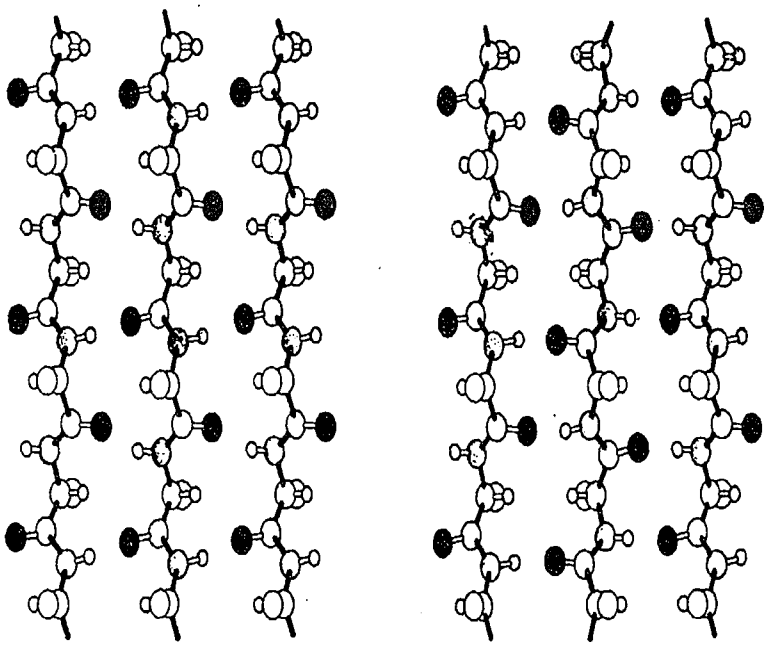

Parallel β-sheet Antiparallel β-sheet

Figure 1- 8. Secondary structure of peptide: β-sheet.

It is well-known that α-helix and β-sheets are major stabilizing structures in proteins. Segments of the protein chain which are neither helical nor β-sheet have been generally designated as random coil or irregular regions. However, it has become increasingly apparent that these so-called random regions of the protein do exhibit regular structural patterns. The third important category of secondary structures are turns.

A turn is defined as a site where the polypeptide chain reverses its overall direction. The terms β– and γ-turns have more restricted definitions and describe turns of four or three residues, respectively. In α-helices and β sheet; each conformations is apparent in physical models because each has backbone torsion angles with repeating values. By contrast, turns are not as conspicuous because their backbone torsion angles are nonrepeating (Figure 1-9).

Turns are enormously important for following reason: First, the turn is a basic element that links other secondary structures together to form tertiary structures in proteins or peptides. Thus, the conformation of turns may be nucleation centers for peptide folding.[1-1b] Second, turns have functions related to their structural characteristics. Turns are intrinsically polar structure with backbone groups that pack together closely and side chains that project outward. Such an array of atoms may constitute a site for molecular recognition, and indeed, the literature abounds with suggestions that turns serve as loci for receptor binding, antibody recognition, and post translation modification. This familiar idea, that function follows structure, must be evaluated with particular care in the case of turns. In proteins, intermolecular recognition takes place upon surfaces that are already densely populated by turns. Hence, the appearance of turn at or near a recognition site does not necessarily imply a relationship of cause and effect. In peptides, turns are the conformations of choice for simultaneously optimizing both backbone-chain compactness (intramolecular nonbonded contacts) and side-chain clustering (to facilitate intermolecular recognition). Present of turns in bioactive conformations may in fact reflect the lack of alternative conformational possibilities[1-1c,-2].

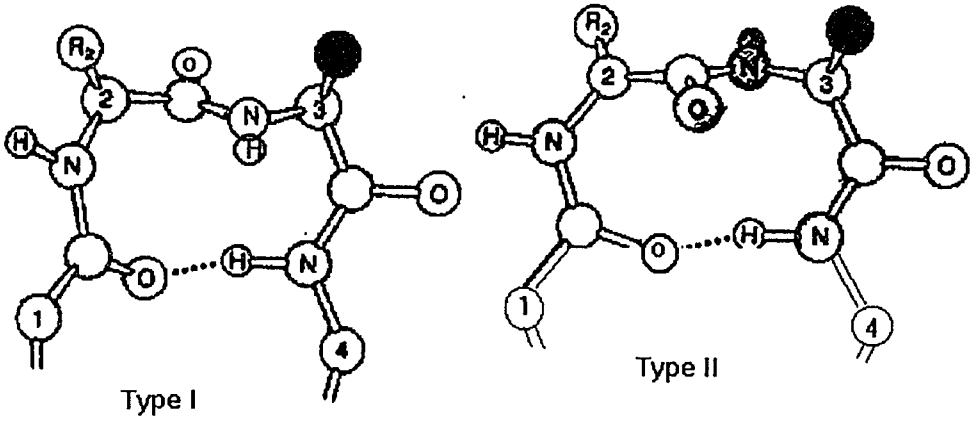

Figure 1-9. Secondary Structure of Peptide: Type I and type II β-turn.

1.1.3. Tertiary Structures of Proteins

(The three-dimensional arrangement of residues)

The tertiary structure of a protein is the complete three-dimensional structure of one effectively indivisible unit. For a protein, this unit is usually one single covalent species, whether it contains a single polypeptide or more than one linked by covalent cross-links. The tertiary structure includes a description not only of local symmetric structure but also of the spatial location of all residues so far as is possible.

1.1.4. Quaternary Structure of Proteins

The highest level of structure we shall consider is quaternary structure. This is formed by the noncovalent association of independent tertiary structural units. The subunits of the quaternary structure may or may not be identical, and their arrangement in the quaternary structure may or may not be symmetric. (Figure 1-10)

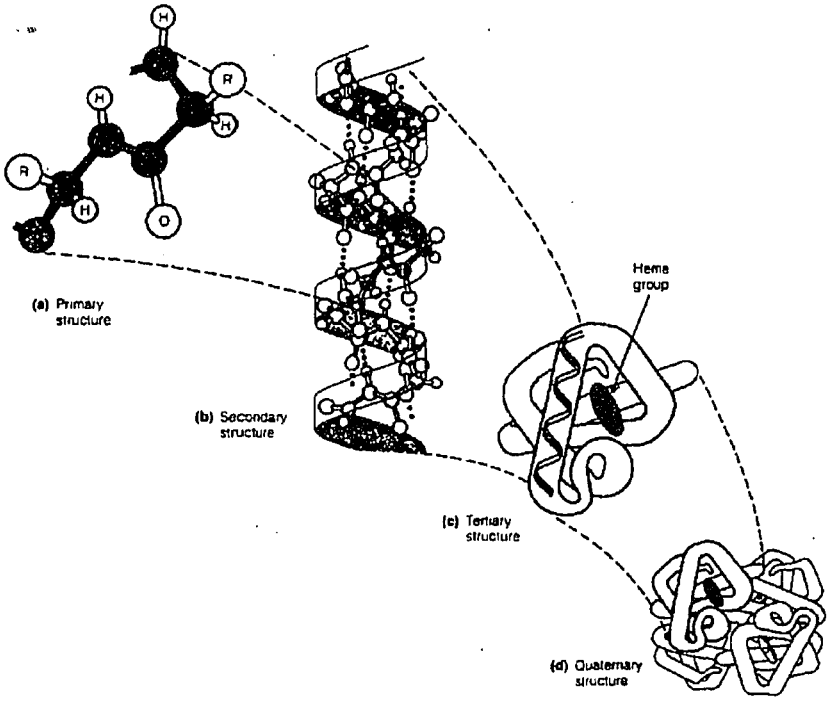

Figure 1-10. Levels of protein structure. This figure summarizes the four levels of structure, using the molecule hemoglobin, a tetramer of myoglobin like chains.

1.2. THE STRUCTURAL STUDIES OF PROTEINS BY PHYSICAL TECHNIQUES

1.2.1 X-ray diffraction

Many methods exist that can yield information about the conformations of peptides; most definitive one being x-ray diffraction. Any peptides of conformational interest ought to be studied by x-ray methods. Much of our current knowledge about the details of conformations is based on observations of peptide crystal structures. However, the drawback of x-ray studies is that the molecule is viewed in conformations that are determined by the interplay of intramolecular and crystal-lattice forces. Intermolecular forces are of primary importance in the formation of the crystal and can have profound effects on the conformations adopted by the peptide (in contrast to the situation in protein crystals where the conformation of the protein is thought to be only slightly perturbed). Still, the observed conformation(s) can always be counted as among those accessible to the peptide. In certain instances, the structure will be closely related to conformations found in other environments of interest.

The restrictions of X-ray crystallography, along with the growing need to understand the conformational properties of proteins in different environments (e.g., water, membranes, micelles, organic solvents and under different physiological and non-physiological conditions) has stimulated the search for spectroscopic methods which can complement the precise crystallographic determination of the secondary structure of proteins. The spectroscopic techniques currently used for such purposes include NMR, circular dichroism, Raman and infrared spectroscopies.

Solution conformational analysis of peptides is hindered by the interrelated obstacles of conformational heterogeneity and dynamics. Small linear peptides are usually flexible molecules and many undergo rapid conformation interconversions. The proportion of time that the peptide spends in each of these conformational states and the rate of interconversion must be considered in choosing methods of conformational analysis and in interpreting data. Conformational conversions not requiring peptide bond rotation may occur at microsecond or faster time scales in linear peptide; on another hand, peptide bond rotations occur on the time scale of seconds[1-3]. If a spectroscopic method has a fast time scale relative to these rates, individual conformers will be "seen" (i.e., the observed spectrum will be sum of the individual spectra). If the spectroscopic method has a slow time scale relative to these rates, observed spectral parameters will be weighted averages of interconversion of those conformers; the weighting functions can be complex [1-4]. Cyclic peptides are less flexible than their linear counterparts and are generally more traceable targets of solution conformational analysis.

1.2.2. Nuclear Magnetic Resonance Spectroscopy

The first nuclear magnetic resonance (NMR) experiments with biopolymers were described over 40 years ago, and the potential of the method for the studies of structure and dynamics of proteins and nucleic acids was long anticipated. However, in practice, initial progress was slow because of limitations imposed both by available instrumentation and by the lack of suitable samples of biological macromolecules. Nuclear magnetic resonance of proteins and nucleic acids is represented in the literature by less than 30 papers during the years up to 1965,

approximately 200 papers up to 1970, 4000 papers up to 1980, and of the order 500 to 1000 papers a year from 1981 onward.

Nuclear magnetic resonance is the most useful method of peptide conformational analysis in solution. NMR yields information about the chemical environment of nuclei (chemical shifts), the geometric relationships between nuclei (coupling constants), the distances between nuclei (Nuclear Overhauser enhancements (NOEs)), accessibility and hydrogen bonding of amide protons, exchange kinetics and sensitivity of resonance positions and line widths to temperature, solvent, or paramagnetic probes [1-6], as well as the dynamics of nuclei (relaxation times). This wealth of information is site specific, so that properties of individual residues can be studied. However, the interpretation of NMR data for peptides must be carried out with caution. NMR is slow method with a time scale between 10^{-6} seconds to 10^{-3} seconds for the usual NMR measurements. Hence conformational interconversions not requiring peptide bond rotations will lead to averaged NMR parameters. As Jardetzky[1-4] has point out, the interpretation of these averaged NMR parameters in terms of one conformation is of little value.

NMR structure determination may be applied effectively to small proteins with molecular weights up to about 12000. For the architecture of the core of globular proteins the result of a high quality NMR structure determination is comparable to that achieved in a high resolution X-ray crystal structure. The onset of structural disorder toward the molecular surface is more pronounced in NMR protein structures than in the corresponding x-ray structures. One line of future research will undoubtedly focus on the functional significance of this observation.

Much effort is currently concentrated on improving the experiment, in particular with the use of stable isotopes, to extend NMR structure determination to large proteins, in the size range 15000-30000.

By comparison with X-ray, since the pioneering work of Perutz and Kendrew in late the 1950s, single crystal X-studies have set the standards for protein and nucleic acid spatial structure determination. They have provided data on over 200 proteins, several tRNA's and a selection of synthetic oligonucleotide. The NMR approach is complimentary to X-ray crystallography in several ways.

1. The NMR studies use noncrystalline samples(e.g., solution in aqueous or nonaqueous solvent, or detergent-solubilized biopolymers in mixed micelles). If NMR assignment and spatial structure determination by NMR can be obtained without reference to a corresponding crystal structure, a meaningful comparison of the conformations in single crystals and in noncrystalline states can be obtained.

2. Nuclear magnetic resonance can be applied to molecules for which no single crystals are available. Thus new structures can be obtained, which are not available from X-ray studies.

3. The conditions for NMR studies (e.g., pH, temperature, ionic strength, buffers) can usually be varied over a wide range. This opens the possibility for comparative studies under native and denaturing solution conditions, or for investigations of intermolecular interactions with other solute molecules.

4. For a characterization of the internal dynamics of biomolecular structures, NMR provides direct, qualitative measurements of the frequencies of certain high activation energy motional processes. It also provides some semiquantitative information on additional high frequency processes. In comparison, X-ray structure determinations may include only an outline of the conformational space covered by high frequency structural fluctuations. Furthermore, both neutron diffraction in single crystals and NMR in solution can be employed to studies the exchange of label protons, potentially enabling the direct comparison of molecular dynamics in different states [1-7].

1.2.3. Vibrational Spectroscopy

The vibrational frequencies of molecules can be determined by two fundamentally different spectroscopic techniques; Infrared spectroscopy; first systematically used by W. Coblentz in 1905 and Raman spectroscopy; first experimentally observed by C.V. Raman and K. Krishman in 1928.[1-8]

Vibrational spectroscopy has been used widely in many different field. It is also applied in biomolecular system as a complementary approach to NMR and crystallography in the determination of the conformation of peptides and proteins. The sensitivity of amide vibrations to hydrogen bonding has been of particular interest.[1-9, 10, 11] As is the fact had, vibrational spectroscopy occurs a fast time scale (10^{-13} sec.).

The amide vibrations of polypeptide linkages are listed in Table 1-2. So, one sees IR bands in virtually all spectral region. Normal coordinate analysis has offered a way of analyzing all of the intrinsic vibrations for a particular conformation of a peptide. Bandekar and Krimm [1-12, 13] have focused on β turns and have reported expected bands for various turns, They compared their predicted spectra with experimental data for cyclized β-turn models (i.e., a β-turn cyclized via a covalent, nonpeptide linkage) and found a consistent fit. These approaches have not been extensively applied as yet, and it remains to be seen how useful they will be.

Infrared spectroscopy is one of the earliest experimental methods recognized for it's potential in estimating the secondary structure of polypeptides and proteins. In the past, the practical usefulness of the method was severely limited by such factors as low sensitivity of the infrared instruments, interfering absorption from the surrounding media or solvents and most importantly, by

Table 1-2. Amide Vibrations of polypeptide linkages.

Vibrations of amide	Constituents	Frequency (cm^{-1})
A	N-H stretching	3300
B	First overtone of amide II	3085
	C=O stretching (80%)	
I	C-N stretching	1690-1650
	N-H in-plane deformation	
	N-H in-plane deformatiom	
II	(60%)	1560-1545
	C-N stretching (40%)	
	coupling of N-H in-plane	
III	deformation and one	1350-1250
	deformation each of αC_i-H	
	and αC_{i-1}-H	
IV	O=C-N in-plane bending	725
	N-H out-of -plane	628
V	deformation	
VI	C=O out-of-plane bending	600
VII	torsion about the C-N bond	206

difficulties in extracting the structural information contained in the conformation-sensitive infrared bands. The first two obstacles have been largely overcome by the development of computerized FT-IR instrumentation. This has improved the signal to noise ratio and also allows extensive data manipulation. The third difficulty appears to be of a more functional nature. It reflects the fact that the conformation-sensitive amide bands of proteins are composites which consist of overlapping component bands originating from different structures, such as a helix, β-strand, turns and non-ordered polypeptide fragments. Due to the inherently large width of the overlapping component bands, they cannot be resolved and /or identified in the broad contours of experimentally measured spectra.

A significant step forward in infrared spectroscopic analysis of proteins was recently made by developing computational procedures for the resolution enhancement of broad infrared bands. These band-narrowing methods allow the decomposition of the complex amide bands into their underlying components. This new methodology not only enriches the qualitative interpretation of infrared spectra, but also provides a basis for the quantitative estimation of protein secondary structure. Today, the most effective procedure for narrowing infrared bands is Fourier self-deconvolution (FSD). This procedure is based on multiplying the Fourier transform function I(x) with an exponentially increasing function to yield a new function I'(x). This can decrease the rate of decay of the exponential term in the Fourier transform function; consequently, the width of the bands in the infrared spectrum is reduced. Several references give detailed explanations about that technique.[1-14, 15, 16].

1.2.4. Circular Dichroism

Circular dichroism (CD) is exquisitely sensitive to conformation, since the arrangement of peptide bond chromophores with respect to each other and to asymmetric fields in the molecule will vary with different conformations. CD has a very fast time scale (10^{-15}sec.) [1-17]. Several spectra of secondary structures of peptides have been documented. Since it is a chiroptical method, the circular dichroism spectrum is determined " first-order" by the molecular conformation. This has led to the wide use of CD measurement in the ultraviolet spectral region for empirical studies of protein conformations [1-18, 19, 20]. Numerous studies have followed the initial proposal of Greenfield and Fasman [1-21] using CD curves obtained from model polypeptides to interpret protein data. The key to success of their approach stemmed form the dominant contribution of the α-helical component in the near-UV CD spectra as compared to that from other elements of the secondary structure. The inherent qualitative advantage of CD can be exploited quantitatively by development of characteristic and transferable "basis" CD spectra that are typical for individual secondary structure. (Figure 1-11) Fitting linear combinations to the experimental data can yield estimates on the composition of the secondary structure. Improving on the original idea that used model polypeptides as the source of reference CD data, these basis spectra were subsequently derived from protein CD spectra by use of X-ray-determined secondary structures. Subsequent studies avoided the use of basis spectra by using an analysis of the protein CD spectra directly. Alternatively, such spectra were used for generation of orthogonal basis CD "vectors" which could then be used in a scheme to generate an analysis of the secondary structure of a protein which was not in the original set.

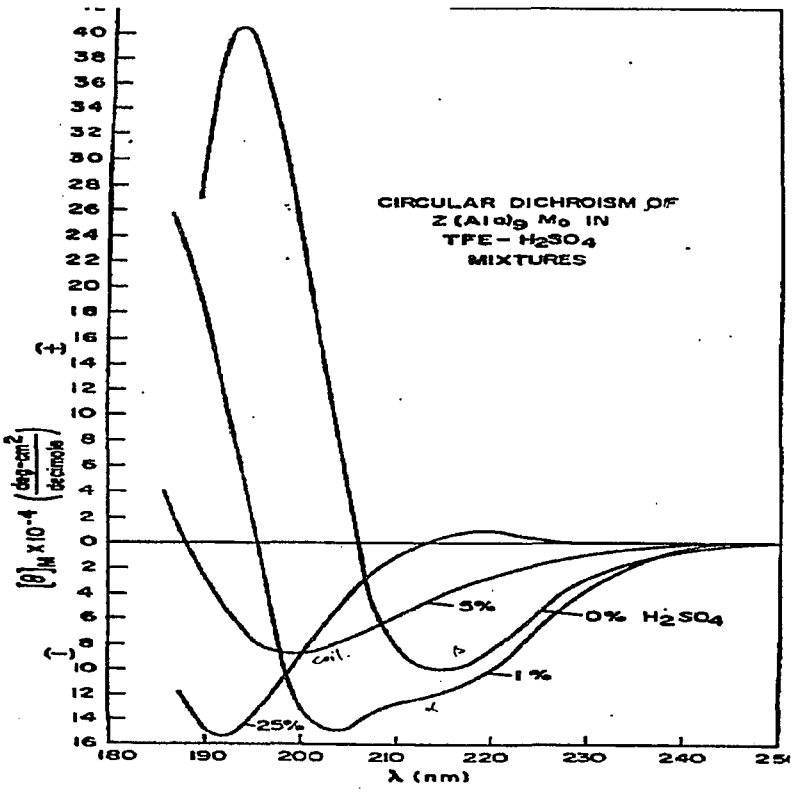

Figure 1-11. The "basic" spectra of secondary structures: α-helix, β-sheet and random coil

Analysis of such results is dependent on the accuracy and stability of the "basis" spectra and on the assumption that there is linear dependence of the CD intensity on the fraction of a given conformational type in a specific protein. This is equivalent to assuming that segments of different secondary structure do not

interact in a way that affects the CD spectrum. This would be true if the UV-CD spectrum was determined by short-range interactions. Since UV-CD spectra are also affected by other factors, the linearity assumption can be a potentially limiting factor in improvements of quantitative conformational analysis.

The CD spectra in the peptide chromophore region are composed of broad overlapping bands arising from an ensemble of $\pi^* \leftarrow \pi$ and $\pi^* \leftarrow$ n transitions of a molecule. Consequently, detailed interpretation of CD spectral for molecules larger than di- or tripeptide is difficult. Furthermore, several different conformational features yield similar CD spectra. Expected CD spectra have been calculated for β [1-22] and γ-turns [1-23]. Model peptide data [1-24, 25] has given support to some of these calculated spectral types and has raised doubts about others. At present it appears that γ turns give rise to a reliable CD band at a long wavelength (- 230 nm), and β-turns yield any of three possible curve shapes that correlate with turn type. It must be kept in mind that these turn spectra have relatively low ellipticities compared to α-helices or β-structures, so that decomposing a complex spectrum into various structural features, including turns, involves large errors.

In the vibrational region of the spectrum, infrared and Raman transitions are typically much better resolved and are straightforward as the assignment and interpretation relative to electronic transitions. The nature and polarization of various characteristic vibrations has been firmly established in many cases. Extensive infrared and Raman studies have demonstrated that certain spectral features are characteristic in frequency or intensity for expected structural aspects of either proteins or nucleic acids. However, in ordinary infrared and Raman spectroscopies, the spectral differences between related structures are quite small. Therefore, even though a great amount of spectral detail is available, sensitivity to conformational change is limited.

1.2.5. Vibrational Circular Dichroism

Vibrational circular dichroism studies combine the advantages of each of these techniques by providing detailed of infrared data with the added conformational sensitivity and bisignate nature of CD. Thus, with VCD, the number and variety of transitions that can be used as structurally sensitive probes of the ground electronic state is significantly increased. These discrete spectral features sample several molecular structural elements whose spectra are strongly influenced by both their local conformation and, by the relative juxtaposition of these elements to chemically similar groups. Furthermore, such transitions are typically resolved sufficiently to enable different transitions with different subunits of a large molecule to be correlated and thus to be studied independently. Therefore, the VCD studies undertaken on biopolymer systems should complement and extend the valuable insight into biochemical structure that has been provided by conventional CD and vibrational spectroscopies.

Compared to other techniques for studying protein and nucleic acid structure in solution, vibrational circular dichroism studies are envisioned to complement, not to replace, existing techniques and to offer additional information to aid in the overall problem of conformational analysis. Since VCD data exhibit a short- range sensitivity to conformation, it will complement the longer range effects sensed with electronic CD [1-26,27,28].

REFERENCES

1-1a) Pauling, L. (1951), *Proc. Natl. Acad. Sci.* 37, 205.

1-1b). Zimmerman, S. S. and Scheraga, H.A., (1977) *Proc.Natl.Acad.Sci.USA*, 74, 4126-4129.

1-1c) Guzzo, A. V. (1965) *Biophys. J.* 5, 809-822.

1-2) G.D. Fasman, (1989) in "Prodiction of Protein Structure and The Principle of Protein Conformation"; Edited by G.D. Fasman. Plenum Press, New York. 193-316.

1-3) L. M. and Sternhell, S. (1969) " *Applications of Nuclear Magnetic Resonance Spectroscopy in Organic Chemistry.*" Pergamon, Oxford.

1-4) Jardetzky,O. (1980) *Biochim. Biophys. Acta* 621, 227-232.

1-5) Kopple, K. D. (1983) . *Int. J. Pept. Protein Res.* 21, 43-48.

1-6) Kopple, K. D. and Zhu, P. P. (1983). *J. Am. Chem. Soc.* 105, 7742-7746.

1-7) Williamson, M. P. & Wuthrich, K. (1985). *J. Mol. Biol.* 182, 295-315.

1-8a) J. Bandekar, (1992) *Biochim. et. Biophys. Acta.* 1120, 123-143.

1-8b) R. W. Sarver Jr. & W.C. Krueger (1991), *Anal. Biochem.* 194, 89-100..

1-9) Kopple, K. D., Go, A., and Pilipauskas, D. R. (1975). J. Am. Chem. Soc. 97, 6830-6838.

1-10) Pease, L. G., and Watson, C. (1978). *J. Am. Chem. Soc.* 100, 1279-1286.

1-11) Aubry, A., and Marraud, M. (1983). *Biopolymers* 22, 341-345.

1-12) Bandekar, J., and Krimm, S. (1979). *Proc. Natl. Acad. Sci.* U.S.A. 76, 774-777.

1-13) Bandekar, J., and Krimm, S. (1980). *Biopolymers* 19, 31-39.

1-14) F. U. P. Leutert and Burger, M.M. (1986) *Pro. Natl. Acta. Sci.* 83, 1315-1319.

1-15) Susi,H. and Byler, D. M. (1983) *Bichem. Biophys. Res. Commun.* 115, 391-397.

1-16) W. K. Surewicz and H. H. Mantsch (1988), *Biochim, Biophys. Acta.* 952, 115-130.

1-17) Cantor, C. R., and Schimmel, P. R. (1980). " *Biophysical Chemistry*," Parts I, II. Freeman, San Francisco.

1-18) Woody, R. W. (1985), *The Peptides*, 7, 15.

1-19) Yang. Y. T., Wu, C.S.C. and Martinez, H. M. (1986). *Methods Enzymol.* 130, 208.

1-20) Johnson, W. C. (1985). *Methods Biochem. Anal.* 31, 61.

1-21) Greenfield, N. J., and Fasman, G. D. (1969). *Biochemistry* 8, 4108.

1-22) Woody, R. W. (1974). In " *Peptides, Polypeptides, and Proteins*". 338-350. Wiley John and Sons, New York.

1-23) Madison, V., and Schellman, J. (1970). *Biopolymers* 9, 569-588.

1-24) Bush, C. A. Sarkar, S. K., and Kopple, K. D. (1978). *Biochemistry* 17, 4951-4954.

1-25) Madison, V., and Kopple, K. D. (1980). *J. Am. Chem. Soc.* 102. 4855-4863.

1-26) Keiderling, T. A. (1990) in "Practical Fourier Transform Infrared Spectroscopy", 203-284. Acad. Press. Inc.

1-27) P. P. Sritana and T.A. Keiderling (1989) *Biochem.* 28, 5917-23.

1-28) P.Pancoska and T. A. Keiderling (1991), *J. Am. Chem. Soc.* 30, 6885-6895.

CHAPTER TWO

OPTICAL ACTIVITY OF MOLECULES

(Theoretical Background of Optical Activity and Computation of VCD)

Optical rotatory dispersion and circular dichroism have been known for more than 100 years.[2-1, 2, 3] Until recently, most applications in chemistry only utilized the optical rotation at some transparent wavelength. Then, in the early 1950s, revolutional progress in the study of optically active molecules was brought about through the introduction of new instruments to measure optical rotatory dispersion routinely. This was possible as a result of developments in electronics(particularly is the Photo-Multiplier Tube and the electro-optic modulator). Conventional optical rotation and circular dichroism can be utilized in visible or near ultraviolet region.

2.1. GEOMETRY OF MOLECULE AND ITS OPTICAL ACTIVITY

One of the essential differences between the chemistry of living and nonliving systems is the greater structural complexity of biological macromolecules. That implies the shape of a molecule is an important feature for

peptides or proteins. Most of their bioactivities attribute the folding of a peptide or protein into a certain tertiary structure.

Moffitt, Moscowitz and Djerassi and co-workers[2-4] classified optically active chromophores into terms of two limiting types:

(a) the inherently dissymmetric chromophore.

(b) the inherently symmetric, but dissymmetrically perturbed chromophore.

Chirality is a structural property of both organic and bio- molecules. Chiral molecules exist in two forms, or enantiomers. They are related to each other the same way a left and a right hand are related; i.e., they are mirror images of each other.

Inherently dissymmetric chromophores occur when the geometry of the chromophoric grouping lacks an S_n alternating axis, so that even in isolation; its transitions will manifest optical activity. A typical example for chiral species are dissymmetric chromophores or asymmetically substituted, tetravalent carbon compounds.(Figure 2-1)

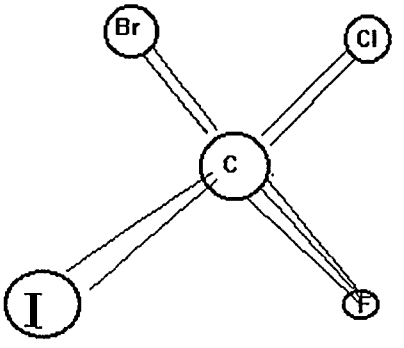

Figure 2-1. The inherently dissymmetric chromophore of carbon.

In terms of rotatory strength (**R**), typical values observed in the visible and near ultraviolet for inherently dissymmetric chromophores on the order of 10^{-38} cgs.

On the other hand, the inherently symmetric chromophore is one where the symmetry of the isolated chromophore is sufficiently high to preclude optical activity. Optical activity is observed only in case of chiral interaction of these symmetric chromophores. As such, the signed magnitudes of the associated rotational strength provide information as to the chemical nature of the molecular environment and its disposition relative to the symmetry planes of the chromophore, whereas inherently symmetric chromophores exhibit rotational strengths that are generally significantly less in magnitude. Mostly, this second case is a major application which would deal with molecular conformation rather than configuration. Whereas the configuration around an asymmetric carbon atom is fixed and can only be altered by the breaking a chemical bond, molecular conformation is less well defined and can change as rotation about single bonds occurs. Molecular conformation may be monitored in optical activity via the coupling of transitions in groups which are arranged in a dissymmetric fashion. One example model of coupling of transition is the "Coupled Oscillator". In that case, CD consists of positive and negative contributions for the coupled transitions. The coupling lifts the degeneracy; thus, produces an absorption spectrum consisting of two overlapping peaks. From the relative magnitudes of the positive and negative CD peaks, the dihedral angle between the groups, on which the transitions are localized, can be deduced.

This last mechanism is mostly responsible for the large CD features of well-ordered polymers, such as peptide α-helices, in which the peptide moieties are arranged in such a manner that their transitions occur in well-predictable geometric patterns. Upon conformational changes of the ordered polymer, for example

during denaturation, significant changes in the CD spectra observed since the geometric order is destroyed or altered.

2.2. THOERETICAL BACKGROUND OF OPTICAL ACTIVITY

A system is called "optically active" if it has the power to rotate the plane of polarization of a linearly polarized light beam. In fact, optical rotation is just one of a number of optical activity phenomena which can all be reduced to the common origin of different response to right and left circular polarized light. Substances that are optically active in the absence of external influences are said to exhibit " natural optical activity". Otherwise, all substances in a magnetic field are optically active. In addition, an electric field can induce optical activity in special situations.

In general, there are two theories that can be followed, based respectively on the theory of oscillators, and the principles of quantum mechanics. Here we only quote briefly results from the quantum mechanics.

The first application of the quantum theory to optical activity was made by Rosenfeld[2-2], and elaborated upon by Condon.[2-3] Moffitt and Moscowitz[2-4] also revised and extended these calculations.

A molecule represented in a system which is not subjected to the action of an external field can presented by the wave function Ψ. The mean value of a variable connected with this system is then given by

$$\langle f \rangle = \int \Psi^* F \Psi d\tau \qquad (2.1)$$

where Ψ^* is the complex conjugate of Ψ and F is the operator connected with the variable under consideration.

A well-known quantum mechanical operator is the energy operator H, called the Hamiltonian. The energy of the system is then:

$$E = \int \Psi^* \mathrm{H} \cdot \Psi d\tau \tag{2.2}$$

Any measurable property of a molecule can be expressed as:

$$B_{0\to F} = \left| \left\langle \Psi_0(q,Q) \middle| \hat{B} \middle| \Psi_F(q,Q) \right\rangle \right|^2 \tag{2.3}$$

Here, $\Psi_{0 or F}(q,Q)$ are the wave functions of the initial and final state of a transition; q and Q are the electron and the nuclei coordinates respectively. The $\boldsymbol{B}$ is the operator of the desired property. For the total absorption of the molecule in electric field:

$$A_{0\to 1} = \frac{1}{2\pi \mathrm{h}^2 \nu^2} \left| \left\langle \Psi_1(q,Q) \middle| \sum_j \frac{e_j}{m_j} e^{i\bar{k}\cdot\bar{r}_j} \cdot \bar{\varepsilon}_U \cdot \bar{p}_j \middle| \Psi_0(q,Q) \right\rangle \right|^2 \tag{2.4}$$

Here, e_j and m_j are the electric charge and mass on the jth particle, respectively. $\bar{K}$ is the light wave vector, $\bar{K} = (2\pi\nu/c)\bar{\varepsilon}_k$. $\bar{\varepsilon}_K$ *and* $\bar{\varepsilon}_U$ are the unit vectors in the propagation direction and the polarization direction of light respectively, and $\bar{p}_j$ is the linear momentum of the jth particle.

The operator $e^{i\bar{K}\cdot\bar{r}_j}$ can be expanded into a converging Taylor series since $\bar{K}\cdot\bar{r}_j << 1$.

$$e^{i\bar{K}\cdot\bar{r}_j} = 1 + i\bar{K}\cdot\bar{r}_j - 0.5(\bar{K}\cdot\bar{r}_j)^2 + \cdots \tag{2.5}$$

The first terms in Eq.(2.5) produces the electric dipole transition moment, μ

$$\mu_{e(0\to1)} = \langle \Psi_1 | \bar{\mu} | \Psi_0 \rangle \tag{2.6}$$

$$\bar{\mu} = \sum_j e_j \bar{r}_j \tag{2.7}$$

where the second term is:

$$\left\langle \Psi_1(q,Q) \left| \sum_j \frac{e_j}{m_j} (i\bar{K}\cdot\bar{r}_j)(\bar{\varepsilon}_U \cdot \bar{p}_j) \right| \Psi_0(q,Q) \right\rangle \tag{2.8}$$

Since $\bar{K} = (2\pi\nu/c)\bar{\varepsilon}_K$, equation (2.8) becomes:

$$2\pi i\nu \left\langle \Psi_1(q,Q) \left| \sum_j \frac{e_j}{m_j} (\bar{r}_j)_K (\bar{p}_j)_U \right| \Psi_0(q,Q) \right\rangle \tag{2.9}$$

This integrate actually contains two terms: the magnetic dipole moment, ***m***:

$$\begin{aligned} m_{(0\to1)} &= \langle \Psi_1 | \bar{m} | \Psi_0 \rangle \\ \bar{m} &= 0.5 \sum_j (\bar{r}_j{}^x \bar{p}_j)_{KxU}{}^* \end{aligned} \tag{2.10}$$

and electric quadrupole transition moment, Θ:

$$\Theta_{0\to 1} = \langle \Psi_1 | \bar{q} | \Psi_0 \rangle \tag{2.11}$$

$$\bar{q} = 0.5 \sum_j \left[\left(\bar{r}_j \bar{p}_j \right)_{KU^*} + \left(\bar{r}_j \bar{p}_j \right)_{U^*K} \right] \tag{2.12}$$

In regular absorption, Θ is small and can be ignored. Therefore, the total absorption of the molecule is:

$$A_{0\to 1} = \frac{4\pi^2 \nu}{\eta c} n \sum_f G_f(\bar{\nu}) \left| \bar{\varepsilon}_{U^*} \cdot \mu_{e(0\to 1)} + (\bar{\varepsilon}_K x \bar{\varepsilon}_{U^*}) \cdot \mu_{m(0\to 1)} \right|^2 \tag{2.13}$$

Here, $G_f(\nu)$ is a band shape function; n is the number of molecules per cm^3, n= CN/1000. N is Avogadro's number.

When the square (dot product) in the equation (2.13) is evaluated, it is composed of three significant terms. If unpolarized light passes through an isotropic solution, the total absorption will involve with the first term in (2.13) only, which is due to the electric dipole transition moment. This is called the dipole strength:

$$D = \left| \mu_{e(0\to 1)} \right|^2 = \mathrm{Re} \langle \Psi_0 | \bar{\mu} | \Psi_1 \rangle \cdot \langle \Psi_1 | \bar{\mu} | \Psi_0 \rangle \tag{2.14}$$

If circularly polarized light passes through an isotropic sample, the total absorption of molecules will involve all three terms in (2.13). They actually are composed of two part: a real and an imaginary part. The latter gives the information about optical activities of both molecules and light beam present. In regular cases, the second component of imaginary part is small and can be ignored. The first imaginary component is the cross term between $\mu_{e(0\to 1)}$ and $\mu_{m(0\to 1)}$, that gives rise to the molecular optical activity called rotatory strength R:

$$R_i = \mathrm{Im}\left[\langle \Psi_0 | \mu_i | \Psi_1 \rangle \cdot \langle \Psi_1 | m_i | \Psi_0 \rangle\right] \tag{2.15}$$

From quantum chemistry, one can derive the following relationship:

Dipole strength:

$$D = \left|\mu_{e(0\to 1)}\right|^2 = \mathrm{Re}\langle \Psi_0 | \bar{\mu} | \Psi_1 \rangle \cdot \langle \Psi_1 | \bar{\mu} | \Psi_0 \rangle = \frac{2.303x3hc}{8N\pi^3} \int \frac{\varepsilon(\bar{\nu})}{\bar{\nu}} d\bar{\nu} \tag{2.16}$$

The second part of this equation can be derived from statistical thermodynamics. The integration represents the area under an absorption peak corresponding to one electronic transition.

The rotational strength, R, is a unique quantity observed in CD, that accounts for the interaction between the electronic transition and the magnetic transition.

$$\begin{aligned} R_i &= \mathrm{Im}\left[\langle \Psi_0 | \mu_i | \Psi_1 \rangle \cdot \langle \Psi_1 | m_i | \Psi_0 \rangle\right] \\ &= \frac{2.303x3hc}{32N\pi^3} \int_{band} \frac{\varepsilon_L(\bar{\nu}) - \varepsilon_R(\bar{\nu})}{\bar{\nu}} d\bar{\nu} \\ &= 2.297X10^{-39} \int_{band} \frac{\varepsilon_L(\bar{\nu}) - \varepsilon_R(\bar{\nu})}{\bar{\nu}} d\bar{\nu} \end{aligned} \tag{2.17}$$

Here, $\varepsilon_L(\bar{\nu}), \varepsilon_R(\bar{\nu})$ are the molar absorptivity due to the left and right circular polarized light (CPL) respectively. Thus circular dichroism measures the absorption difference between left and right CPL of molecules. The optical activity of molecules can be characterized by a dissymmetric factor, or anisotropy (g), which is defined by:

$$g = \frac{\Delta\varepsilon(\bar{\nu})}{\varepsilon(\bar{\nu})} = \frac{\varepsilon_L(\bar{\nu}) - \varepsilon_R(\bar{\nu})}{0.5[\varepsilon_L(\bar{\nu}) + \varepsilon_R(\bar{\nu})]} = \frac{4R}{D} \qquad (2.18)$$

g is a dimensionless quantity. To be more detailed, $\Delta\varepsilon(\nu)$ and $\varepsilon(\nu)$ should be the areas under the respective absorption bands. The latter part of the equation is easily obtained, from equations (2.16) and (2.17). The anisotropy, g, is a characteristic constant which is used to identify a compound and its optical activity.

2.3. Computational Method: Coupled Oscillator Model

To predict the conformation of a molecule in solution, one needs to compare the experimentally observed IR and VCD spectra to calculated ones, which are based on certain theoretical models. There are several methods that have been applied to compute the CD and VCD spectrum of biopolymer. Here we like to introduce the simplest method to calculate a VCD spectrum, called " coupled oscillator model". The pioneers of this work are Moffiit and Tinoco, who started it in the 1950's.[2-5, 6, 7, 8, 9, 10.]

In a biopolymer (protein or DNA), the polar transitions of certain functional group, such as C=O stretching vibration, are arranged by the geometry of the fixed secondary structure of a biopolymer. For example, the C=O amid I transitions aligned almost parallel to the axis of α-helix in peptide. If one vibrational quantum is absorbed by these degenerate oscillators, the resulting vibrationally excited state is best described by sum over all possible one-quantum excitations. This implies that the excitation is no longer localized on one of the oscillators, but is delocalized over the entire array of identical oscillators. This delocalized excitation is referred to as an " exciton"[2-2]. The dipolar coupling

between the transitions lift their degeneracy; consequently, one observes as many discrete exciton energy levels as there are interacting dipoles.

The coupled oscillator model considers the interaction among identical or near identical dipoles. When they are radiated by an appropriate wavelength, the dipoles can oscillate in correlated manner, as if they saw each other instead of independently. For example, the absorption intensity of a dimer is equal to twice the monomer absorption plus a small correction caused by the interaction of the monomers. However, the rotation of a dimer is all due to the monomer interaction, if the monomers are chosen to have no optical rotation. The dimer will also have new energy levels which will affect both the absorption and the rotation. The magnitudes and wavenumbers of the couplet depend on the geometry of the dipoles (direction of dipole and distance between dipoles). However, the coupling is not limited to two dipoles, and can be extended to any number of dipoles (called n-mer) until infinity (polymer).

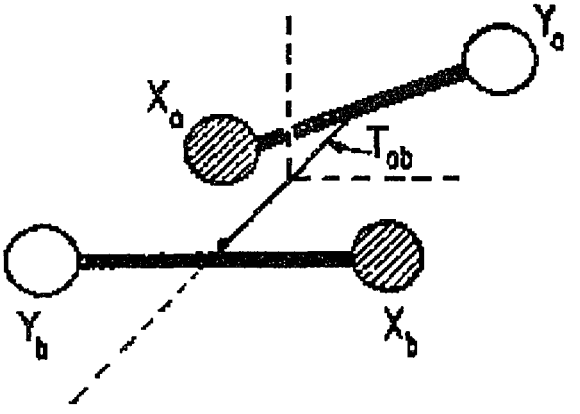

Figure 2-2. An optically active dimer consisting of two identical diatomic molecules X and Y. The vector tab connects the center of mass of monomer A to the center of mass of molecule B

For simplicity, consider a hypothetical, optically active dimer composed of two diatomic, polar molecules, 1 and 2. The distance vector, T_{12}, links the centers of mass of the each dipole. The properties of such a dimer provide useful insight into the behavior of real molecules. Let us consider the ground state and first excited states of monomer 1 $\psi_g^1(q,Q)$ and $\psi_f^1(q,Q)$, with similar function for monomer 2, where q and Q symbolizes electronic and nuclear coordinates respectively. The total wavefunction of the dimer for ground state is:

$$\Psi_g = \psi_g^1(q,Q)\psi_g^2(q,Q) \tag{2.19}$$

Because of degeneracy between the function $\psi_f^1\psi_g^2$ and $\psi_g^1\psi_f^2$, the zero order vibrational excited states of the dimer will consist of symmetrically and antisymmetrically coupled monomer functions. Designating these by Ψ^+ and Ψ^-, one has

$$\Psi^{\pm} = (\psi_f^1\psi_g^2 \pm \psi_g^1\psi_f^2)/\sqrt{2} \tag{2.20}$$

The energies corresponding to the functions Ψ^+ and Ψ^- will generally differ because of coupling between the monomers; this may be viewed as a form of Fermi resonance.

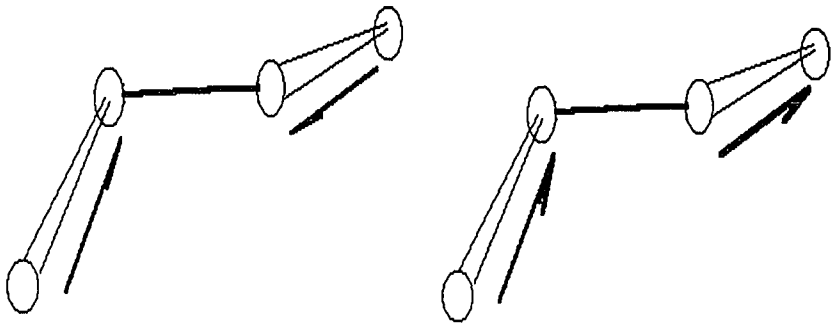

Symmetric Oscillation Antisymmetric Oscillation

Figure 2-3. Oscillation Model of Chromophomers

As mentioned above, the infrared optical activity of dimer, i.e. its circular dichroism and vibrationally induced optical rotation, are most succinctly characterized by the rotational strengths R of the vibrational transitions. The rotational strength R of a transition from state g to state f is given by $R = \mathrm{Im}(\mu_{gf} \bullet m_{fg})$ where μ_{gf} is electric transition dipole moment for the transition g to f and m_{fg} is the magnetic transition dipole moment for transition f to g. Thus, in order to evaluate the rotational strength R_+ and R_- for the transitions $\Psi^0 \rightarrow \Psi^+$ and $\Psi^0 \rightarrow \Psi^-$, we need to evaluate the electric and magnetic dipole moments of these transitions.

For the dimer or two coupling dipoles,

$$D_{\pm} = \mu^2 \pm \bar{\mu}_1 \cdot \bar{\mu}_2 \tag{2.21}$$

$$\begin{aligned} R_{\pm} &= \pm(\pi\bar{\nu}_0 / 2c)(\bar{T}_{1,2} \cdot \bar{\mu}_1 x \bar{\mu}_2) \\ &= \pm(\pi\bar{\nu}_0 / 2c) R\ \mu^2 \sin\phi_1 \cos\theta_2 \end{aligned} \tag{2.22}$$

θ, ϕ give the orientation of μ in spherical coordinate system. Notice that:

$$\nu_{\pm} = \nu_0 \pm V_{1,2} \tag{2.23}$$

$$V_{1,2} = \frac{\overline{\mu}_1 \cdot \overline{\mu}_2}{\left|\overline{T}_{12}\right|^3} - \frac{3(\overline{\mu}_1 \cdot \overline{T}_{12})(\overline{\mu}_2 \cdot \overline{T}_{12})}{\left|\overline{T}_{12}\right|^5} \tag{2.24}$$

$$D_+ + D_- = 2D = 2\mu^2 \tag{2.25}$$

$$R_+ + R_- = 0 \tag{2.26}$$

$$\nu_+ + \nu_- = 2\nu_0 \tag{2.27}$$

Also the values of D, R, and V_{12} are all proportional to μ^2, the monomer absorption. The rotational strengths $R_{\pm}$ have the worrisome property of becoming large as the distance between monomers increases. However, the actual rotation at any wavelength will approach zero as the distance increases, because ν_+ approaches ν_- rapidly.

Therefore, from those equation, the optical activity of the dimer strongly depends on the orientation of transition moments in the dimer. For example, if one branch is absent, however (this corresponds to parallel moments), then $R\pm = 0$. Also, of course, coplanarity leads to $R\pm = 0$, and colinearity with R_{12} leads to $R\pm = 0$. The latter two conformations have planes of symmetry which preclude optical activity. A special case is the dimer with perpendicular transition moments. Then $R_{\pm} \neq 0$, but there is no splitting ($\nu_+ = \nu_-$), and therefore no rotation.

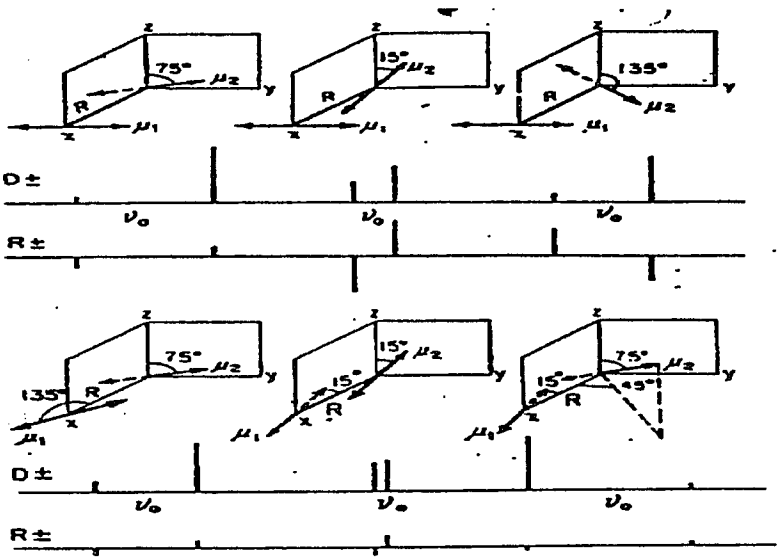

Figure 2-4. The absorption frequencies, dipole strengths and rotational strengths for various dimers. The bond joining the two parts of the dimer R_{12} is along the x-axis and μ_1 is in the xy-plane.

For a system of n coupled dipoles, the kth resultant exciton transition is given by:

$$R_k = -(\pi \nu_0 / c) \sum_{i=1}^{n} \sum_{j>i}^{n} c_{ik} c_{jk} \left[T_{ij} \cdot \mu_i \times \mu_j \right] \tag{2.28}$$

where c is velocity of light, and the c_{ij} are the eigenvector components of the (dipole-dipole) interaction matrix:

$$V_{i,j} = \frac{\overline{\mu}_i \cdot \overline{\mu}_j}{\left|\overline{T}_{ij}\right|^3} - \frac{3(\overline{\mu}_i \cdot \overline{T}_{ij})(\overline{\mu}_j \cdot \overline{T}_{ij})}{\left|\overline{T}_{ij}\right|^5} \tag{2.29}$$

here, T_{ij} is the distance vector between dipoles μ_i and μ_j. ν_0 is the center frequency of the unperturbed transition, and the subscript k refers to the k'th exciton component ($1< k<n$). The infrared absorption intensities can be obtained from the dipole strengths D, defined by:

$$D_k = \sum_{i=1}^{n} c_{ik}^2 \mu_i^2 + \sum_{i=1}^{n} \sum_{j<i}^{n} c_{ik} c_{jk} (\mu_i \cdot \mu_j) \tag{2.30}$$

For near-degenerate vibrational transition, such as certain C=O and C=N stretching vibrations in nucleic acid bases, equation (2.28) needs to be modified as follows:

$$R_k = -(\pi_0 / c) \sum_{i=1}^{n} \sum_{j>i}^{n} c_{ik} c_{jk} \left[(\bar{\nu}_j X_j - \bar{\nu}_i X_i) \cdot \mu_i \times \mu_j \right] \tag{2.31}$$

In this " nondegenerate extended coupled oscillator (NECO)" equation, the X are the coordinates of the center of mass of an oscillator. If $\nu_i = \nu_j$, Eq. (2.31) simplifies to the DECO expression presented in Eq. (2.28).

The computations of dipole and rotational strengths for the polymers are carried out using cartesian coordinates of the C and O atoms of the various carbonyl groups on the purine and pyrimidine bases or the peptide linkages. Furthermore, the transition frequency ν_0 of an unperturded carbonyl transition is needed, and its monomeric dipole strength D, which is proportional to μ^2. For the conversion between rotational (or dipole) strengths (in esu cm)^2 and the extinction coefficients (in L mol^{-1} cm^{-1}) the approximations

$$D \approx 9.2\mathrm{D} \approx 9.2\times 10^{-39}\, \pi \varepsilon_{max} \mathrm{w} / \nu_0 \tag{2.32}$$

and

$$R \approx 2.3\times 10^{-39}\, \pi\Delta\varepsilon_{max} w / \nu_0 \qquad (2.33)$$

were used. Here w denotes the width of the observed VCD or absorption band. Equations 2.32 and 2.33 hold for Lorenzian shapes; for Gaussian bands, the factor π needs to be replaced by $\sqrt{\pi}$.

Once the geometry of the dipole transition moments is defined, the interaction energies of all dipoles with each other is calculated according to equation (2.29) , and the interaction matrix is diagonalized numerically. The eigenvalues of V_{ij} are the frequency displacements for each of the exciton components from ν_0 and the eigenvector components are used, according to equations (2.29) and (2.30), to compute the rotational and dipole strengths of the exciton components.

Atomic coordinates of the carbonyl groups can be derived from crystallographic data, or from any of a number of molecular graphics program, such as Hyper Chem. To predict the conformation of a molecule in solution, one needs to compare the experientially observed IR and VCD spectra to the calculated ones, and to find a reasonable fit with the observed one. Several results were reported by Diem group [2-11]. In following chapters we will in detail discuss results from such computation in examples of small peptides.

REFERENCES

2-1) Kuhn, W. (1958) *Ann. Rev. Phys Chem.* 9, 417.

2-2) L.Rosenfeld, (1929), *Z. Physik*, 52,161

2-3) E. U. Condon, (1937), *Rev. mod. Physics* 9, 432.

2-4) W. Moffitt and A. Moscowitz, (1959), *J. Chem. Physics* 30, 648

2-5) Moffit, W., (1956) *J. Chem. Phys.*, 25, 467- 78.

2-6)C. W. Duetsche, (1969) *Ann. Rev. Phys. Chem.* 20 407-448.

2-7) Tinoco, I. (1963), *Radiation Research*, 20, 133-39.

2-8) Holzwarth, G. and Chabay, I. (1972), *J. Chem. Phys.* 57, 1632-1635.

2-9) T. R. Fraulkner (1977) *J. Chem. Chem. Soc.* 99, 8160-8168.

2-10) C. Marcott (1977) *J. Am. Chem. Soc.* 99, 8169-8175.

2-11) Birke, S. S. and Diem, M. (1992) *Biochemstry* 31, 450-455.

CHAPTER THREE

INSTRUMENTATION AND MEASUREMENT OF VIBRATIONAL CIRCULAR DICHROISM

In this chapter we will discuss the instrumentation and measurement method of vibrational circular dichroism. The detailed principles and design details of the instruments have been reported in the literature.[3-1, 2, 3] Thus, we like only to concentrate on the key points in VCD measurements, for example: the principle of photoelastic modulator and the electronics of dispersive VCD.

Although VCD was first reported nearly two decades ago in 1974, [3-4] progress in the field has been slow, and observation of VCD in the mid-infrared region (5 to 10 nm , or 2000 to 1000 cm^{-1}) from aqueous solution has not been possible until the mid 1980's. Most unfortunately, the number of research groups involved in this area has remained constant, at best, or even decreased somewhere, due to the difficulties in constructing the necessary equipment, which is not yet commercially available.

In the past, VCD was observed by one of two experimental approaches, dispersive or Fourier Transform instrumentation. For biological samples, there are normally no enantiomeric samples available to check for the accuracy of the measurement, dispersive instruments have been used nearly exclusively.

3.1 THEORY AND PRINCIPLES OF THE MEASUREMENT OF VCD

The differential absorbance ΔA, observed in VCD is very small, typically on the order of $5x10^{-4}$ to $5x\ 10^{-5}$ of the infrared absorption A. In order to observe effects of this magnitude, sophisticated modulation techniques need to be employed. Instruments with very high light throughput and extremely sensitive detectors need to be constructed. This is particularly true for the studies of biological molecules via VCD, since water is a necessary solvent for these studies, and the transmission of H_2O or D_2O is low in the infrared spectral region.

For the measurement of differential absorption spectra in the visible and ultraviolet spectral region, a light modulation technique was introduced over two decades ago. The principle of this measurement also governs the measurement of infrared VCD. This technique involves the high frequency modulation of the exciting beam between left and right circular polarization states via a photoelastic modulator, and measuring the differential absorption with a lock-in amplifier tuned the modulation frequency.

3.1.1 Photoelastic Modulator (PEM) and Circular Polarized Light (CPL)

The heart of all chiroptical instruments is the device that produces alternating left and right circular polarized light. In VCD we use a device called photoelastic modulator (PEM). It is based on the phenomenon of stress birefringence to introduce a phase difference between two orthogonally polarized components of light incident on the modulator. The PEM crystal consists of a

uniaxial piece of material which is transparent in the spectral region of interest and is aligned with its unique axis (the Z axis) along the propagation direction of the light.

Under the influence of the mechanical or electrical stress or strain, applied perpendicularly to the propagation direction of the light and along the crystal X or Y axes; the refractive indices along the axes, n_x and n_y become unequal, causing light waves polarized along the X and Y directions to travel with different velocities through the crystal. At the exit face of the crystal circularly polarized light is produced if the retardation between the two orthogonal components of light is $\lambda / 4$ ($\pi/2$).

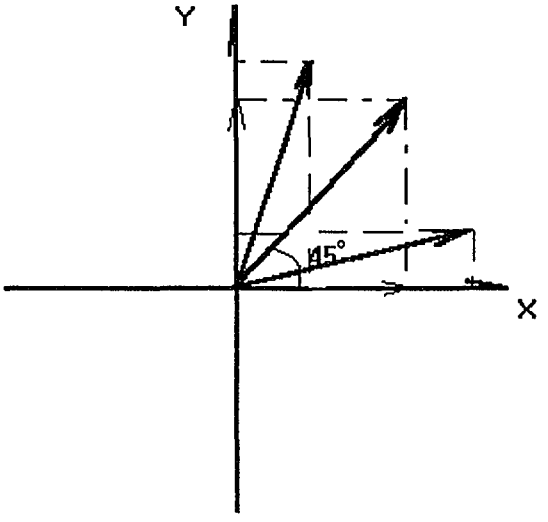

Figure 3-1. Linear polarized light can be decomposed into two components of linear polarized light (LPL) along in x and y axes. Under the strain/stress of PEM, the LPL along with either X axis or Y axis is retarded.

The polarizer axis is set at 45° with respect to the optical axis of the PEM (X axis). As the light reaches the PEM, it is considered a superposition of two linearly polarized waves, one parallel to the X axis, and the other parallel to the Y-axis of the PEM axis (Figure 3-1).

The alternating strain / stress is produced by squeezing the modulator crystal between two piezoelectric drivers. An AC voltage is applied to the piezoelectric crystals, and the amplitude of this voltage determines the stress/strain and therewith, the retardation. Commercial modulators are available for the infrared region, using CaF_2 above 1200 cm^{-1}, and ZnSe down to about 600 cm^{-1} as stress optical materials. The retardation varies sinusoidally at the modulator frequency ω_M, which is determined by the crystal material, and its size. Since the modulation frequency is fixed, the retardation for each individual wavelength depends on the voltage applied to the piezoelectric drivers.(Figure 3-2)

3.1.2 Principles of Vibrational Circular Dichroism

For VCD measurement, the actual differential signal, at constant circular dichroism of the sample, will vary with the light level transmitted at a given wavelength. Denoting the signal at modulator frequency as I_{AC} (ν), and the overall transmission of the instrument and the sample as I_{DC} (ν), it can be shown from an analysis of the radiant energy at the detector, the electronic output of the detector is proportional to the time averaged intensity. The intensity is:

$$I = 0.5E_0^2\left\{[1+\sin\alpha]10^{-A_+(\nu)} + [1-\sin\alpha]10^{-A_-(\nu)}\right\} \qquad (3.1)$$

$$I = I_{DC}(\nu) + I_{AC}(\nu) \qquad (3.2)$$

Only the ratio of I_{AC} (ν) over I_{DC} (ν) is of importance to a dichroism measurement.

$$I_{AC}(\nu) / I_{DC}(\nu) = \tanh(1.15\Delta A)\sin\alpha \qquad (3.3)$$

Here, α denotes the retardation between two linearly polarized components of light used for the production of circularly polarized light, and equation (3.3) demonstrates that the ratio I_{AC} (ν) / I_{DC} (ν) is proportional to ΔA. The term sin(α) itself varies sinusoidally with time, since the retardation α may be rewritten as

$$\alpha = \alpha_0 \sin (\omega_M t) = \alpha_0 \sin (2\pi f_M t) \qquad (3.4)$$

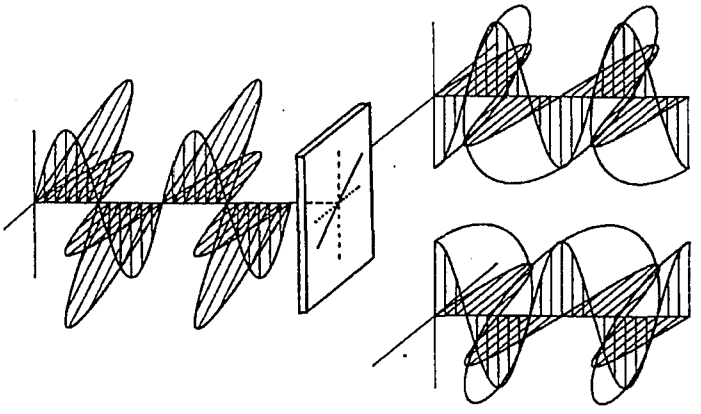

Figure 3-2. The circular polarized light. a) left polarized light; b) right polarized light.

Here, ω_M is the oscillation frequency of the modulator. The sine of a sine function may be expressed in terms of the Bessel function, $J_1(\alpha)$. Thus,

$$I_{AC}(\nu)/I_{DC}(\nu) = \tanh(1.15\Delta A(\nu))J_1(\alpha_0)\sin(2\pi f_M t) \qquad (3.5)$$

where $J_1(\alpha_0)$ is the first order Bessel function. Obviously, α_0 is chosen to have the maximum $J_1(\alpha_0)$ for a maximum observable signal; therefore, $\alpha_0 = 1.84$. Equation (3.5) becomes,

$$\begin{aligned} I_{AC}(\nu)/I_{DC}(\nu) &= 2(1.15\Delta A(\nu))J_1(1.84) \\ &= 2 \text{ x } 0.5819 \text{ x } 1.152\ \Delta A(\nu) \\ &= 1.340\ \Delta A(\nu) \end{aligned} \qquad (3.6)$$

The term $\sin(2\pi f_M t)$ disappears because the output of the lock-in amplifier, tuned to f_M, is a direct current (DC) signal proportional to the amplitude of the sine $(2\pi f_M t)$ term. Thus, by taking the ratio of $I_{AC}(\nu) / I_{DC}(\nu)$, the VCD spectrum, $\Delta A(\nu)$, is acquired rather simply. This ratio-taking process is called normalization of $I_{AC}(\nu)$.

Inspection of equation (3.6) yields that for the observation of ΔA, a signal in phase with ω_M must be monitored via a lock-in amplifier and continuously divided by the DC signal. Here, the $I_{DC}(\nu)$ should be due to an absorption of the functional group which contributed to $I_{AC}(\nu)$ rather than the total absorbency.

3.2. THE DOUBLE MODULATION AND A PHASE SENSITIVE DETECTOR

As mentioned before, the difficulty for VCD is that the differential absorption ΔA is very small. A special electronic techniques, double modulation and phase-sensitive detection via lock-in amplifiers, is employed to extract the small signal out of noise level that is much larger.

The intensity of polarization components is described in Figure(3-3). The PEM works at 31.2 kHz with λ /4 retardation time. The shape of modulation voltage is a regular sine function. Ahead of the PEM, a polarizer is set up to produce linear PL oriented at 45° with modulator axis. The linear polarized light consist of two components (X and Y). During the first half period (0-180°) of modulation, the positive voltage is applied to the crystal. Right CPL is produced and reaches a maximum when the voltage is maximum. During the second half period (180°-360°) of modulation, a negative voltage is applied to the crystal. Left CPL is produced and a maximum left CPL is reached at minimum of modulation voltage. The retardation of the crystal is controlled by adjusting the amplitude of voltage applied to crystal. The right and left CPL have same intensity and the phase difference between them is 180° . When the applied voltage is zero, the light is still linear polarized. At this point the total light intensity is constant and is equal to $I_{DC}(\nu)$; $I_{AC}(\nu)$ is equal to zero. It is shown at (a) in Figure 3-3. Because the absorption coefficients of a chiral sample toward right CPL and left CPL are different, the intensities of right and left CPL become different after

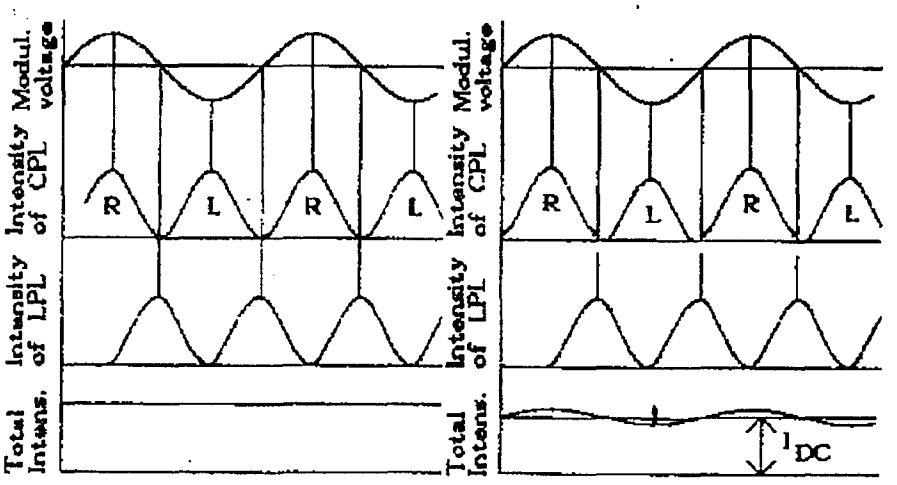

Before Sample After sample

Figure 3-3. Intensity of R, L and linear polarized light components during cycle before and after sample.

sample. The total intensity of light, I_{DC} (ν), depends on the absorption of sample. At that time, the difference between the right and left CPL $I_{AC}(\nu)$ is not zero any more and depends on the difference between the intensity of right and left CPL and has same frequency as that of modulation voltage.

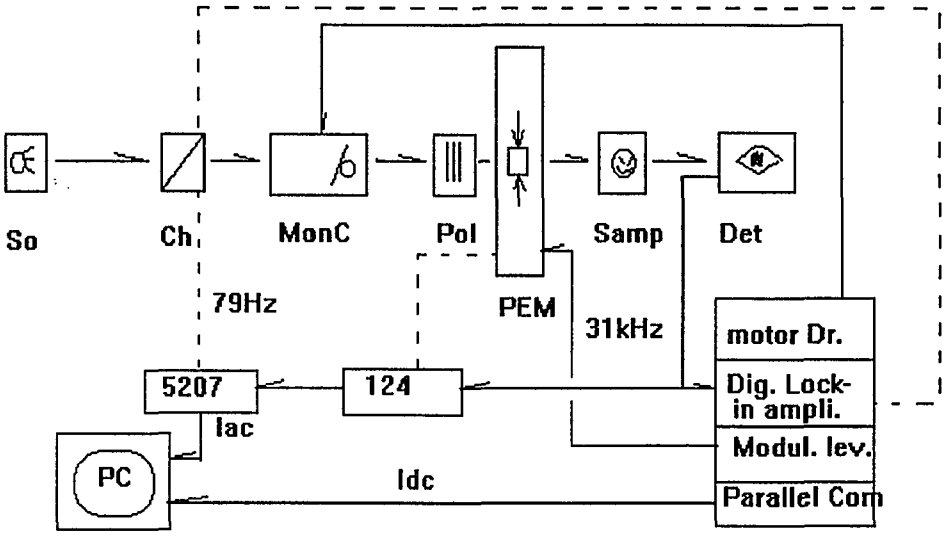

Figure 3-4. Electronic schematic of the infrared dichrograph. So: source of infrared; Ch.: chopper; Monc.: monochrometor; Pol.: polarizer set at 45°; PEM.: photoelastic modulator; Samp.: sample; Det.: detector.

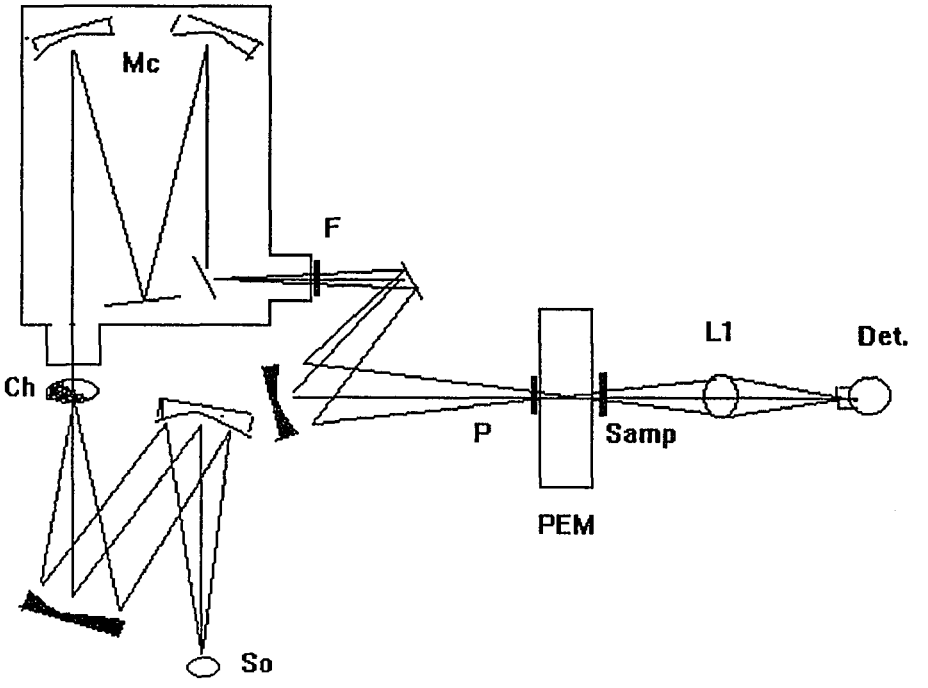

Fig. 3-5. Optical schematic of the dispersive infrared dichrograph. So: source; Ch: chopper; Mc: monochromator; F: filter; P: polarizer; L1: lens; Det: detector.

REFERENCES

3-1.L. A. Nafie (1976), *J. Am. Chem. Soc.* 98 2715.

3-2) L.A. Nafie and M. Diem (1979), *Accts. Chem. Res.* 12, 296.

3-3) L. A. Nafie and M. Diem (1979) *J. Am. Chem. Soc.* 101, 496.

3-4) G. Holzwearth (1974) *J. Am. Chem. Soc.* 96, 252.

3-5) M. Diem,. (1988), *Appl. Spectr.* 42, (1) 20-27.

3-6) O. Lee and M. Diem, (1992) *Analy. Instr.* 20(1) 23-43.

3-7) M. Diem, (1992), *SPIE Proceedings* 1681, 67-78.

CHAPTER FOUR

ARTIFACTS IN AND OPTIMIZATION OF DISPERSIVE VCD

Artifacts, or spurious signals are common problems in any optical activity measurement. They have limited application of VCD in peptide structural studies. Artifacts in dispersive VCD can be from both hardware, such as design and alignment of optical parts in the light path of VCD, and software problems, such as data processing methods. Sources of artifact in dispersive VCD are discussed in this chapter. A new data processing method employed can efficiently reduce system artifacts in VCD measurement, particularly for a sample which has a weak ellipticity.

4.1. INTRODUCTION

Essentially all measurements of circular dichroism (CD) are made by use of modulation spectroscopy techniques.[4-1] The polarized state of the light beam is modulated by either an electro-optic or photoelastic modulator.[4-2-6] Differential absorption of left- and right-circular polarized light then produces a flux variation

at the modulation frequency, which is detected by the phase-sensitive detection technique.

The sensitivity of a CD experiment depends on a variety of obvious factors such as the amount of light transmitted by the apparatus, and the detector's sensitivity. It also depends on the magnitude of spurious signals that can arise from nonideal polarization properties of the optical components. Incomplete polarization by the polarizer, birefringence of modulators, samples, windows, lenses, and mirrors, together with the polarization sensitivity of the detector, can create pseudo-CD signals or modify the magnitude of the true CD signal. For attainment of optimum CD sensitivity and accuracy, it is important to minimize such effects.

Generally speaking, the effects of spurious signal must be viewed with respect to the real CD signal from an optically active sample. For instance, the real signal from ECD is much stronger than that from VCD. So the artifact effect in ECD is less important and can be ignored. But in VCD, since its ellipticity of sample is much weaker, in order to reach better signal / noise ratio, the concentration of sample has to be high. Such a high concentration is a potential factor for the observation of artifacts.

Spurious signals in a system can be defeated by reducing the number of optical elements and carefully choosing and aligning all optical components. However, techniques for reducing them further are highly desirable. Several methods to optimize VCD instruments were reported by other research groups. For example, Nafie[4-7] suggested that a second photoelastic modulator can be used immediately after the sample to reduce artifact in VCD. Keiderling [4-8] used a high

quality lens after the sample, instead mirrors in the light path, to eliminate spurious signals in his FT-VCD.

In this chapter we will discuss sources of artifacts in VCD and methods to reduce these spurious signals by careful alignment of optical parts in dispersive VCD. To consider artifacts from software, a new calibration method of data processing is employed.

4.2. MATERIALS AND EXPERIMENTAL

The infrared absorption and VCD spectra were collected by broad band, dispersive VCD (VCD-I) in 1500 - 1800 cm^{-1} region. Samples used are poly-L-lysine (PLL), poly-D-lysine (PDL) and poly-DL-lysine (PDLL), as well as acetone.

4.3. ABSORPTION ARTIFACT IN DISPERSIVE VCD

The definition of an artifact or pseudo-CD signal in CD or VCD is a signal in the VCD spectrum that arise from sources other than the optical activity of sample itself. In order to eliminate the effects of pseudo-CD signals from a system, the "real background" spectrum of an instrument, instead that of solvent, should be measured and subtracted from the CD spectrum of a sample. Such a "real background" of the instrument would contain all pseudo-CD signals from system itself. In the case of small molecules and homopolymers, such a "real background" spectrum of system can be obtained by measuring its racemic sample under a

condition identical to measurement of sample. Obviously, the difference between two spectra from a racemic sample and from solvent is the artifact signal from the system.

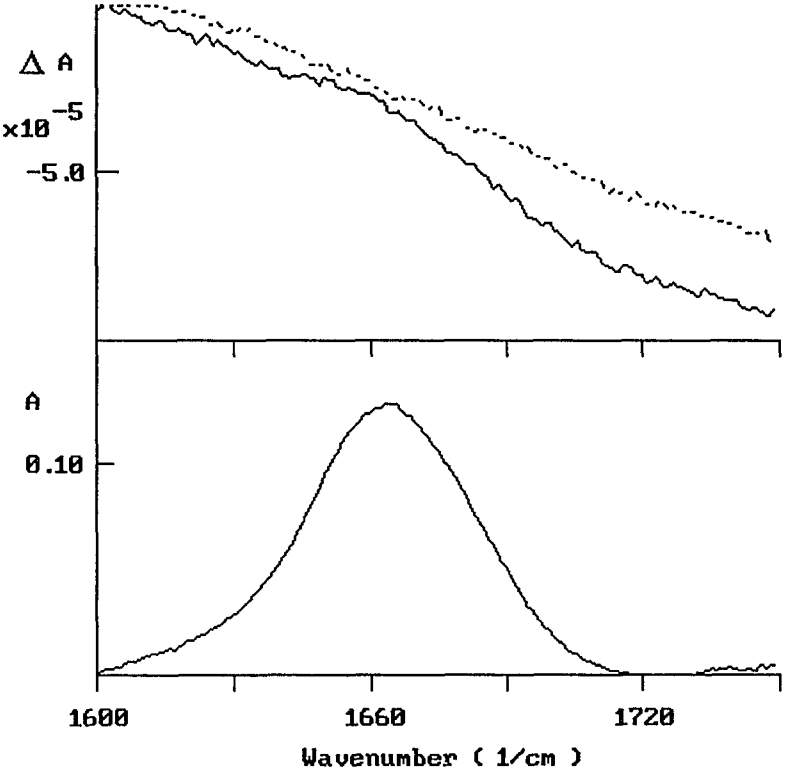

Figure 4-1. Infrared absorption (bottom) and VCD background spectrum (top) from poly DL-lysine in DMSO (solid line), and VCD background spectrum from pure DMSO (dotted line).

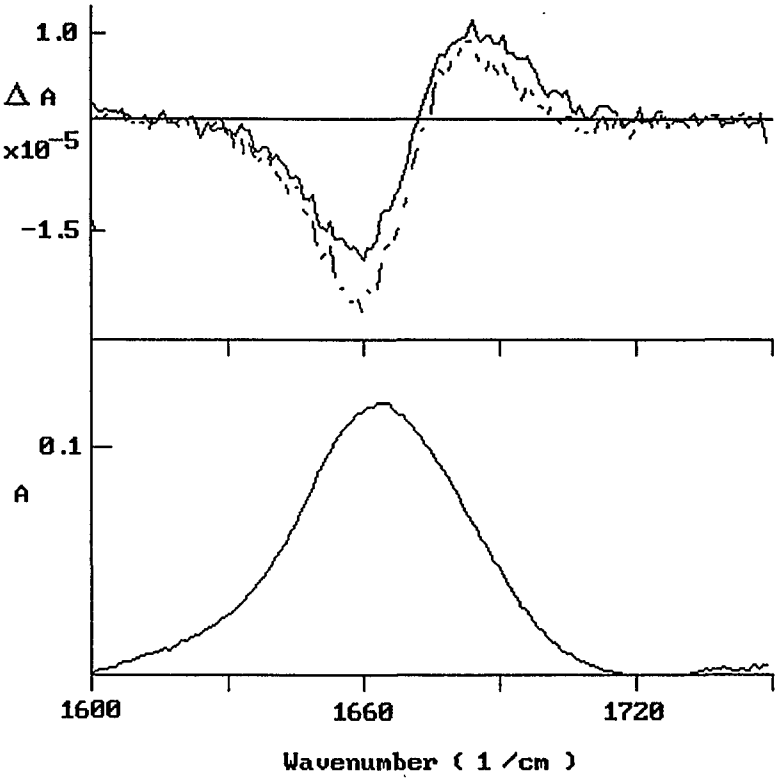

Figure 4-2. The difference between VCD spectra of poly-L-lysine in DMSO subtracted from "realback ground spectrum" (from racemic sample, solid line) and from pure DMSO (dotted line)

Figure 4-1 shows two VCD background spectra from pure solvent DMSO and from poly-DL-lysine in DMSO, respectively. For an artifact free instrument, those two spectra should be identical. Therefore an artifact in the VCD spectrum of the sample can be canceled out by using a spectrum of its racemic sample as the background. Figure 4-2 exhibits the VCD spectra of poly-L-lysine in DMSO, in which a spectrum of solvent and "the real background" from its racemic modification are subtracted from that of PLL, respectively. The different shapes of the background spectra have modified the VCD spectrum of PLL, although PLL has a relatively strong ellipticity.

These artifacts can result from defects in hardware or software, such as data treatment. In fact, it is impossible to have a totally artifact free instrument, because no any optical elements or electronic parts used are perfect.

4.4. THE BEHAVIOR OF ARTIFACTS IN DISPERSIVE VCD

As mentioned before, artifact in an instrument can be checked by comparing VCD spectrum of a racemic sample with a VCD spectrum from solvent used. We found that absorption artifacts can be observed in different ways.

4.4.1. Solvent Dependence of Artifacts

The level of artifacts in the VCD spectra varies with the solvents used. Figure 4-3 shows the observed VCD background spectra of PDLL in DMSO and

in D_2O, respectively. PDLL should not show any optical activity in the amide I region, because it is racemic. Consequently, the spectra shown here are a system artifact. The artifacts in Figure 4-3 exhibit different amplitude depending on the solvent. In D_2O, PDLL induced less of an artifact than in DMSO or other less absorbing solvents. The shapes of two artifact spectra resemble the corresponding absorption spectra. This suggests that the artifact is related to the sample absorption.

4.4.2. Absorbance Dependence of Artifact

Artifact from the VCD instrument does depend on the absorption level of the sample used. Figure 4-4 exhibits the magnitudes of artifacts from PDLL in DMSO at different concentrations. Higher absorption created larger artifacts in ΔA spectrum. The ΔA here is proportional to the concentrations of PDLL and is due to absorption by the carbonyl groups in polylysine.

4.4.3. The Artifact Dependence on Amplitude of Signal From Sample

The observed amplitude of the artifact in the VCD instrument is inversely proportional to the magnitude of the optically active signal of the sample.

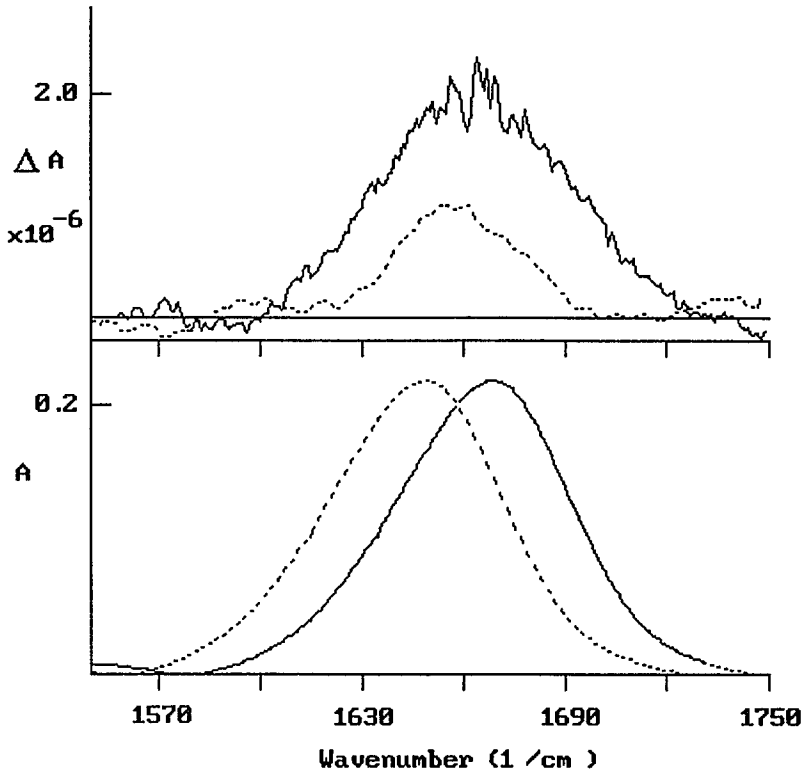

Figure 4-3. The solvent dependence of artifact in VCD-I by using racemic poly-DL-lysine in DMSO (solid line) and D_2O (dotted line), respectively .

Poly-L-lysine can establish well-defined secondary structures under given condition, such as, α-helix , β-sheet and random coil. Its VCD signal is expected to be strong, because all the carbonyls of peptide in those structures align in a certain direction and the total dipole changes are large. Almost all carbonyls in the peptide participate in the dipole-dipole coupling and contribute to the VCD spectrum. In that case the system artifact effect on measurement of VCD is relatively weak and can be ignored. But the artifact from system is still able to interfere with the shape of an observed VCD spectrum, if is measured at a low sample concentration.

By contrast, the turn structures in peptides do not have a unique shape, and only a few carbonyls are involved on this particular structure, and total coupling between carbonyls is relatively weak. Therefore the signal ΔA from carbonyl coupling in β-turns is much weaker than that in α-helix and β-sheets. Therefore, the effect from system artifact, in that case, would have much more contribution to the entire spectrum, especially in low concentration of sample.

For example, we consider the concentration dependent VCD spectra of PLL shown in Figure 4-5. The observed VCD spectrum of poly-L-lysine at a relatively high concentration (18 mg / ml), subtracted from racemic background spectrum, is similar to the spectrum subtracted from its solvent spectrum, with a negative and positive pattern (Figure 4-2). In this case, the system artifact is too small to be considered. With reduction in the concentration of poly-L-lysine, the variations in the spectra become significant, even though they are measured under the same condition and have same conformation. Figure 4-5 shows that with reducing the concentration of poly-L-lysine to 6.25mg / ml, the artifact created a

negative pattern in VCD spectrum of PLL at high frequency region, if VCD spectrum of PLL is directly subtracted from its solvent spectrum. This means that the artifact effects become a dominant factor, when the real signal from sample is getting weak.

Furthermore, defects in optical part also can generate spurious signals in a VCD spectrum. In general, the background curve from solvent of VCD (I_{AC} / I_{DC}) should be a straight line. Figure 4-6 shows the differentiation between background spectra from a regular lens and a cracked lens, respectively. Of course, such a system error can be eliminated by subtracting the solvent spectrum from sample spectrum. But it is only successful for a system that has a large signal amplitude from the sample. Such a defective lens can cause enormous changes on the spectrum of both background and sample. Obviously, it is difficult to obtain a correct VCD spectrum by using such a cracked lens, particularly in the case of the weak VCD signal. Finally, lower amplification of detector or electronics exhibit much less artifact.

To sum up the phenomenon of artifacts in VCD measurement, it appears that the artifacts impose limitations on the application of VCD. Essentially, the range of concentration of samples is restricted by the system artifacts. The concentration of samples should be neither too high (larger than 0.3 absorbency unit) nor too low (below 0.1 absorbency unit). This limitation would bring inconvenience for its application to biomolecules. For instance, DNA, exhibits weaker VCD than peptides and proteins do. To obtain a good spectrum, a higher sample concentration should be used. The higher absorbance, in turn, will render the observed VCD spectrum more susceptible to artifact.

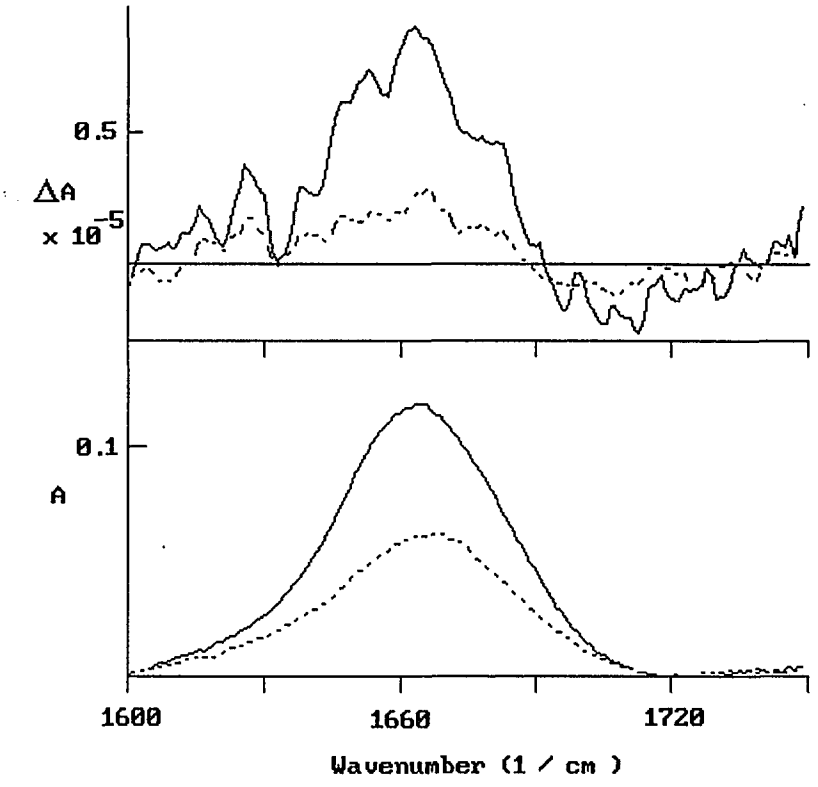

Figure 4-4. The concentration dependence of artifact from VCD-I. The spectra from poly-DL lysine in DMSO at concentration 18 mg/ ml (solid line) and 12 mg/ ml (dotted line)

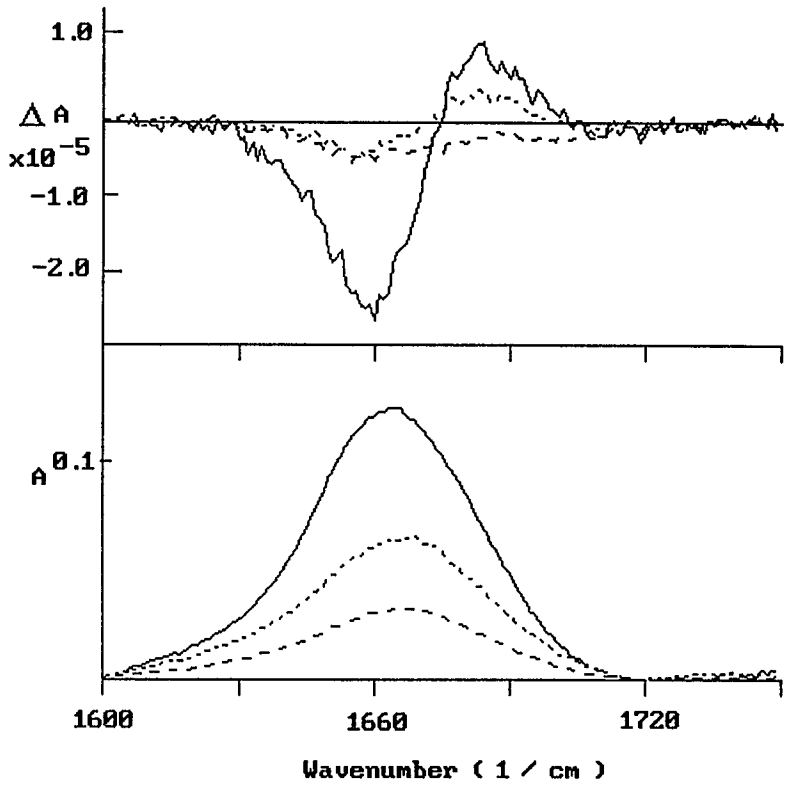

Figure 4-5 The VCD spectra of poly-L-lysine in DMSO were changed with a varied concentration. Concentration are 18 mg / ml (solid line); 12 mg / ml (dotted line); 6.25mg / ml (broken line).

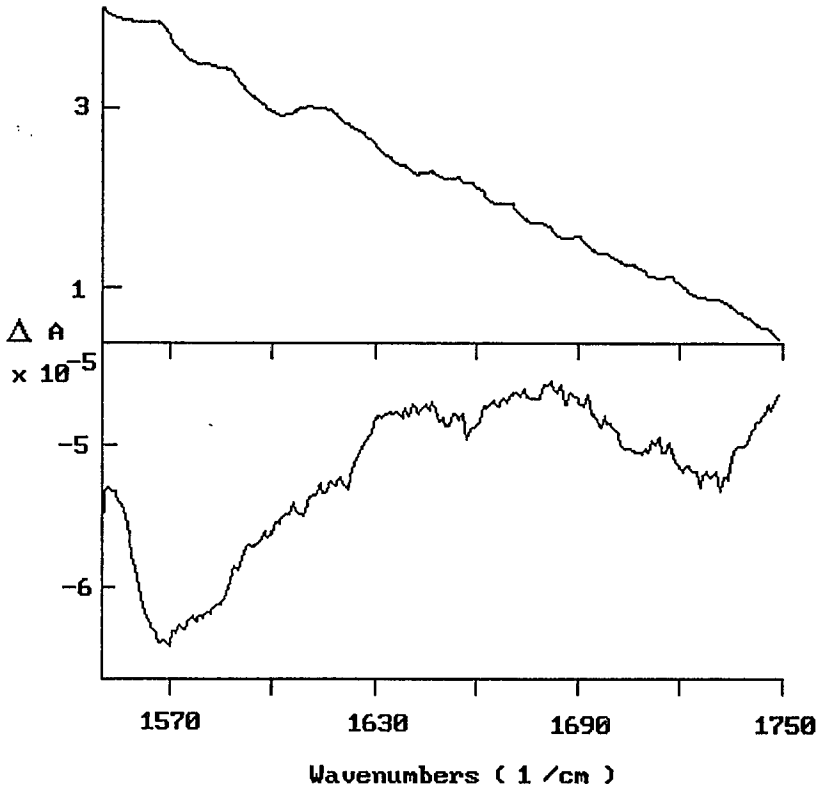

Figure 4-6. The background spectra of VCD-I from new lens (top) and from old, cracked lens (bottom).

Secondly, some solvents can not be used, because they might exhibit more system artifact than others. However, peptides can exist in some interesting conformations in various chemical environments as compared with that in pure water. That will help us to understand the driving force in protein's folding.

Presently, one critical weakness for application of VCD in biomolecular systems is that such a measurement has to be done at a relatively high concentration, because of its small magnitude of ΔA. The concentration used in VCD measurement has been about 10-fold higher than that used for measurement of electronic CD. The high concentration of proteins will create a series of problems, such as aggregation and interaction between molecules. Peptide or protein might alter its conformation due to these interactions. Reducing the concentration, in other hand, decreases the signal/ noise ratio of ΔA, and the system artifacts become a significant factor in VCD measurement. In order to extend the application of VCD, the primary problem is to overcome the absorption artifact from system.

4.5. CALIBRATION METHOD BY USING A RACEMIC SAMPLE SPESTRUM AS VCD BACKGROUND

To eliminate the comprehensive effect from either hardware or software on VCD measurement, the calibration by standard samples is a elegant and simple way to cancel out artifact from instrument. In particular, the subtraction of a background spectrum from the instrument from the ΔA spectrum of the sample is an ideal way to avoid an influence from any artifact in most measurements of

optically active property. Ideally, the background spectrum contains all the artifact from both hardware and software.

One popular means of obtaining such a background spectrum in chiroptical measurements is to use a spectrum from the racemic sample modification as a background spectrum. This background is acquired under measurement conditions identical to that of sample. For a homopolypeptide, such as polylysine, samples of poly-L-lysine and poly-D-lysine as well as its racemic copolymer PDLL are commercial available. But, it is impossible to find racemic samples for polypeptides and proteins or DNA. The standard methods used in VCD measurement for such biomolecules are by subtracting the solvent VCD spectrum from that of the sample, if the system artifacts are minimized. But it is only successful for samples at high concentration having a large ellipticity.

Another method employed by Keiderling is the subtraction of the VCD spectrum of the sample and VCD spectrum of a racemic homopolypepetide, if the two samples have the same or similar absorption peaks. The problem with this method is that the peptide usually has a wider absorption region, because it contains various peptide linkages and more than one peptide conformation. Since a multitude of conformations is involved, the VCD spectrum of such peptide would be more complex than that of homopolymer. Thus, the absorption the homopolymer will not match those from heteropolypeptides.

4.6. SOURCES OF ABSORPTION ARTIFACT IN DISPERSIVE VCD

Previously, it was realized that most of system artifacts in CD or VCD result from the non-ideal polarization properties of the optical components. This is particularly so in the case of an instrument that is misaligned. After carefully choosing the optical parts and realignment, those effects can be minimized. In the case of VCD instruments, there are minor problems after realignment, which can induce an artifact and obstruct we work at low sample concentrations. Those remaining artifact in dispersive VCD are caused by the sample absorbance and the solvent absorbance.

The differential absorbance, ΔA, observed in VCD, is obtained by simultaneously measuring the I_{AC} and I_{DC} and continually dividing I_{AC} by I_{DC}, *cf.* Eq. 3.6. Then, each spectrum obtained from a sample has to be subtracted from a spectrum obtained from background, such as the solvent. This procedure is described in following:

$$\Delta A = \sum \left(\frac{I_{AC}}{I_{DC}}\right)_{sample} - \sum \left(\frac{I_{AC}}{I_{DC}}\right)_{solvent} \qquad (4.1)$$

ΔA here is summation over number of scans. The observed I_{DC} on detector from dispersive VCD can be written as following:

$$I_{DC} = I_0 - (I_{DC_{Sol}} + I_{DC_{C=O^*}} + I_{DC_{C=O}}) \qquad (4.2)$$

$I_{DC_{C=O^*}}$ is the absorption from the optically inactive carbonyls in peptide, $I_{DC_{C=O}}$ is due to the absorption from C=O groups, whose geometry is constrained by a specific structure of peptide. They can interact or couple with each other and produce optical activity. Denoting the total light intensity without sample as I_0, and component due to solvent as $I_{DC_{Sol.}}$.

In the following discussion, we assume that the total absorption of the optically active sample is due to the solvent absorption, the absorption due to optically active amide vibration, and to some C=O or amide intensity not involved in optical activity. We assume there are some peptide linkages with free rotation or no discernible secondary structure.

According to the definition of ΔA in Eq.(3.6), only the third term, $I_{DC_{C=O}}$ in Eq.(4.2) is of interest for the measurement of an optical activity. Therefore, the I_{AC} should be exclusively divided by the change of light intensity from such functional carbonyls ($I_{DC_{C=O}}$) instead by total light intensity change (I_{DC}) in Eq. (4.1). In case of poly-DL-lysine in DMSO, for instance, the $I_{AC_{C=O}}$ should be zero, because PDLL is racemic and does not derive any optical activity from its carbonyl groups. The $I_{DC_{C=O}}$ and $I_{DC_{C=O^*}}$ are the same. The total I_{DC} varied with frequency is due the absorption from solvent and the carbonyl groups, which do not related to the structure of this peptide. If such an I_{AC} is divided by the total I_{DC}, the total ΔA changes with I_{DC}. Therefore, the VCD spectrum has the same shape as the absorption peak. Thus, it becomes clears: why the I_{AC} / I_{DC} from PDLL in Figure 4-1 is not a straight, sloped line like that of the solvent.

This I_{AC} should be only divided by $I_{DC_{C=O}}$ to obtain ΔA. Practically, it is difficult to separate the $I_{DC_{C=O^*}}$ from the term $I_{DC_{C=O}}$. However, the term $I_{DC_{C=O^*}}$ is usually a small portion of the total carbonyl groups in peptides and proteins. But

the first term in Eq. (4.2), I_{DCsol}, may be a significant part in total I_{DC} changes. For example, D_2O has broad absorption peak in the 1600-1630 cm^{-1} region. It causes a lot of change in I_{DC}, compared to the weak signal of I_{AC} from sample.

Table 4-1 I_{AC} / I_{DC} variation with I_{DC} measured at 1660 cm^{-1} with PLL.[a]

I_{DC}	I_{AC} /I_{DC}
0.30	-0.033
0.40	-0.035
0.50	-0.038
0.60	-0.040
0.70	-0.043
0.80	-0.048
0.90	-0.055
1.00	-0.063
1.10	-0.075

a: The voltages of I_{AC} and I_{DC} was measured at 1640 cm^{-1}, at which PLL has maximum ΔA. The light intensity are varied by adjusting the slit of monochromator.

Table 4-2. I_{AC}/I_{DC} variation with I_{DC} measured at 1660 cm^{-1} with PLL (reducing signal to 1/2 amplitude)[b]

I_{DC}	I_{AC} / I_{DC}
0.3	-0.045
0.4	-0.043
0.5	-0.045
0.6	-0.047
0.7	-0.049

b: The voltage divider was connected before Lock-in amplifiers.

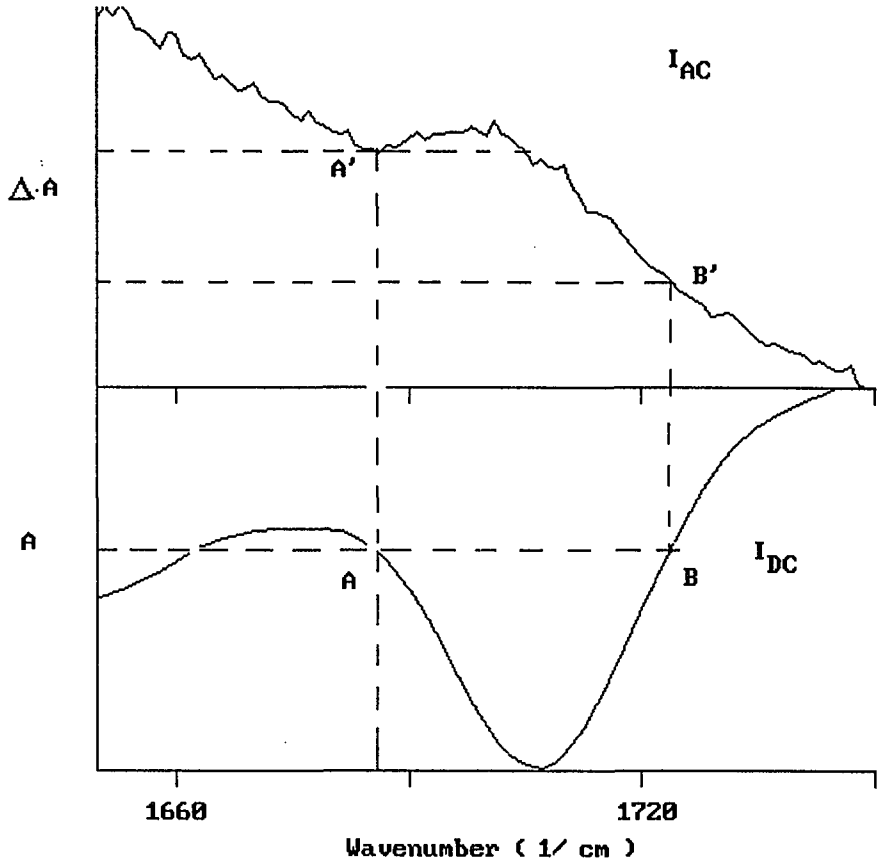

Figure 4-7. The variation of I_{AC} (top) and I_{DC} with wavenumber in VCD-I (Acetone in DMSO).

The observed I_{AC} spectrum in VCD measurement depends on the present light level, and also the ellipticity of amide groups in the peptide. A well-defined conformation will exhibit a strong VCD signal and an ill-defined conformation shows a weak signal. Furthermore, the VCD intensity follows Beer-Lambert law. Thus, ΔA should not change with the intensity of light, because the effect of light intensity on I_{AC} would be canceled out, if I_{AC} is divided by $I_{DC_{C=O}}$. In fact, it is not so. Table 4-1 shows the variation of I_{AC} / I_{DC} with the differences of present I_{DC} . The fact that the ΔA varies with intensity of light must mean that the observed I_{AC} from detector contains other terms, which depends on the intensity of light. The observed I_{AC} in detector of VCD may be composed of:

$$I_{AC} = I_{AC}^{0} - (I_{AC_{C=O}} + I_{AC_{IDC}}) \qquad (4.3)$$

$I_{AC_{IDC}}$ is a term in total I_{AC}, which varies with the I_{DC} or intensity of present light. Such a change is likely due to the nonlinearity of detector and electronics. By using a voltage divider, by which the total signal is reduced to half amplitude of regular one, ΔA is nearly constant with change of light intensity under same measurement condition (Table 4-2). It is apparent that the detector and electronics lost the linearity, if the light intensity beyond a certain level.

Theoretically, the frequency dependence of I_{DC} on the observed I_{AC} can be canceled out, when the observed I_{AC} is divided by the I_{DC} from an absorption of the optically active carbonyl groups. If those carbonyl groups do not show optical

activity, finally, a sloped straight line can be obtained from racemic sample such as PDLL. This is called the normalization. The background, I_{AC}, of the instrument should is a straight, sloped line with a negative slope. The I_{DC} background, from the VCD instrument is a straight line with a positive slop. A sample, which has no optical activity, such as acetone, has an absorption in the carbonyl region. Its absorption is symmetric peak. The observed I_{AC} and I_{DC} from acetone in DMSO are shown in Figure 4-7, respectively. The points A and B show equal light level in I_{DC} curve, but the points A' and B' on I_{AC} curve, corresponding to points A and B on I_{DC} curve, do not have same values. Therefore, directly dividing I_{AC} by I_{DC} would modify the ΔA spectrum.

Thus, those effects should be considered that can induce artifacts from unsuitable data treatment:

1) $I_{AC_{C=O}}$ should be divided by $I_{DC_{C=O}}$ instead total I_{DC}.

2) How to separate the components of I_{DC} to normalize data.

3) How to cancel out the effect of non linearity of the detector and electronics.

4.7. OPTIMIZATION OF DISPERSIVE VIBRATIONAL CD

There are several steps that were employed for reducing absorption artifacts in VCD in the literature. Foremost, it is probably a good idea to reduce the number of optical elements in the light path, at least between sample and detector, to a minimum to reduce the sources of birefringence, and to avoid an effect from any defects in the optical parts used. Second, all optical elements in

light path must be carefully aligned. The basic principle of alignment is that the center of light beam should hit the center of each optical elements and the light distribution after each optical component has to be uniform. In order to do that, the laser beam is a good tool. Two laser beam can be employed in both forward and backward directions, respectively.

In order to eliminate the effect of solvent on I_{DC}, the I_{DCsol} should be subtracted from total I_{DC} before dividing by I_{AC} spectrum of sample. The I_{AC} spectrum from racemic sample, or from solvent, should be first subtracted from the sample I_{AC} spectrum. This procedure is described as following:.

$$\Delta A = \frac{\sum I_{AC\,sample} - \sum I_{AC\,background}}{\sum I_{DC\,sample} - \sum I_{DC\,backgound}} \qquad (4.4)$$

The effects of non linearity of the detector and electronics can be calibrated by putting a sample, which has same absorbance (both frequency and amplitude) as real sample, but does not have optical activity, at sample position. Thus, a corrected background spectrum of instrument can be obtained. It should contain all $I_{AC}/_{DC}$ changes from non linearity of detector and electronics. However, such as a racemic sample does not exist for peptides and proteins.

This problem can be solved by hardware. One can simulate an absorption from a real sample by a computer controlled, light attenuator, which is installed on beam path. This attenuator can trace the intensity changes of light with various frequency in exactly same way as that from real sample. Such an I_{AC} spectrum from the attenuator will be identical to that from its racemic sample. It can serve as a universal racemic sample. This method can be applied in any optical active

measurement. But the complicated electronic system might create other new effects into system.

Based on same idea above, another method was attempted. If one puts the sample in a position in front of PEM, it exposed to regular light instead to CPL. This sample will accurately reproduce the I_{AC} spectrum as that from a racemic sample. In that case, the peptide behaves as if had no optical activity. The ΔA collected here is the background spectrum of instrument. Since it is collected under identical condition as real sample, such a VCD spectrum contains all effects or information from both instrument and sample itself. The artifact are the same as those produced by the sample in a position behind PEM.

Figure 4-8 shows the difference between two background spectra that were obtained by using pure DMSO at regular position and PLL in DMSO on front PEM, respectively. The difference between the spectra of PDLL in DMSO and pure DMSO modify the spectrum of poly-L-lysine, which loses the positive VCD peak in high frequency area at low concentration of sample.(Figure 4-5) After these improvements, the artifact of the dispersive VCD I is much smaller. Figure 4-9 exhibits the difference between VCD spectra of PLL at concentration 6.25 mg / ml in DMSO by using new method and regular one, respectively. Those data were collected under same condition. This is also a piece of evidence that when the signal is getting weaker, VCD spectrum is modified by a system artifact.

The most significant progress in VCD is that VCD spectrum of biomolecules can be measured in any solvents and in low and reasonable concentration. (about 0.05 absorbance units, about 10-20 mM for peptides) Figure 4-10 shows the spectra of VCD from poly-L-lysine in DMSO with various concentrations. Those spectra are treated by the new data processing method. It

is not surprising that the VCD spectrum for poly-L-lysine at lower concentration (6.25 mg / ml) demonstrates the same pattern and ratio of negative and positive part as that from one at high concentration.

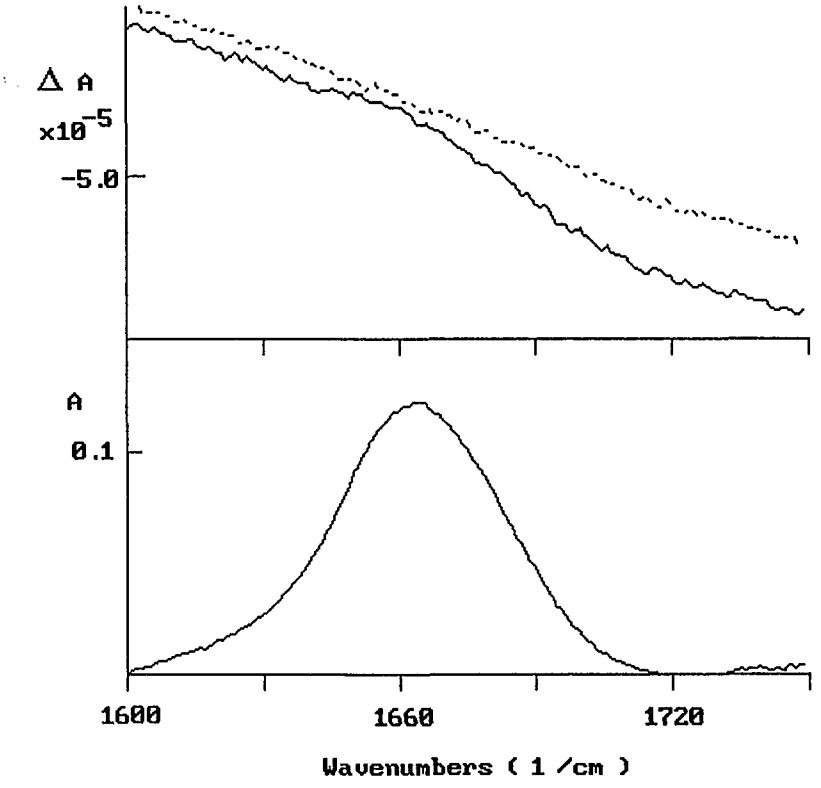

Figure 4- 8. The comparison background VCD (top) from PLL in front of PEM (solid line) and with one from pure solvent in regular sample position (dotted line).

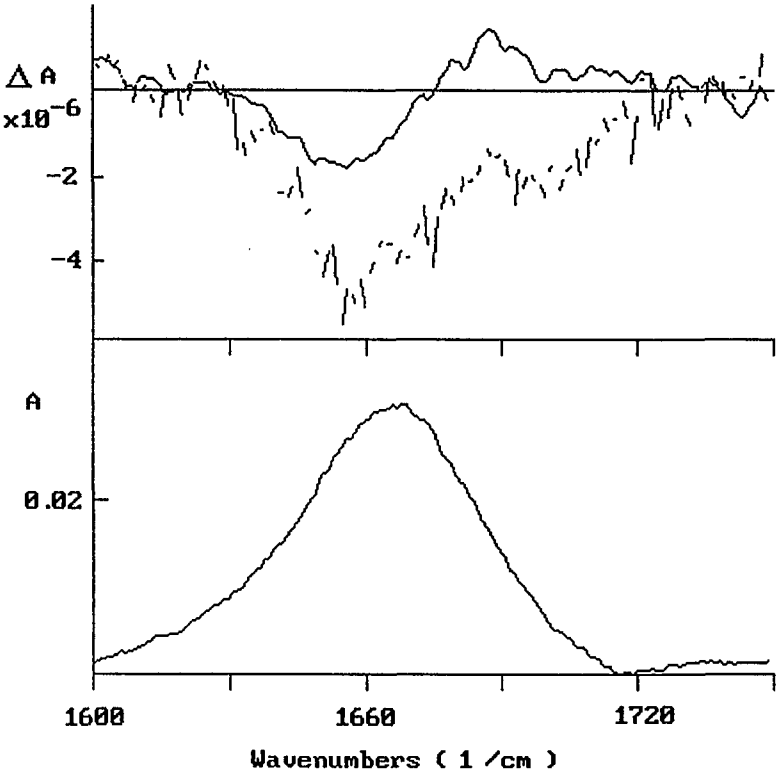

Figure 4-9. The difference of VCD spectra between poly-L-lysine (PLL) in DMSO subtracted from a spectrum of PLL, located in front of PEM (solid line), and from spectrum of pure solvent as background (dotted line).

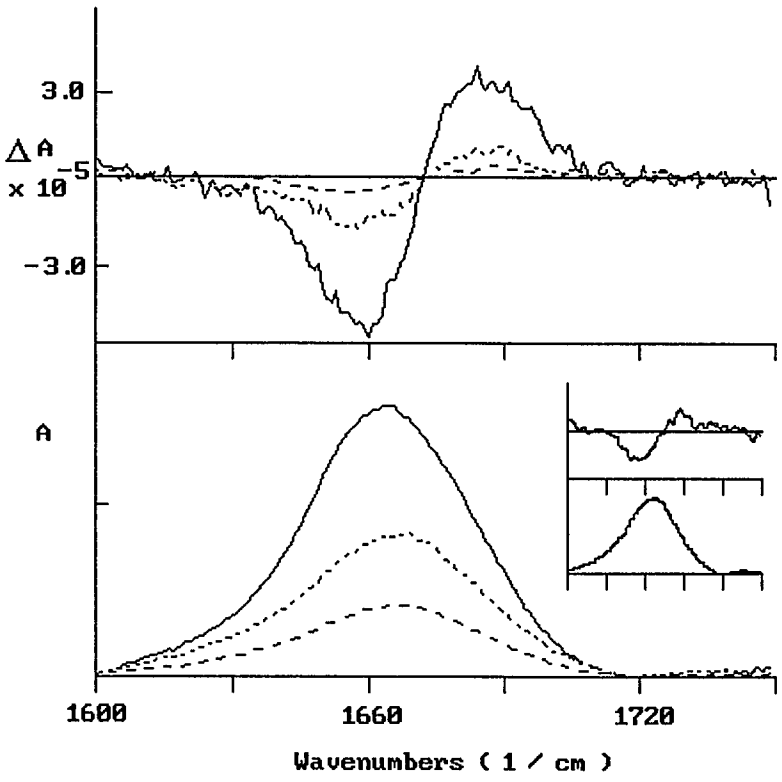

Figure 4-10. VCD spectra of poly-L-lysine at varied concentrations (18 mg / ml (solid line); 12 mg / ml (dotted line) and 6 mg / ml (broken line and small image), which were subtracted from a spectrum of PLL on front PEM. Inset spectrum shows detail spectrum of PLL at lower concentration.

There are two advantages, that results directly from this data acquisition method. First, the procedure of subtracting a background spectrum of I_{AC} and I_{DC} from I_{AC} and I_{DC} of sample, respectively, then dividing this I'_{AC} by a corresponding I'_{DC}, will cancel out the interference of background, such as the contribution in I_{DC} from absorption of solvent. But to offset the influence of non active carbonyl groups is too complicated to be practical. Since they contribute a small portion in peptides, their effects can be neglected. Secondly, the separate cumulation of I_{AC} and I_{DC} leads to a higher signal/noise ratio. Because both I_{AC} and I_{DC} fluctuate individually, the division of such two data increase the amplitude of data fluctuation. However, separately cumulating each data series will smooth the data itself and increase its signal/ noise ratio of I_{AC} / I_{DC}.

4.8. CONCLUSIONS

In retrospect, it is clear why artifacts show up in dispersive VCD and why may depend on the concentration of sample as well as solvent used. Furthermore, it is clear why some detectors produce more artifacts: the non linearity of the detector and electronic devices is a significant factor in VCD measurement. The data treatment is also a partial reason for artifact in dispersive VCD, which people have not realized before. The new data processing method employed here has more significantly improved results from VCD measurement, particularly, for a system that has low ellipticities, such as the carbonyls in β-turn conformation of peptide.

REFERENCES

4-1). L.F. Mollehauer, D. Downie, H. Engstrom, and W. B. Grant. (1969). *Appl. Opt.* 8. 661.

4-2) S.N. Jasperson and S.E. schnatterly. (1969) *Rev. Sci. Instrum.* 40, 761.

4-3) J. C. Cheng, L. A. Nafie, and P. J. Stephens. (1975) *J. Opt. Soc. AM.* 65, 1031-35.

4-4) L. F. Mollehauer, D. Downie, H.Engstrom, and W. B. Grant,(1969), *Appl. Opt.* 8. 661.

4-5) S, N, Jasperson and S. E. Schnatterly, (1969), *Rev. Sci. Instrum.* 40, 761.

4-6) J . C. Cheng, L. A. Nafie, and P. J. Stephens, (1975) *J. Opt. Soc. Am.* 65, 1031-35.

4-7) E. D. Lipp, and L. Nafie (1984), *Appl. Spectr.* 38, 20-26.

4-8) P. Malon and T. A. Keiderling (1988), *Appl. Spectr.* 42, 32-38.

CHAPTER FIVE

CONFORMATIONAL STUDIES OF *cyclo*-(-PRO-GLY-)3 AND ITS COMPLEXES WITH CATIONS BY VIBRATIONAL CD

In this chapter we report VCD and infrared absorption spectra of a cyclic hexapeptide, *cyclo*-(-Pro-Gly-)$_3$ in aqueous and non-aqueous media, and in the presence of a number of mono- and divalent metal cations. *Cyclo*-(-Pro-Gly-)$_3$ was studied previously by CD, Raman and NMR spectroscopies, and its ionophoric properties were recognized.

VCD in the amide I spectral region monitors the relative orientation of amide linkages of the peptide with respect to each other. We find that VCD is an enormously sensitive technique to monitor the conformation of small peptides, and can distinguish more than a dozen different molecular shapes, depending on the ionic strength of the solvent media.

5.1. INTRODUCTION

Infrared or vibrational circular dichroism (VCD) is a relatively new spectroscopic technique[5-1] which bears several advantages over conventional methods used for the determination of peptide solution conformation. Compared with electronic CD, it provides the possibility to monitor the optical activity of a number of specific functional groups, such as the amide linkage, which exhibits a C=O stretching vibration between 1600-1700 cm^{-1}. These amide vibrations undergo dipolar coupling to produce the observed VCD. Since vibrational transition moments are smaller than those encountered in electronic CD (ECD) observed in the UV spectral region, the coupling in VCD extends over shorter distances than in ECD[5-2]. Therefore, VCD is sensitive to short range structural order. This advantage, coupled with the selectivity of vibrational spectroscopy toward different chemical environments, and the high resolution and narrow band widths achievable in vibrational spectroscopy, make VCD a nearly ideal tool to monitor conformational changes of biological molecules. Due to its chiroptical origins, it adds an enormous amount of information to that available from standard vibrational techniques.

Even compared to other structural techniques used previously to study biomolecules, such as X-ray crystallography and NMR and Raman spectroscopy, VCD offers significant advantages. Obviously, it is a solution conformational technique and is therefore free from crystal effects which may distort the shape of molecules. Furthermore, it circumvents the difficulties associated with crystal growth. Compared to NMR spectroscopy, VCD offers the advantages of permitting a qualitative interpretation of spectral changes in terms of structural

changes without requiring elaborate calculations, although quantitative information is available from VCD as well. In addition, there are a number of arguments involving vibrational *vs.* NMR time scale, which are favorable for VCD.

However, one problem persists with the understanding of VCD of biomolecules: it is presently impossible to perform detailed VCD intensity calculations on molecules of the size discussed here. Empirical VCD calculations, to be discussed later, have been carried out for some biological molecules, but they yield best results for molecular systems were the interacting groups exhibit only dipolar and no mechanical coupling. In peptides, however, both dipolar and mechanical coupling, as well as other factors, contribute to the overall VCD intensity.[5-1] Therefore, we restricted ourselves in this paper to a qualitative interpretation of the VCD results, using mostly geometric parameters to assess whether or not dipolar coupling occurs and contributes to the observed VCD intensities.

5.2. PRIMARY STRUCTURAL CONSIDERATIONS

Cyclo-(-Pro-Gly-)$_3$, to be abbreviated CPG3 henceforth, is a model for ion carrier peptides. Its conformations were studied systematically by Blout's group in the 1970's, mostly by NMR and CD spectroscopies.[5-4,5] Raman[5-4] and X-ray data[5-4,5] are available as well. Results from these techniques will be reviewed briefly in the next section.

CPG3 is composed of the two amino acids proline and glycine. Proline has a -$(CH_2)_3$- sidechain linked to the amide nitrogen atom, which makes it a tertiary amide and restricts the conformational freedom about the N-C_α bond .

Thus, incorporation of a proline residue into a peptide sequence reduces the number of possible rotamers. Proline also plays an important role in peptide turns which reverse the direction of the peptide chain. Turns are particularly common when proline is followed by glycine in a peptide. Glycine, which has a H as the side group, can fit into structures where amino acids with large side groups would be excluded.

Proline and glycine exhibit different amide linkages with quite different amide I vibrational frequencies: a Pro-Gly peptide bond contains N as a secondary amide, whereas in a Gly-Pro group, the nitrogen is a tertiary amide. The carbonyl stretching vibration of secondary amide linkage, such as the $C{=}O_{(pro)}$ in Pro-Gly, is observed at 1670 cm^{-1}, whereas the corresponding vibration in a tertiary amide such as Gly-Pro is observed at 1640 cm^{-1}. These frequencies and assignments have been established through studies of model peptides such as Pro-Gly and Gly-Pro by Asher and coworkers[5-5]. The *cis* and *trans* forms of a tertiary (Gly-Pro) amide linkage exhibit nearly the same potential energy, and the corresponding vibrations can be distinguished by the slightly higher amide I frequency of the *cis*-form (about 1650 cm^{-1}). The ability to form *cis*-linkages increases the conformational flexibility of CPG3, for which *cis*-peptide bonds have been found to occur in polar solvents.[5-4]

CPG3 has six carbonyl but only three N-H groups. Even when intramolecular hydrogen bonds are formed, three carbonyl groups can form hydrogen bonds with the solvent, or interact with metal ions. These factors contribute to the conformational variety of CPG3, which is determined primarily by the solvent environment. In most complexes with metal ions, it appears that the three $C{=}O_{(pro)}$ point toward one side of the molecular ring whereas the three $C{=}O_{(gly)}$ groups point toward the other side.

5.3. RESULTS FROM OTHER TECHNIQUIS

The conformations of CPG3 were studied previously by NMR, electronic CD and Raman spectroscopies,[5-6] as well as by X-ray crystallography.[5-7,8] The 3-fold repetition in the primary sequence of CPG3 allows this molecule to form a conformation with 3-fold symmetry under certain conditions. In non-polar solvents, for example, CPG3 exhibits three γ-turns, which are stabilized by intramolecular 1 → 3 H-bonds between the glycine residues. These are chemically equivalent as indicated by the fact that only one N-H proton signal is observed. This symmetric structure is called conformation **S**. In aqueous or polar solvents, on the other hand, some or all intramolecular hydrogen bonds may break, and the tertiary amide linkage of the prolyl groups may assume the *cis*-conformation. Results from crystallography confirm that in crystals grown from polar solvents (methanol : water = 2:1), CGP3 exhibits one *cis*- and five *trans*-peptide linkages. The occurrence of one *cis*-linkage causes a loss of symmetry, and the resulting asymmetric structure is referred to as conformation **A**. This conformation, for which NMR spectroscopy detects three different N-H resonances, also exists in solution.

Because of the alternating Pro-Gly sequence, one can visualize all prolyl and all glycyl carbonyl groups to be located above and below the peptide ring, respectively. Metal ions can therefore bind to two faces, or binding sites, composed of either prolyl or glycyl carbonyl groups. The complexation with cations can move either set of carbonyl groups closer together toward the center of the ring. Several conformations of cation complexes are possible, depending on the solvent medium and the nature of the cation. These can be classified into 1:1

complexes, peptide sandwiches (peptide/metal ion/peptide) or salt sandwiches (metal ion/peptide/metal ion).

X-ray results show [5-7] that CPG3 can form a peptide sandwich with Ca^{2+} ions. Here, calcium binds with only the glycyl carbonyls of two separate peptide molecules. The Ca-O distance is 2.26Å, which is about the same as the length observed between a calcium and the carbonyl oxygen in proteins. CPG3 also can form longer sandwich structures in sodium/calcium containing crystals,. Here, one finds solvent/Na^+/peptide/Ca^{2+}/peptide/ Na^+/solvent structures in which the sodium ion binds to the three prolyl carbonyls which are on the face of the peptide ring not occupied by the calcium ions. With magnesium ions, one finds a 1:1 complex, with the Mg^{2+} ion coordinated to the three glycyl carbonyls as in the case with calcium ions. In addition, three water molecules are found complexed with the magnesium ion. The carbonyl Mg-O distance was found to be 2.03 Å, and the Mg-O distance with the water molecule is 2.11 Å. This complex exhibits 3-fold symmetry.

In solution, NMR results suggest two kind of complexes formed between CPG3 and cations. One of them, called conformation **S1***, is formed by Ca^{2+}, Na^+, and K^+ at 1:1 stoichiometry. In these complexes, the prolyl carbonyl groups are rotated by 80° as compared to the **S** conformation, and form an open cup on one face of the molecule. The rotation of the prolyl carbonyl groups also brings the glycyl carbonyls together to form a similar cup on the other side of the molecule. The other conformation, **S2***, is a salt sandwich formed with magnesium ions only. Thus, the NMR results on complexes formed in solution are quite different from the X-ray results discussed above.

Raman spectroscopy can distinguish the tertiary amide I band of $C{=}O_{(gly)}$ in Gly-Pro at 1651 cm^{-1} and the secondary amide I band of $C{=}O_{(pro)}$ in Pro-Gly at 1677 cm^{-1}. Two bands observed in crystalline CPG3 at 1634 and 1671 cm^{-1}

were assigned accordingly, although the shift of the glycyl carbonyl frequency from 1651 cm^{-1} in Gly-Pro to 1634 cm^{-1} in CPG3 was not explained satisfactorily. In solution in chloroform, the observed frequencies were 1674 and 1641 cm^{-1}, with the latter number very uncertain because proper band analysis was not carried out by the authors.[5-6] In fact, we believe that the Raman data for the uncomplexed peptide, as well as for the peptide/ion complexes, are so strongly influenced by crystal effects that the interpretation presented is questionable.

The Raman data of the complexes were interpreted in terms of the Na^+ and K^+ ions binding to the prolyl carbonyls, because a band attributed to the $C{=}O_{(pro)}$ amide I vibration shifted from 1674 to 1706 cm^{-1}. This band is strong and sharp, with three more Raman bands observed at 1672, 1653 and 1643 cm^{-1}. We contend that the highest frequency peak at 1706 cm^{-1} is due to crystal effects or overtones of the anion vibrations (SCN^-). This is based on a comparison of its intensity with those of other peptide Raman bands, and bands marked with (an unexplained) letter S in Figure 2 of reference 5-6.

Calcium binding was observed for the deuteriated peptide in the solid phase. The amide I' vibrations were observed at 1690, 1656 and 1619 cm^{-1}. The vibrations of the anion used, perchlorate, are very strong and again might contribute overtone and combination bands. Based on the Raman frequency shifts observed for the carbonyl groups, Asher and coworkers[6] concluded that Na^+ and K^+ bind with prolyl carbonyls, and Ca^{2+} binds with glycyl carbonyls. We do not observe in solution phase FT-IR spectra any comparable frequency shifts, and believe that the Raman data are dominated by solid phase artifacts.

5.4. EXPERIMENTAL ASPECT

Experimental details of infrared VCD and absorption data acquisition are discussed in the literature.[5-1] Absorption data were verified at higher resolution using a MIDAC, Inc., M-Series FT-IR spectrometer equipped with a HCT detector. CPG3 was purchased from Bachem Biochemicals, Inc. and used without further purification. However, the peptide was lyophilized from D_2O to exchange the three labile protons to deuterons. The reason for doing so is that VCD spectra obtained from solution in D_2O are naturally those of the deuteriated peptide linkage. Thus, in order to avoid problems of comparing deuteriated peptide linkages in D_2O and protonated linkages in other solvents, only deuteriated peptide samples were used. Consequently, our reported frequencies are those of the amide I' vibration, which is about 10 - 15 cm^{-1} lower than the corresponding amide I frequencies reported in the Raman data.

The solvents, DMSO, $CDBr_3$, D_2O and ethanol-d_1 were obtained from Sigma Chemical Co., respectively, and were used after distillation. All salts utilized were the chlorides, and were obtained from Sigma Chemical Co., as well.

The visualization of molecular shapes, and the determination of the distances and the geometry of the prolyl and glycyl carbonyl groups, were carried out using the program HyperChem (SciVision, Inc., Lexington, MA) operating on a desktop computer equipped with a 90 MHz Pentium processor.

5.5. RESULTS

In the following section, the observed VCD spectra of CPG3 and its complexes with metal cations will be presented. These spectra will be interpreted qualitatively in terms of the dipolar coupling mechanism used before by us and others to describe the origin of VCD features. Previous comparisons of observed and computed VCD intensities have demonstrated that dipolar coupling provides a significant portion of the observed VCD intensity, but that other mechanisms may contribute as well. However, to fully exploit the conformational information contained in VCD, intensity calculations at the *ab initio* level need to be carried out.

Although it is anticipated that such calculations will become practical for a molecule of the size of CPG3 in the future, it is presently impossible to carry out the numerous calculations necessary to interpret the observed spectral data, considering the large number of different structures and environments studied. We feel that empirical VCD calculations, on the level of the non-degenerate extended coupled oscillator (NECO) model, may be helpful in the interpretation of the observed VCD data.

However, in this paper, we shall concentrate on the experimental results and a qualitative interpretation of the VCD results. This interpretation will use distance arguments alone to determine whether or not coupling between carbonyl transitions is possible. Since structural data on a number of different conformations are available, we are able to assess the validity of our approach. A favorable coupling geometry is given, for example, for the S conformation in low polarity solvents, where all three glycyl carbonyl groups point toward the inside of the peptide to form three γ-turn. Here, the glycyl carbonyl groups are very close (3.2 Å) whereas the prolyl groups are about 8 Å apart. Under these

circumstances, the coupling is nearly exclusively due to the glycyl groups. Similarly, in mixed solvents of somewhat higher polarity, the **S** conformation is destroyed, and a structure appears which may be described as having a binding cavity, or "cup", on both faces of the molecule. In this conformation, both the glycyl carbonyl as well as the prolyl C=O groups can undergo dipolar coupling *(vide infra)*. Consequently, very different VCD spectra result. The solution structural arguments based on changes in VCD spectra, and absorption frequency shifts, do not necessarily agree in detail with the crystallographic data of the ion/CPG3 complexes. Previously available Raman spectroscopic results of crystalline CPG3 probably cannot be used to make any statements about the solution structure of these complexes.

5.5.1. Conformational Studies of CPG3 in Solvents with Various Polarity

The conformation of CPG3 is determined in a sensitive way by the solvent environment. In a low polarity solvent such as bromoform, CPG3 shows an infrared absorption spectrum shown in Figure 5-1. The amide I' band has its absorption maximum at 1663 cm^{-1} which is a relatively high frequency for a amide I' vibration. This high value is determined, in part, by the absence of hydrogen bonding with the solvent. The absorption peak, which is asymmetric with a low frequency shoulder, was resolved into two components at *ca.* 1636 and 1668 cm^{-1} *via* second derivative spectroscopy. Subsequent band deconvolution into Gaussian envelopes resulted in two peaks at 1642 and 1671 cm^{-1} which we assign to the $C{=}O_{(gly)}$ and $C{=}O_{(pro)}$ vibrations, respectively, in agreement with the previous Raman data. Alternatively, one could argue that the difference in frequencies is mostly determined by the presence or absence of hydrogen bonding

in the glycyl and prolyl carbonyl groups, respectively, in the **S** conformation. However, the relatively small shifts discussed below with different solvents, or in the presence of metal ions, make us favor the former interpretation.

The VCD spectrum shows a strong positive couplet (implying positive VCD intensity at lower wavenumber) with a zero crossing point of about 1642 cm^{-1} (*cf.* Figure 5-2 and Table 5-1), near the center of the glycyl carbonyl vibrations. Thus, we conclude that the VCD couplet is due to the three $C{=}O_{(gly)}$ groups, held close to each other (3.2 Å, measured from the center of the C=O bonds) in this 3-fold symmetric structure by the three $1 \rightarrow 3$ H-bonds of the γ-turns, and that these C=O groups undergo dipolar coupling which is responsible for the appearance of the observed VCD spectrum. The three $C{=}O_{(pro)}$ groups, on the other hand, are far away from each other (8 Å), and do not contribute significantly to the observed VCD. Here, we used structural data available from other techniques to interpret the observed VCD features.

1,4-dioxane is a nonpolar solvent, but a strong H-bond acceptor. In 1,4-dioxane, CPG3 shows VCD spectra identical to those in bromoform (data not shown). This result implies that the polarity, rather than the H-bond acceptor properties, determine the conformation of CPG3. In more polar solvents, however, the symmetric conformation observed in bromoform or dioxane will be perturbed. In a 1:2 mixture of bromoform : ethanol, CPG3 exists in another conformation which exhibits different spectral features than those in bromoform. The absorption band is symmetric and shifted to lower frequency (1654 cm^{-1}). A band deconvolution revealed the prolyl and glycyl carbonyl frequencies at1665 and 1642 cm^{-1}, respectively. For this and subsequent interpretations, we assume that differences in H-bonding do not change the order of glycyl and prolyl carbonyl stretching frequencies, *i.e.*, that the prolyl carbonyl frequencies are always larger than those of the glycyl groups. This assumption is well justified,

since band deconvolution in all cases studied here do not reveal a shift in the components by more than 10 cm^{-1}.

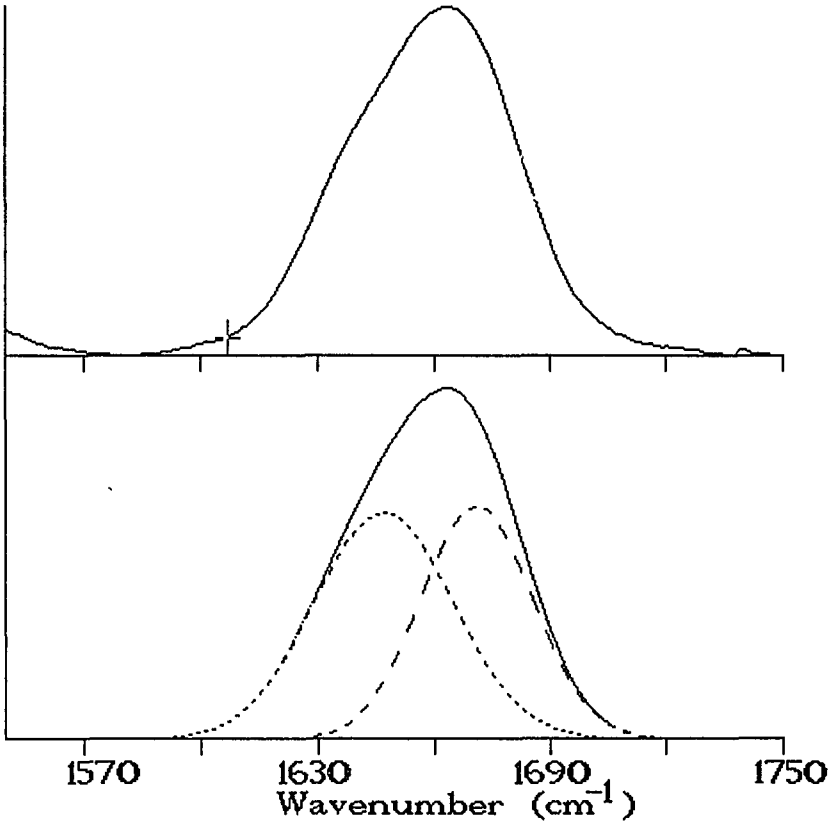

Figure 5-1. Observed (top) and Band Fitted Infrared Absorption Spectra of *cyclo*-(-Pro-Gly-)$_3$ in $CDBr_3$.

Fitting Parameters: Gaussian Envelopes

Frequencies:	1642	1671	cm^{-1}
FWHH:	42	34	cm^{-1}
Intensities	0.0709	0.0731	OD units

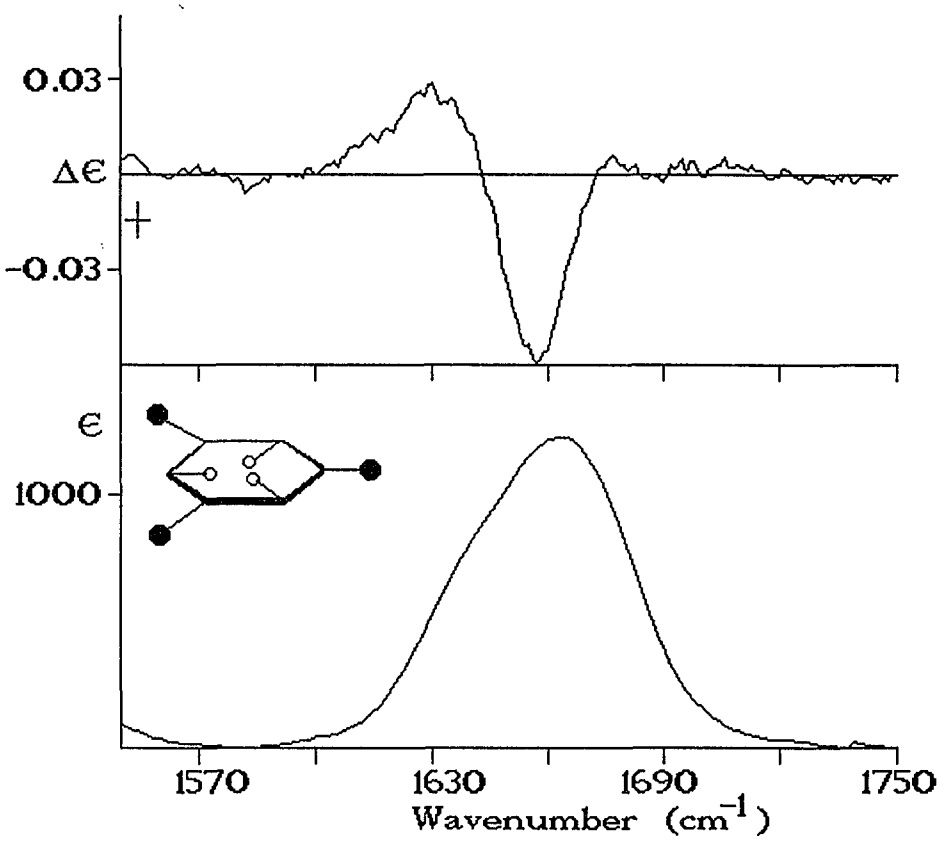

Figure 5-2. Infrared VCD (top) and Absorption (bottom) Spectra of *cyclo*-(-Pro-Gly-)$_3$ in $CDBr_3$. The Inset Presents a Schematic Structure of the Peptide.

Black Circles: Prolyl Carbonyls, White Circles: Glycyl Carbonyls

TABLE 5-1. Observed Frequencies [cm^{-1}] and VCD Intensities of CPG3 and its Metal Ion Complexes.

	Absorption Maximum [cm^{-1}]	Wavenumber of VCD Maxima and Zero Crossing [cm^{-1}]	VCD Intensity in Units of $\Delta\varepsilon$ [L/(mol cm)]
CPG3 in $CDBr_3$	1663 (1642 / 1671)*	M 1630 / 1657 Z 1642	0.029 / -0.060
CPG3 in $CDBr_3$ / Ethanol 1: (v/v)	1654 (1642 / 1665)*	M 1633 / 1654 / 1680 Z 1645 / 1667	-0.026 / 0.032 / -0.032
CPG3 in DMSO	1656	M 1679	-0.066
CPG3 in D_2O	1638 (1632 / 1657)*	M 1619 / 1667 Z 1642	0.018 / -0.012
CPG3 / Ca^{2+} 1 : 1in D_2O	1643 (1636 / 1659)*	M 1621 / 1641 / 1665 Z 1626 / 1652	-0.009 / 0.032 / -0.031
CPG3 / Na^{+} 1 : 1 in $CDBr_3$ / Ethanol 1: 2 (v/v)	1664 (1649 / 1669)*	M 1636 / 1661 / 1689 Z 1648 / 1676	-0.042 / 0.054 / -0.023
CPG3 / K^{+} 1 : 1 in $CDBr_3$ / Ethanol 1: 2 (v/v)	1664	M 1635 / 1662 / 1692 Z 1647 / 1681	-0.046 / 0.070 / -0.016
CPG3 / Ca^{2+}/Na^{+} 1 : 0.5 :1 in D_2O	1643	M 1641 / 1665 Z 1652	0.027 / -0.025
CPG3 / Mg^{2+} 2 : 1 in $CDBr_3$ / Ethanol 1: 2 (v/v)	(1638 / 1666)*	M 1624 / 1656 / 1685 Z 1636 / 1677	-0.018 / 0.074 / -0.010
CPG3 / Mg^{2+} 1 : 1 in $CDBr_3$ / Ethanol 1: 2 (v/v)	1642 / 1661 (1637 / 1670)*	M 1621 / 1652 / 1683 Z 1631 / 1670	-0.016 / 0.088 / -0.044
CPG3 / Mg^{2+} 1 : 2 in $CDBr_3$ / Ethanol 1: 2 (v/v)	1653	M 1624 / 1656 / 1684 Z 1636 / 1677	-0.018 / 0.075 / -0.018

* These frequencies were obtained from second derivative spectra to approximately locate the composite bands, followed by a band decomposition into mixed Gaussian/Lorentzian band shapes.

A negative/positive/negative VCD spectrum is observed for CPG3 in this solvent which is interpreted to be due to the superposition of a negative couplet of the glycyl carbonyl groups, with a zero crossing at 1645, and a positive couplet of the prolyl carbonyl groups with a zero crossing at 1667 cm^{-1}. The zero crossing points are remarkably close to the calculated band maxima of the curve fitted absorption peak (*cf.* Table 5-1). The fact that there are couplets under both prolyl and glycyl absorptions makes us believe that coupling among the prolyl and among the glycyl carbonyl groups does occur. In order for such coupling to be possible, the distances between the glycyl and the distances between the prolyl carbonyls should be below 4 Å, and should be approximately equal. Inspection of the structures formed by CPG3 and metal ions *(vide infra)* reveals that the distances between glycyl carbonyl groups may vary from 3.1 to 3.7 Å, and those between prolyl carbonyl groups between 3.1 and 3.9 Å in these complexes. Thus, we conclude that the structure of CPG3 in bromoform : ethanol exhibits a geometry where the distances between the prolyl and the glycyl carbonyl groups are approximately equal. We represent this conformation schematically by the inset in Figure 5-3.

DMSO is a more polar solvent system, but a weak H-bond acceptor. In DMSO, the frequency of the amide I' mode is shifted to 1656 cm^{-1}, and shows increased intensity and a high frequency shoulder (Figure 5-4). The VCD is negative, and has its largest intensity under the high frequency shoulder (1673 cm^{-1}). The high frequency VCD suggests that it is due to the prolyl carbonyls, which must have turned even closer to allow interactions. The strong VCD signal implies a well-defined conformation with some intra-molecular H-bonds still existing. Previous NMR studies have shown that in more polar solvents, an

asymmetric structure called conformation **A** exists which appears to contain one *cis*-peptide linkage.

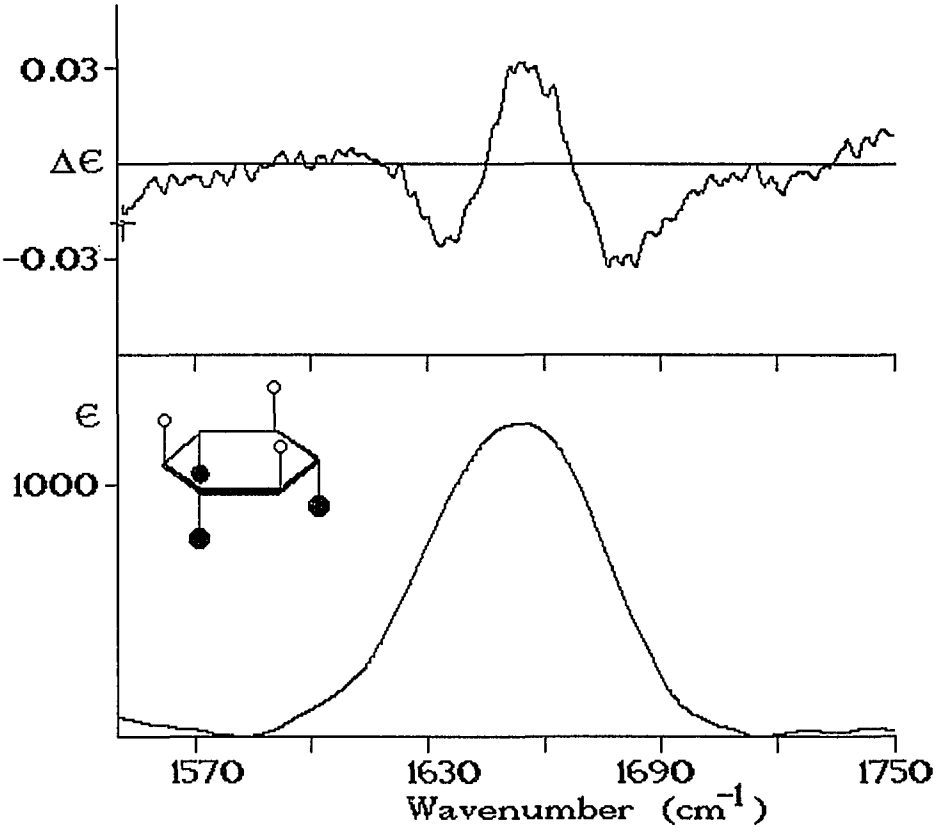

Figure 5-3. Infrared VCD (top) and Absorption (bottom) Spectra of *cyclo*-(-Pro-Gly-)$_3$ in $CDBr_3$/Ethanol (1:2 by volume). The Inset Presents a Schematic Structure of the Peptide.

Black Circles: Prolyl Carbonyls

White Circles: Glycyl Carbonyls

D_2O is still more polar, and a good H-bond acceptor and donor. It can form intermolecular H-bonds with both the C=O and N-D groups, which may release the constraint of the peptide even further. The absorption maximum occurs at 1638 cm^{-1} with both the prolyl and glycyl frequencies are shifted to lower wavenumber, to 1632 and 1657 cm^{-1}, respectively. We attribute this shift to solvent exposure, and hydrogen bonding, of all carbonyl groups. The VCD spectrum exhibits a weak positive couplet. Since the zero crossing point of the VCD couplet (1645 cm^{-1}) is located near the center of the IR peak and not under the individual prolyl and glycyl components, it appears that the VCD is due to small, residual VCD of uncoupled prolyl and glycyl groups. The weak VCD intensities point toward a poorly defined structure, or an equilibrium of many structures, with water molecules bridging the carbonyl groups.

The VCD and infrared absorption spectra of CPG3 in D_2O and DMSO are quite different, indicating different solution structures for the peptide in these solvents. Interestingly, these differences were not obvious in other spectroscopic experiments. We believe that the fast time scale and high spectral resolution of VCD allow these different conformations to be detected, whereas NMR and CD spectroscopic methods cannot do so.

An inspection of Table 5-1 reveals frequency shifts of the absorption maxima from 1663 (in bromoform) to 1638 cm^{-1} (in D_2O). However, the shifts in the band maxima of the component bands is much smaller, between 1632 and 1642 cm^{-1} for the glycyl, and between 1657 and 1665 cm^{-1} for the prolyl carbonyl groups. The observed shifts in the band maxima are actually due to relatively small shift of the component bands, accompanied by intensity variations in the components.

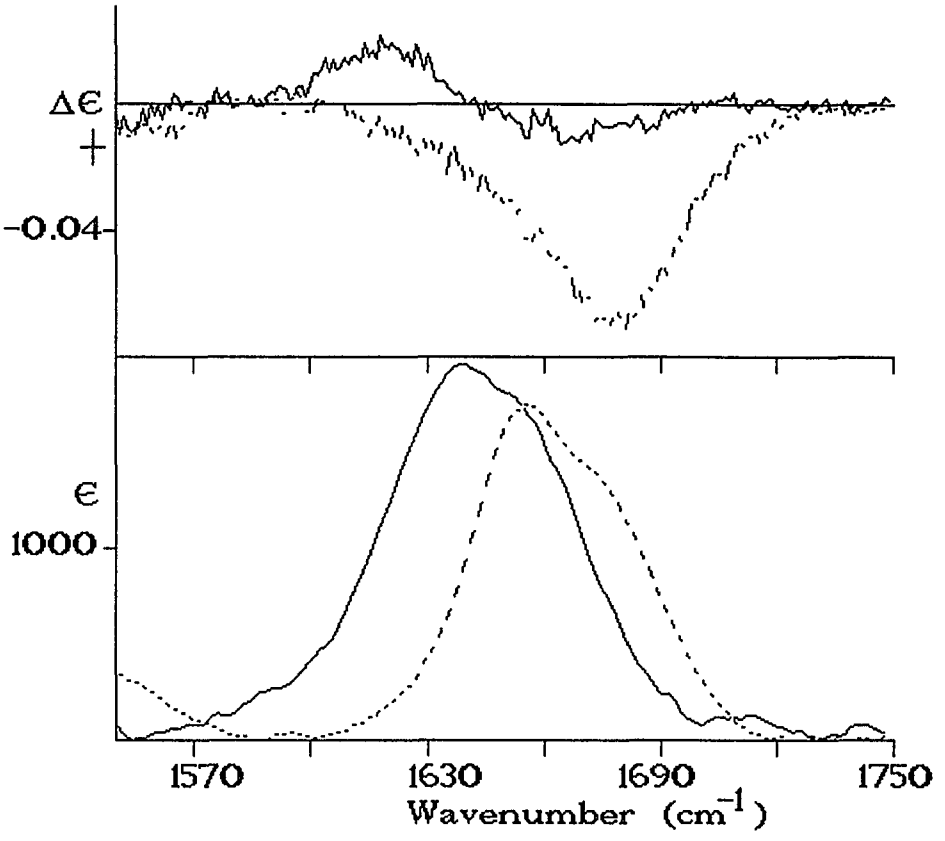

Figure 5-4. Infrared VCD (top) and Absorption (bottom) Spectra of *cyclo*-(-Pro-Gly-)$_3$ in D_2O (solid traces) and DMSO (dashed traces).

5.5.2. Conformational Studies of CPG3 with Various Metal Ions

An interesting feature of CPG3 is its ability to act as an ionophore, that is, to bind to metal ions while undergoing a conformational change. Peptides with such properties are thought to fulfill important biological tasks *in vivo*, such as the transport of metal ions through membranes. The cations studied here change the geometry of the C=O groups, mostly by twisting either the glycyl or the prolyl carbonyl groups toward the center of the molecule. The formation of such complexes depends on the charge and size of the cation as well as the solvent used.

Some properties of the metal ions of interest are listed in Table 5-2, along with peptide binding constants of the cations. Calcium plays a very important role in biological systems, especially its interactions with proteins. Calcium is a large, divalent cation, which favors coordinate numbers of 8, 7, 6, 9 (in order of preference). Thus, calcium has the flexibility to bind with ligands which have binding pockets of different sizes.

Figure 5-5 shows VCD and absorption spectra of CPG3 in the presence of Ca^{2+} ions in aqueous solution at a ratio CPG3 : Ca^{2+} = 1 : 1. The absorption maximum shifts up to 1643 cm^{-1} from 1639 cm^{-1} in water. The band decomposition results in two peaks at about 1636 and 1659 cm^{-1}, as compared 1632 and 1657 cm^{-1} found in D_2O. The small changes in the absorption maxima, as well as the positions of the component bands, suggest that the order of prolyl and glycyl frequencies is unchanged. The changes in the solution phase infrared spectra are very small and inconclusive. In light of these results, the enormous changes observed in the Raman spectra of the solid CPG3 / Ca^{2+} complex is most likely due to solid state effects.

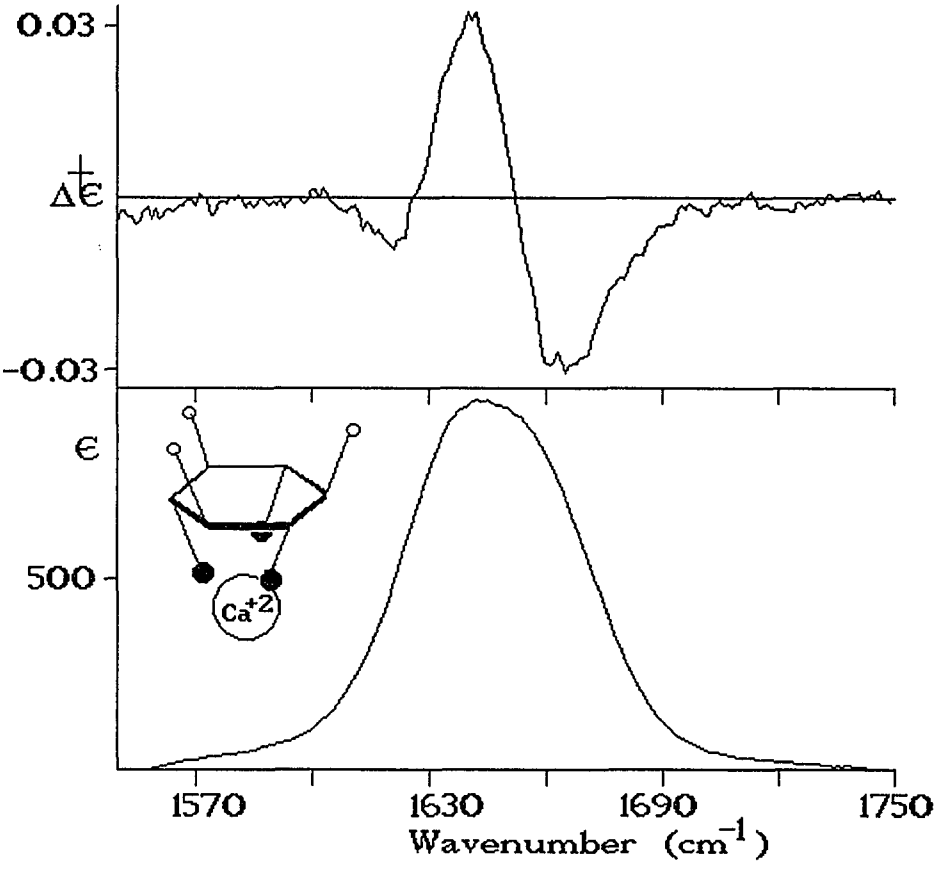

Figure 5-5. Infrared VCD (top) and Absorption (bottom) Spectra of *cyclo*-(-Pro-Gly-)$_3$ in D_2O in the Presence of Equimolar Ca^{2+}. The Inset Presents a Schematic Structure of the Peptide.

Black Circles: Prolyl Carbonyls.

White Circles: Glycyl Carbonyls

Table 5-2 . Properties of Metal Ions Used in This Study

Metal Ion	Ionic radius[a] at coordination # 6 [Å]	Binding Constant[b] for Protein binding	Comments
Ca^{2+}	1.02	$< 10^6$	prefers oxygen as electron donor; donor-ion distance 2.2-2.6Å coordination character: ionic.
Mg^{2+}	0.72	10^3	higher affinity for N than O; donor-ion distance 2.0-2.1 coordination character: more covalent.
Na^+	1.02	$<10^3$	
K^+	1.38	$<10^3$	

a) From: Howard Einspahr and Charles Bugg, "Crystal Structure of Calcium Complexes and Implications for Biological Systems", in *Metal Ions in Biological Systems*, Helmut Sigel, Ed., Marcel Dekker, New York, Vol. **17**, 51-97 (1984)

b) J.J.R. Frausto da Silva and R.J.P Williams, *The Biological Chemistry of Elements: The Inorganic Chemistry of Life*, Clarendon Press, Oxford, UK, p. 104 (1991)

The VCD exhibits a (weak negative)/positive/negative pattern with a zero crossing at 1653 cm^{-1}. Since the main VCD couplet is formed in the high frequency range of the amide I ' peak, we conclude that the calcium ion binds to the peptide in such a fashion that the prolyl carbonyl groups are able to undergo dipolar coupling. We believe that this implies that the calcium ion actually binds *via* the prolyl carbonyl groups and distorts the peptide as shown in the inset in Figure 5-5. However, the possibility exists that the calcium ion actually binds to the glycyl carbonyl groups, and that the spectral change observed in the prolyl region is due to a better coupling geometry of the prolyl residues once the calcium ion is in the glycyl pocket. However, further results with other ions make us favor the first interpretation.

Upon increasing the CPG3 : Ca^{2+} ratio to 1 : 2 or even 1 : 10, no further spectral changes are observed, except for a slight shift toward lower wavenumbers, of the zero crossing point of the VCD trace. We believe that this indicates that no Ca^{2+}/ peptide/Ca^{2+} complex is formed, and that Ca^{2+} binds selectively to prolyl carbonyls. This finding is in contrast to results from the solid phase, and the different conclusions drawn in this study will be elaborated upon in the discussion section below.

We found that in aqueous solution, other cations such as Li^+, Na^+, K^+ and Mg^{2+} cannot induce similar conformational changes in CPG3 due to their lower binding constants. Although they may cause a frequency shift in the IR absorption spectrum, due to the weak interaction between the ions and the carbonyl oxygen atoms, they cannot compete with the solvent and produce a complex with a discernible conformation. Thus, the solvent polarity is the dominant factor controlling not only the conformation of CPG3, but also its complexes with metal ions.

However, in moderately polar environments, the carbonyls of CPG3 exhibit weaker interaction with the solvent medium, and therefore, allow some cations to bind with CPG3. Figure 5-6 shows the VCD and absorption spectra of Na^+ and K^+ with CPG3 in bromoform : ethanol (1:2). Na^+ and K^+ have relative large sizes (*cf*. Table 5-2) and a single positive charge. Addition of these cations induces a shift of the absorption maximum to 1664 cm^{-1} from 1654 cm^{-1} in bromoform/ethanol, with the glycyl and prolyl components appearing at 1649 and 1669 cm^{-1}. This shift toward higher wavenumber, as compared with the pure bromoform/ethanol solvent, is due to the metal ion binding; however, when comparing the prolyl and glycyl components in the Na^+ / peptide complex with those of the Ca^{2+} / peptide complex (*cf.* Table 5-1), one has to remember that the calcium data were collected in aqueous solution, which always exhibit lower frequencies. Furthermore, the symmetric band shape observed in bromoform/ethanol in the absence of metal ions (*cf.* Figure 5-3) is lost, and the absorption spectra in the presence of Na^+ and K^+ ions show distinct low frequency shoulders.

The observed VCD spectra are more intense than that shown in Figure 5-3, and this increase occurs mostly in the glycyl carbonyl couplet at the expense of the prolyl couplet. Since the spectral changes between the complexed and uncomplexed peptide in bromoform/ethanol occur in the low frequency shoulder (the glycyl carbonyl groups) of the amide I' band, we conclude that both Na^+ and K^+ bind with the glycyl carbonyl groups, and that a similar distortion of the carbonyl groups occurs that was discussed for the Ca^{2+} ion in D_2O before. It is interesting to note that the shape of the VCD spectrum of the CPG3/K^+ complex is related to that of the calcium complex in D_2O by a reflection by a vertical plane, indicated by the dashed line in the dashed line in the small (upper) inset in Figure 5. We conclude that the binding cups formed on both faces of the

molecule are similarly related by a mirror image. Available structural data[5-7,8] have allowed us to assess the distances between the carbonyl groups. In the calcium complex, the distance between the glycyl-glycyl carbonyl groups is 3.15 Å, and the prolyl-prolyl distance 3.89 Å. In the sodium complex, these distances are 3.68 and 3.51 Å, respectively

A further increase in the sodium or potassium ion concentration does not change the observed spectral features, and the formation of an ion/peptide/ion sandwich can be excluded. This can be understood in terms of the two binding sites of CPG3 being sufficiently different that they cannot easily interact with a second sodium or potassium ion (*vide infra*).

The previously presented data suggest that calcium and sodium (or potassium) ions bind to different faces of CPG3. Therefore, it should be possible to form ion/peptide /ion sandwich complexes with a mixture of these ions. In Figure 5-7, we present the VCD data of a CPG3 / Ca^{2+} / Na^{+} complex at a ratio 1: 0.5 : 1 in D_2O. Sodium ions at any concentrations cannot induce a conformational change of CPG3 in aqueous solution since sodium shows a weak interaction with the glycyl carbonyl groups; consequently, complexation of sodium ions was observed in non-aqueous solutions only.

However, at a ratio CPG3 / Ca^{2+} / Na^{+} of 1: 0.5 : 1, the observed VCD spectrum is the same as that of CPG3 in the presence of a 1:1 ratio of Ca^{2+} ions. Thus, we conclude that the binding of sodium and calcium occurs cooperatively: since one cation binding to one side of the peptide can produce a conformational change which facilitates the binding of the other cation, binding proceeds preferentially in the presence of both ions.

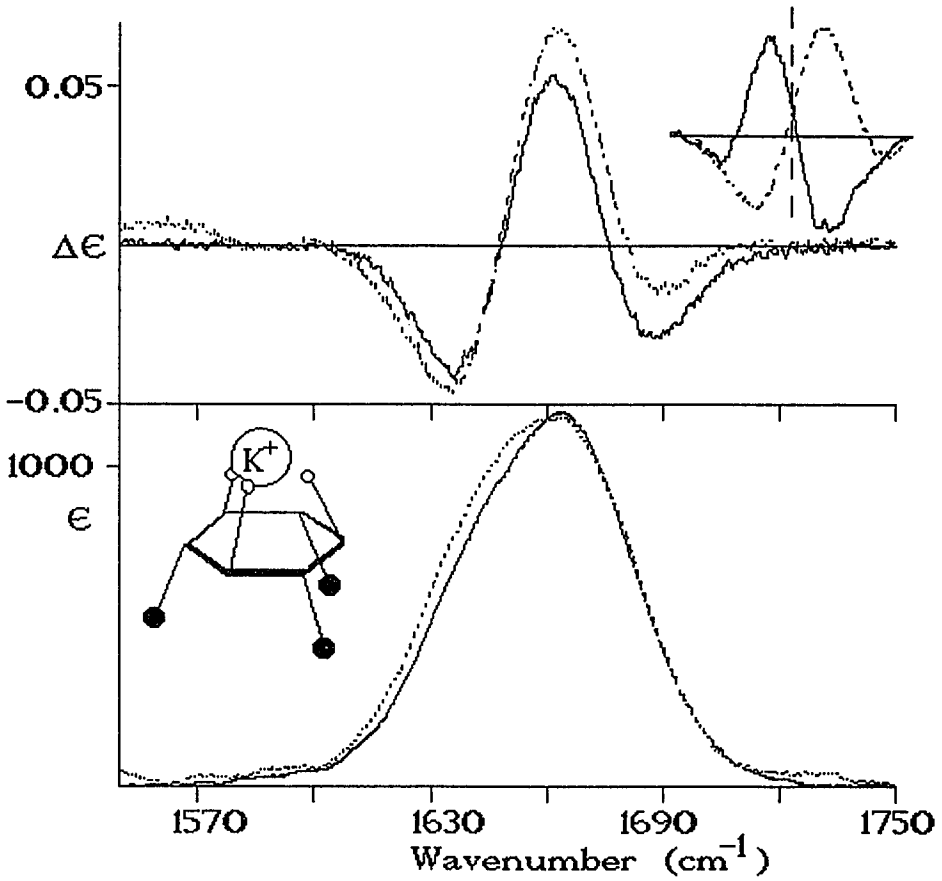

Figure 5-6. Infrared VCD (top) and Absorption (bottom) Spectra of *cyclo*-(-Pro-Gly-)$_3$ in $CDBr_3$/Ethanol (1:2 by volume) in the Presence of Equimolar Na^+ (solid traces) and K^+ ions (dashed traces). The Inset at the Upper Right Corner Compares the Ca^{2+} and the K^+ spectra. The Lower Left Inset Presents a Schematic Structure of the Peptide.

Black Circles: Prolyl Carbonyls

White Circles: Glycyl Carbonyls

VCD data do not allow us to determine the exact nature of the complex formed in the presence of both sodium and calcium ions. However, since x-ray crystallography has suggested the structure Na^+ /peptide/ Ca^{2+}/peptide/Na^+ (*vide supra*), which has the same stoichiometry as the solution used in the VCD study, we are inclined to suggest that a similar complex might be formed in solution, with the calcium ion being sandwiched by two peptide molecules, and one sodium ion binding to each of the peptide rings *via* the glycyl groups.

Different binding behavior was observed for Mg^{2+} in bromoform/ethanol. Mg^{2+} is chemically quite different from the other cations. Its small size, combined with its high charge, give the interaction of magnesium ions with the carbonyl groups more covalent character. Consequently, it exhibits totally different bioactivity from the other cations. In bromoform/ethanol, Mg^{2+} can bind with CPG3 in at least two distinct ways, depending on the molar ratio of peptide to metal ion. In Figure5- 8, the VCD and absorption spectra of 0.5 : 1 , 1:1 and 1: 0.5 ratios of CPG3 : Mg^{2+} are shown.

At a ratio of CPG3 : Mg^{2+} of 1:1, one observes that the absorption peak is broader and nearly resolved into two components, which are found by band deconvolution to occur at 1638 and 1666 cm^{-1}. The VCD spectrum exhibits a strong couplet in the $C{=}O_{(pro)}$ region with a much weaker couplet in the $C{=}O_{(gly)}$ band. The observed band shape is very similar to that observed for the Ca^{2+} ion complex, but with larger splitting of the components. Thus, we conclude that the preferential binding site of the magnesium ion is the prolyl pocket as well.

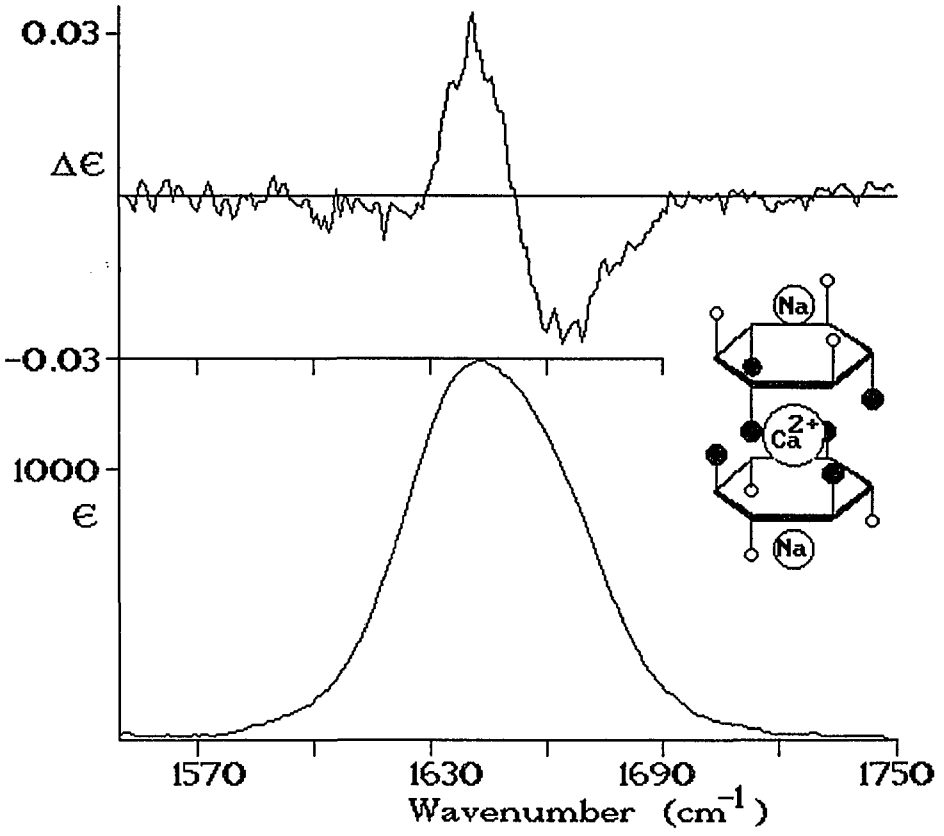

Figure 5-7. Infrared VCD (top) and Absorption (bottom) Spectra of *cyclo*-(-Pro-Gly-)$_3$ in D_2O in the Presence of Ca^{2+} and Na^+ at a ratio CPG3: Ca^{2+} : Na^+ = 1: 0.5 : 1. The Inset Presents a Schematic Structure of the Peptide/Ion Complex.

Black Circles: Prolyl Carbonyls

White Circles: Glycyl Carbonyls

The VCD and absorption data observed for a 1:2 ratio of CPG3 : Mg^{2+} are similar to those observed for the 1:1 ratio, except that at higher cation concentration, the prolyl absorption and VCD shift to somewhat higher wavenumber. We interpret the similarity between the 1:1 and 1:2 complexes in terms of the absence of an ion/peptide/ion complex, in which metal binding would have to occur at both prolyl and glycyl carbonyl groups. In this case, we would expect that their VCD couplets be equal. This is clearly not the case.

At a 2:1 ratio of CPG3 : Mg^{2+}, however, both IR and VCD spectra become symmetric with respect to the absorption center at about 1655 cm^{-1}. The strong VCD spectrum, with a dominant positive center and two negative peaks on each side, shows two zero crossing point at 1636 / 1677 cm^{-1}. We have interpreted this spectrum in terms of a peptide / ion / peptide sandwich in which both faces of the peptides are involved. The magnesium ion binds with $C{=}O_{(gly)}$ from one CPG3 and $C{=}O_{(pro)}$ from another. This hypothesis is based on a comparison of the observed spectrum of the 2:1 complex (Figure 8) with a coaddition of the VCD spectra of a glycyl / metal interaction (such as the 1:1 Na^{+} / CPG3 complex) and a prolyl /metal interaction (such as the 1:1 Mg^{2+} complex). The resulting coadded spectrum has a similar shape as the experimental data of the 2:1 complex. We believe that at this ratio, the complex formed is a peptide / Mg^{2+} / peptide sandwich where the metal ion binds to both the $C{=}O_{(gly)}$ and $C{=}O_{(pro)}$ of different CPG3 molecules.

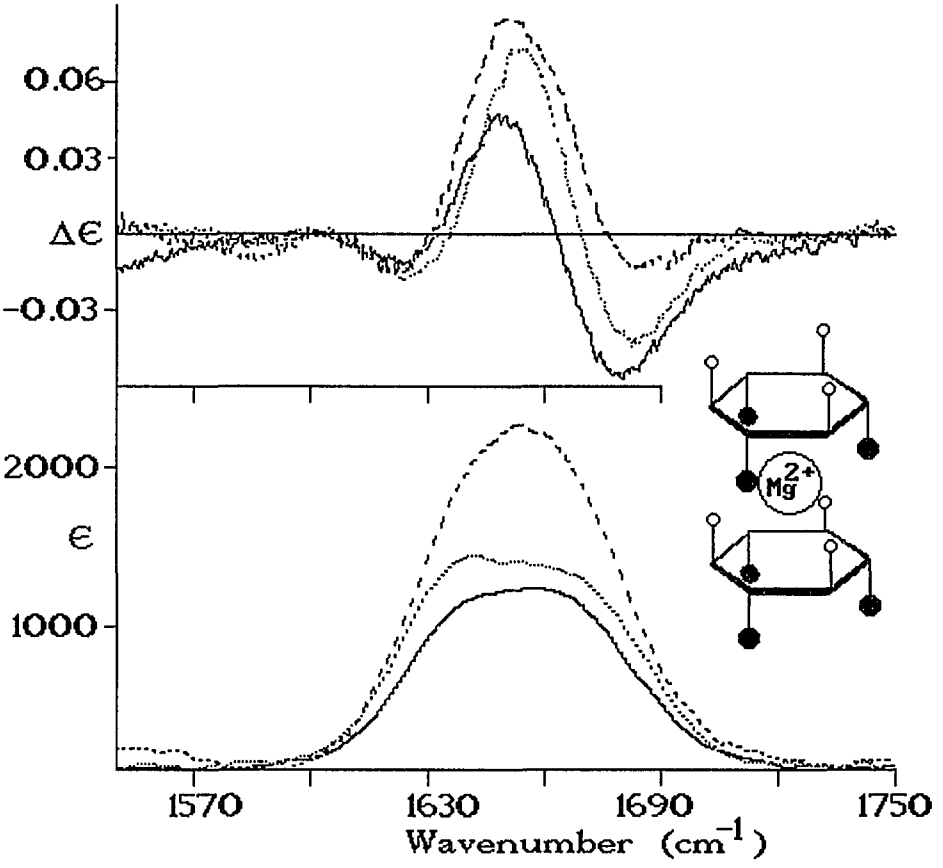

Figure 5-8 Infrared VCD (top) and Absorption (bottom) Spectra of *cyclo*-(-Pro-Gly-)$_3$ in $CDBr_3$/Ethanol (1:2 by volume) in the Presence of Mg^{2+} Ions.

Solid Trace: CPG3: Mg^{2+} = 1 : 1

Dotted Trace: CPG3: Mg^{2+} = 1 : 2

Dashed Trace: CPG3: Mg^{2+} = 2 : 1

The Inset Presents a Schematic Structure of the Peptide/Ion Complex.
Black Circles: Prolyl Carbonyl; White Circles: Glycyl Carbonyls

5.6. DISCUSSION

The solution conformation of CPG3 in low polarity solvents is well established from CD and NMR spectroscopies.[5-3] This solution structure serves as the starting point of the interpretation of the VCD results. The VCD peak of CPG3 in bromoform has the same sign pattern as the VCD observed in other molecules containing a γ-turn;[5-2] however, band frequencies and relative intensities are quite different. We attribute the distinct shape of the VCD peak in CPG3 in bromoform to the fact that there are three highly coupled, identical γ-turns in very close vicinity, whereas previously studied γ-turns were either isolated species,[5-10] or occured next to a Type II β-turn.[5-2]

In solvents of increasing polarity, such as bromoform/ethanol, a conformational change occurs in CPG3 which turns both the glycyl and prolyl carbonyl groups to form binding pockets, or cups, which are accessible to metal ions. It is interesting to note that the spectra of CPG3 in bromoform/ethanol is nearly symmetrical (Figure 5-3), indicating nearly equally good coupling geometry for both the prolyl and the glycyl carbonyl groups. This spectrum is quite similar to the spectra of CPG3 with certain metal ions. Thus, we may conclude that the largest conformational change occurs between very weakly polar and more polar solvents, and that metal ions produce subsequent and smaller conformational changes. We believe that the best representation of the solution conformation on bromoform/ethanol is given by the inset in Figure 5-3.

The interaction of calcium ions with CPG3 produces a number of interesting features. In aqueous solution, in the absence of metal ions, the structure of CPG3 is ill-defined. The presence of Ca^{2+} ions re-establishes a

structure which is most likely highly symmetric, and which shows strong VCD features. Compared with the symmetric structure observed in pure $CDBr_3$, it is apparent that the main VCD couplet occurs in the prolyl, rather than the glycyl carbonyl groups. Thus, we conclude that the prolyl carbonyl groups are pulled toward each other by the calcium ion, and undergo coupling. The glycyl carbonyl groups, on the other hand, are solvent exposed and are expected to be hydrogen bonded to solvent molecules. In crystalline CPG3/Ca^{2+} complexes, water molecules actually were found bound to the glycyl carbonyl groups. These solvent molecules, along with the unfavorable geometry of the glycyl pocket, will not permit a second calcium ion to bind at the glycyl face.

However, even in the CPG3/Ca^{2+} complex in aqueous solution, there is evidence for some coupling of the glycyl groups, which we believe is manifested by the small negative couplet at low frequency. A schematic structure proposed for the Ca^{2+} complex with CPG3 is shown in the inset of Figure 5-5; the glycyl carbonyl groups will point away from each other, but will still be in reasonably good coupling geometry. In a less polar solvent, sodium and potassium ions bind in a very similar manner, but on the face opposite to the calcium ion binding site.

At this point, it is appropriate to comment once more on the different conclusions derived from the Raman studies on the solid complexes. We present here not only the VCD data, but also absorption spectra which were collected independently on the VCD spectrometer, and on a commercial FT-IR instrument. Thus, we believe that an error in our frequency measurement is unlikely. The IR absorption frequencies do show some variation with metal ions, but not nearly as much as the Raman data reported. Furthermore, band deconvolutions reveal that the component bands stay within a 12 cm^{-1} range for the glycyl and a 10 cm^{-1} range for the prolyl carbonyl groups. Although band resolution algorithms have some inherent uncertainties, the calculated band positions do agree very well with

the zero crossing points of the VCD spectra. Thus, we are confident that our results represent an accurate picture of the vibrational frequencies as a function of solvent polarity or the presence of metal ions. We believe that using shifts of band maxima may be very misleading, since in a composite band, intensity variations may contribute to the apparent shifts of a band.

The VCD data, much more so than the absorption spectra, identify the binding site (*i.e.*, prolyl *vs.* glycyl pockets) occupied by the cation in a complex in solution. We believe that these changes in VCD patterns are much more reliable than changes in frequency and intensity observed in standard vibrational spectroscopy, especially in the solid phase. Furthermore, we have ensured that all anions used in this study are the same (chloride), and are therefore not concerned about vibrational bands and/or overtones contributed by the anions. It is certainly possible that the solid phase data reported earlier are correct, but we claim that they do not represent the structure of CPG3 complexes with calcium, sodium or potassium ions in solution phases.

Next, we shall attempt to present a rationale for the different binding of CPG3 to calcium and magnesium ions. Calcium has a less rigidly defined coordination number than magnesium. It prefers to interact with neutral oxygen donors such as carbonyl groups and alcohols, and prefers to form a loose complex. Magnesium, on the other hand, prefers sites with high charge density and small cavity size. It forms tight complexes with a coordination number of six. Thus, the binding of magnesium to many ligands is much more restricted than, for example, the binding of calcium to the same ligands.

In general, the binding of CPG3 with metal ions will depend on four factors: the polarity and size of the peptide cavity, and the charge and size of the cation. The cavity size of CPG3 depends on the geometry of the carbonyl groups, which, in turn, depends on the polarity of the solvent as discussed before. The

data of CPG3 in solvents of various polarity show how the alignment of the carbonyl groups varies; since the $C=O_{(pro)}$ and $C=O_{(gly)}$ groups are linked by the peptide backbone, the rotation of any carbonyl group is not arbitrary, but is correlated to the rotation of other carbonyl groups in the ring. Based on this consideration, we may postulate a first binding step that causes the carbonyl groups on one side of the ring to complex the metal ion, whereas the carbonyl groups on the other side form a binding pocket that may induce another ion to bind.

In water, for example, the conformation of CPG3 is such that both C=O and N-H groups can form hydrogen bonds with the solvent. The cavity size is relatively large, and a calcium ion can fit in it. In less polar medium, it has a shape with two well defined, and much smaller, binding pockets, or cups. In this situation Mg^{2+} forms a tight complex with a coordination number of six with either two peptide molecules, or one peptide molecules and anions or solvent molecules.

Mg^{2+} / peptide / Mg^{2+} or Ca^{2+} / peptide / Ca^{2+} sandwiches were not found in either case because the binding of one ion leaves the binding pocket on the other side of the molecules so distorted that a second ion does not fit. Only in the case of Ca^{2+} and Na^{+} did we find evidence for such a sandwich, since the sodium and the calcium naturally prefer different faces of the peptide, which have totally different binding properties. The glycyl site favors monovalent cations, whereas the prolyl site prefers divalent cations.

At this point, we need to discuss the unusual structure of the peptide / Mg^{2+} / peptide complex, which we believe is formed *via* the prolyl carbonyl groups on one of the CPG3 molecules, and *via* the glycyl carbonyl groups of the other. If both CPG3 molecules were binding *via* the prolyl groups, the VCD spectrum of the magnesium complex will not change as the peptide concentration

is raised. This behavior was observed in the case of calcium ions. Thus, we offer the following explanation for the formation of the peptide / Mg^{2+} / peptide complex. After the first magnesium ion binds to the three prolyl carbonyl groups form one CPG3 molecule (we call this the first binding step), this magnesium ion loses some of its polarity and behaves more like a monovalent cation. Therefore, it will no longer interact and complex with prolyl carbonyls from a second CPG3, but rather with its glycyl carbonyl groups. Larger sandwich structures, such as:

$\bullet\bullet Mg^{2+}{}_{(gly)}CPG3_{(pro)}\ Mg^{2+}{}_{(gly)}CPG3_{(pro)}\ Mg^{2+}\bullet\bullet$

have 1:1 stoichiometry and should exhibit the VCD spectrum shown in Figure 5-8 for the 1:1 ratio. Thus, we believe that the 2:1 ratio complex contains peptide molecules binding with different faces to the magnesium ion.

5.7. CONCLUSION

We find that VCD is an enormously sensitive tool for monitoring conformation changes in peptides. Its ability to identify different kinds of C=O groups allows for a qualitative interpretation, and its sensitivity to detect local dipolar coupling interactions allows one to determine which carbonyl groups are nearby in a given conformation. Therefore, VCD is an extremely powerful solution conformational probe for small peptides.

CPG3 is an excellent model to study the interaction of various metal ions with an ion-binding peptide. The results of uncomplexed CPG3, several 1:1 complexes of CPG3, and two peptide sandwiches, lead to the following conclusions:

- The solvent is the most important factor determining the conformation of the peptide.
- The size of the ion binding cavity, formed by carbonyls, and the size and charge of the metal ions play important, but secondary roles to the solvent polarity.
- For metal ions, the real size depends on the coordination of the ion prior to peptide complexation. Solvent molecules attached to the cavity may determine the shape of the binding cup. The differences in binding geometries of various cations with CPG3 confirms why these cations have different properties in biological systems.

REFERENCES

5-1) Diem, M., (1994), *Volume 14. Analytical Applications of Circular Dichroism"*, Purdie, N. and Brittain, H.G., Editors, Elsevier Science Publishers, Amsterdam, The Netherlands, pp. 91 - 130

5-2) Keiderling, T.A., (1990), *"Practical Fourier Transform Infrared Spectroscopy: Industrial and Laboratory Chemical Analyses"*, Ferraro, J.R. & Krishnan,K., Eds, Academic Press, NY, pp. 203-283

5-3) Baur, P. and Keiderling, T.A., (1992) *J. Amer. Chem. Soc.*, 114, 9100 - 9105

5-4) Madison, V., Atreyi, M., Deber, C.M. and Blout, E.R., (1974) *J.Amer.Chem.Soc.*, 96, 6725 - 6734

5-5) Deber, C.M., Madison, V. and Blout, E.R., (1976) *Acc. Chem. Res.*, 9, 106-113

5-6) Kartha, G., Varughese, K.I. and Aimoto, S., (1982) *Proc. Natl. Acad. Sci. USA*, 79, 4519-4522

5-7) Krishna, K. and Kartha, G., (1985) "*Peptides: Structure and Function. Proceedings of the Ninth American Peptide Symposium*", Deber, C.M., Hruby, V.J and Kopple, K.D., Editors, Pierce Chem.Comp., USA, p. 163-166

5-8) Diem, M., Roberts, G.M., Lee, O. and Barlow, A., (1988) *Appl.Spectrosc.* 42, 20 - 27

5-9) Lee, O., Roberts, G.M. and Diem, M., (1989) *Biopolymers*, 28, 1759-1770

5-10) Birke, S.S., Agbaje, I. and Diem, M., (1992) *Biochemistry*, 31, 450-455

5-11) Baur, P. and Keiderling, T.A., (1994) *J. Amer. Chem. Soc.*, in press

5-12) Xiang, T., Goss, D.J. and Diem, M., (1993) *Biophysical Journal*, 65(3), 1255-1261

5-13) Xie, P., Zhou, Q., and Diem, M., (1994) *Proc. Faraday Soc.*, submitted

CHAPTER SIX

CONFORMATIONAL STUDIES OF β-TURNS IN CYCLIC PEPTIDES BY VIBRATIONAL CD

In this chapter we report the infrared absorption and Vibrational Circular Dichroism (VCD) spectral features of peptide β-turns observed in small cyclic peptides dissolved in non-aqueous solvents. The molecules studied, *cyclo*-(Cys-Pro-Xxx-Cys), with Xxx = Gly, Phe, D-Phe, all form 14-member rings closed by a -S-S- linkage. The VCD spectra of these molecules vary enormously when the polarity and H-bonding ability of the solvent is varied. Furthermore, type I and type II β-turns can be formed, depending on the chirality of the residue Xxx in the 3-position. VCD intensity calculations, based on standard type I and type II geometries, were carried out and found to agree well with the observed VCD spectra.

6.1. INTRODUCTION

Turns are common structural motifs in proteins, comprising on average about 25% of the residues.[6-1] A survey of 29 proteins[6-2] showed that the frequency for turns is 32%, compared to 38% for helices and 20% for β-sheets. Specific turns, linking strands of anti-parallel β-sheet structures, were first recognized over 20 years ago by Venkatachalam,[6-3] and are referred to as β-turns.

Thus it is clear that turns in general, and β-turns in particular, are an essential and fundamental class of polypeptide structures.

In globular proteins, the secondary structures are organized in specific ways to bring together functional groups form different regions of the protein sequence to create the active site. The turn structures between structurally rigid peptide sections allow the polypeptide chains to adopt the appropriate globular structures. Turns have also been portrayed as nucleation sites for the protein folding process,[6-4, 5] and it has been suggested that turns function as recognition sites in complex immunologic, metabolic, genomic and endocrinologic regulatory mechanisms because of the location of turns on the surface of proteins, and because of the predominance of reactive functional groups in the side chains of amino acids involved in turns.

The general definition of a β-turn is the area where a polypeptide chain reverses its overall direction. In β-turns, this area comprises four amino acid residues, whereas γ-turns involve three residues. Turns may or may not be stabilized by an intramolecular hydrogen bond. Compared to other peptide conformations, such as α-helices or β-sheets, the geometry of β-turns is less unique, and several different β-turns, categorized as Type I, II, III (as well as Type I', II', III'), are found in proteins, *cf.* Table 6-1. The most common β-turns in proteins are the Type I , II and III structures. The standard geometry for each type of turn, based on X-ray crystallographic data of proteins, is defined by the ϕ and ψ angles of residues at the i+1 and i+2 positions. However, due to the variations in amino acid residues in a β-turn region, the angles may vary by as much as ±30°.

These large variations make the Type III and Type I turns indistinguishable in extreme cases, and also imply that the geometry of β-turns is less well defined than that of other secondary structures. The conformational angles in a turn depend on the environment involved, the sequence of amino acids in the β-turn, and the secondary structures connected by the β-turn: two single, β-sheet strands may be connected by a tight, U shaped β-turn that consists of four residues. On the other hand, the turn between two bulky secondary structures, such as α-helices, would exhibit a different shape and resemble an open helical structure (it is referred to as an "open turn" in the literature). This kind of turn might have a left or right handed chirality depending exclusively on the side chains. In these structures, it is not necessary to have a $1 \rightarrow 4$ intramolecular hydrogen bond.

Since β-turns consists of only a few residues, the spectroscopic signatures of these turns are hard to detect in larger proteins. In addition, the large degree of variation in the conformational angles of turns, as compared to other secondary structures, makes the conformational analysis much more complicated. Therefore, the structures of turns in peptides in solution is less well understood, and novel spectroscopic results can enormously enhance our present understanding of these structures.

In this paper we present the results of conformational studies of β-turns using VCD, which is a relative new technique for the study of peptide conformation. Therefore, this paper is aimed at establishing whether or not there are characteristic VCD patterns for β-turns, and whether or not different types of

turns can be distinguished from each other by VCD. Recent VCD results shows that VCD is a particularly sensitive probe for the conformation of small peptides containing turn motifs.[6-6,7,8] It combines and enormously enhances the sensitivities of CD and FTIR spectroscopies, and overcomes some disadvantages of both techniques.

Table 6-1 Dihedral Angles for Hydrogen-Bonded β–turns

	i+1		i+2	
Turn	ϕ	φ	ϕ	φ
Type I	-60	-30	-90	0
Type I'	60	30	90	0
Type II	-60	120	80	0
Type II'	60	-120	-80	0
Type III	-60	-30	-60	-30
Type III'	60	30	60	30
Type VIa (cis)	-60	120	-90	0
Type Vib(cis)	-120	120	-60	0

We find from the VCD results that small, cyclic peptides incorporating β-turns exhibit large conformational differences when the chemical environment is changed, although they are conformationally restricted. This change in environment was accomplished by varying the solvent polarity and hydrogen bonding ability. In spite of the perceived rigidness of the peptides reported here, we find that polar and hydrogen bonding solvents interfere with the internal hydrogen bonds between the peptide linkages, cause the polar group of the β-turn to be solvent exposed, and therewith induce conformational changes. In inert solvents, peptides tend to form intramolecular hydrogen-bonded structures and to be conformationally more restricted.

Finally, in order to understand the relationship between the observed VCD spectra and the conformations of peptides, we carried out VCD intensity simulations using the Non-degenerate Extended Coupled Oscillator (NECO) model.[6-9] The patterns of calculated VCD spectra for standard Type I and II β-turns, based on literature conformational data, agree well with experimental data. We conclude that the NECO model is useful for interpreting VCD data in peptides of the size reported here. The coupling between carbonyl group of the peptide linkages, which is considered the major mechanism for generating VCD intensity within the NECO model, will be different in single β-turns and in fused turns in larger peptides. We find that even these differences can be interpreted through the calculated VCD spectra.

6.2. PREVIOUS STRUCTURAL STUDIES ON β-TUTNS

6.2.1. Previous Spectroscopic Methods

Because of the complicated properties of β-turn, a variety of techniques have been employed to study the conformation of β-turns. The first systematic study of β-turns was carried out by Venkatachalam[6-3] using conformational computations. In the 1970's, the most accurate structural information available for turns was obtained by crystallographic techniques.[6-10,11] In recent years the NMR, CD, and FT-IR spectroscopies have become the most popular techniques to study β-turns,[6-12-16] because these techniques are sensitive to conformation and conformational changes of peptides and proteins in solution.

CD is very useful technique for conformational determination, especially for biomolecules. Because of its fast time scale, population-weighted average conformations will be measured, from which individual populations can be extracted. Thus, all existing conformer populations are observed simultaneously. For β-turns, four classes of CD spectra were established computationally by Woody[6-17,18] for the different subtypes. However, their direct observation proved to be difficult,[6-14] because the CD features of the turns are generally weak, and because there will be a population distribution of different turn subtypes. Furthermore, in model peptides and proteins, the signatures of the turn was found to be overlapped by the strong CD spectrum of other conformations or side-chain and disulfide bond contributions.

Several techniques in NMR can be used to determine conformation of β-turn, such as J-J coupling, ROSEY and chemical shift temperature dependence.[6-10,11,15] A common and powerful method to distinguish between Type II and other types of β-turns is NOE spectroscopy. β-turns exhibit a number of NOEs, but the most significant one is the interaction of the α-proton on carbon atom C_{i+1} with the amide proton on N_{i+2} in the Type II β-turn. In general, NOEs are observable when two protons are less than 3Å apart. In a standard Type II turn, the distance between the two protons, henceforth referred to as $C_{\alpha i+1}H$ and HN_{i+2}, is typically 2.1 Å, and strong NOE is observed. However, since there is a large variation of the conformational angles ϕ and ψ, the distance between $C_{\alpha i+1}H$ and HN_{i+2} can vary to such an extent that no NOE's are observable. In addition, the intensity of NOE is proportional to the population of each type of turn that may co-exists; therefore, interproton distances generated by NMR experiments may not fit a unique structure. Furthermore, the slow time scale of NMR, which is generally longer than the time scale of conformational interconversions, will further reduce the intensity of NOE's, particularly in small peptide system.[6-15] Many of the peptides studied via NMR techniques were linear and cyclic tetrapeptide, which were found to exhibit different conformations in various environments. In addition, they were found to be more flexible than the turns in large peptides or proteins, in which the conformation of the turn is limited by the entire protein environment .

IR absorption spectroscopy has been used quite extensively to investigate turn structures, particular in recent efforts. The assignment of absorption bands to given conformational angles, however, is not a unique one, particularly since infrared absorption peaks are broad and solvent dependent. We found in some previous studies on γ-turns, and in the present study, that the changes in infrared absorption spectra are relatively small and insignificant compared to the changes

in VCD features.[6-6,8] However, the amide I stretching frequency of a proline containing peptide linkage is quite different from that containing other amino acid residue: In a Gly-Pro peptide linkage, where the nitrogen is a tertiary amine, the $C=O_{(Gly)}$ stretching frequency is observed around 1640-1655 cm^{-1}, whereas in Pro-Gly where nitrogen is a secondary amide, the $C=O_{(Pro)}$ frequency is observed at 1670-1685 cm^{-1}. Thus, these frequency shift caused by changes in the chemical environment of peptide linkages can interfere with the frequency shift generally associated with changes in secondary structure, causing the results of vibrational work to be inaccurate.[6-6] In this study, we use the different frequencies of the secondary and tertiary amide groups to our advantage, since they allow us to differentiate between the various possible interactions of the carbonyl groups.

6.2.2. β-turn Structural Considerations

Type I and Type II β-turns are composed of four residues. In the case of a tight β-turn, the $C=O_i$ can form an intramolecular hydrogen with HN_{i+3}. The $C=O_{i+1}$ is approximately perpendicular to the plane of the ring, pointing either down (Type I) or up (Type II), *cf.* Figure 6-1. It is able to interact with solvent molecules and exhibits large conformational flexibility. Thus, the geometry of β-turn is determined by the arrangement of the three carbonyl groups $C=O_i$, $C=O_{i+1}$ and $C=O_{i+2}$. The advantage of VCD as a structural tool is that it monitors the orientation of these three probe groups.

The peptides reported in this study are cyclic tetrapeptides closed by a disulfide bond, and a cyclic pentapeptide. The cyclization reduces the flexibility of the peptides, and the disulfide bond will constrain the distance between $C_{\alpha i}$ and $C_{\alpha i+3}$. This latter factor may determine whether the particular peptide sequence will prefer a Type I or Type II turn. The peptides all have proline

residue at the i+1 position, because proline is well known to play a key role in β-turn conformations of proteins.[6-2] On the basis of x-ray crystallographic data in proteins, proline is the most frequently occurring residue in the i+1 position of β-turn. In addition, the sequence Pro-Y, in position i+1 and i+2, with Y= Ser, Asp, Asn or Glu, is found almost exclusively in type I or III turns, whereas the Pro-Gly sequence may occur both in type I(III) and type II turns. The limitations on conformational freedom is due to the constraint of the ϕ angle of proline.

In this study, we concentrate on solution conformations derived from the amide I' vibration of the peptide linkage. This vibration, which can be describes mostly as the carbonyl stretching motion of the amide moiety, occurs between 1630 and 1700 cm^{-1}, and has a dipole transition moment of 0.29D. The VCD spectra reflect the dipolar coupling among the different C=O groups of neighboring peptide linkages which depends on the distance between C=O groups and their dihedral angles. Since the turn geometry is directly related to the orientation of the carbonyl groups, the VCD results in this spectral region is particularly sensitive to the peptide conformation.

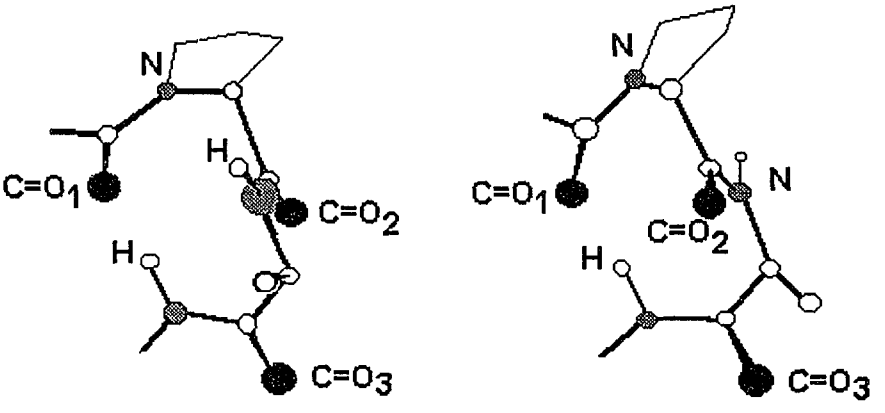

Figure 6-1. The schematic structure of Type I (left) and Type II (right) β- turn.

6.3. MATERIAIS AND METHODS

All data presented in the following publication were collected on the broadband (800-1800 cm^{-1} spectral range), dispersive VCD spectrometer at Hunter College described previously.[6-19] Several improvements were implemented since the earlier description of the instrument. Mostly, these improvements deal with further lowering the artifact levels. Thus, VCD spectra with amplitudes of about $3 \cdot 10^{-7}$ ΔA units can now be measured reliably. Details of the modifications will be reported at a later date.

Sample handling in VCD is entirely analogous to that in infrared spectroscopy. Samples are contained between CaF_2 plates, separated by Teflon spacers of appropriate thickness, typically 25 μm. Sample volumes of 10 - 20 μL, at peptide concentrations of 5 - 20 mg/mL, were utilized. These peptide concentrations result in peak absorbances of about 0.15 at the pathlength indicated. To check for association effects, VCD data of some peptides at lower concentration were collected as well. At present, the lowest absorbance levels at which VCD can be collected reliably is about 0.06 absorbance units. At these lower concentrations, no change in the VCD spectra were observed in the cyclic peptides, although the linear precursors did show concentration dependent VCD features.

The cyclic peptides *cyclo*-(-Cys-Pro-Gly-Cys-) [*c*(GPGC)], *cyclo*-(-Cys-Pro-Phe-Cys-) [*c*(GPFC)] and *cyclo*-(-Cys-Pro-D-Phe-Cys-) [*c*(GPdFC)], were prepared by standard F-Moc solid phase synthetic methods as described

previously.[6-8] The cyclic molecules were obtained from the linear precursors by oxidative ring closure in the presence of H_2O_2. *Cyclo*-(-Gly-Pro-Gly-D-Ala-Pro-) [*c*(GPGdAP)] was provided by H. Wyssbrod.[6-7] All peptides were lyophilized from D_2O prior to dissolving them in the solvents discussed for each experiment. Thus, all reported C=O stretching vibrational frequencies will be for the deuteriated peptide linkage, referred to as the amide I' vibration.

Molecular modeling, the calculation of atomic coordinates and the generation of structures shown, were carried out using program HyperChem running on a personal computer equipped with a 90 MHz Intel Pentium processor. The simulated VCD and infrared absorption spectra were obtained using exciton-type calculations allowing for non-degenerate frequencies of prolyl and glycyl carbonyl groups.[6-8,9]

6.4. RESULTS

The observed IR and VCD spectra of three cyclic peptide, *c*(GPGC), *c*(GPFC) and *c*(GPdFC) in three different solvent systems are shown in Figures 6-2 to 4. The solvent systems, DMSO/$CDBr_3$ (1:1, v:v), DMSO and DMSO/D_2O (1:2, v:v) were selected to represent different polarity and hydrogen bonding ability. In principle, the pure solvents $CDBr_3$, DMSO and D_2O would have been preferable since polarity and dielectric constants may be reproduced more accurately, but low solubilities prevented us from using the pure solvents. Figure 6-5 shows the observed VCD and infrared absorption spectra of the pentapeptide *c*GPGdAP in bromoform.

6.4.1. Absorption Spectra

The changes in the absorption spectra in Figures 6-2, 3 and 4 are relatively small. The general band shapes are very similar for the three peptides in the three different solvents, even if the amino acid at the 3-position is changed. However, the choice of solvent influences the frequency of the absorption maximum: there is a trend toward lower wavenumber of the peak absorbance between DMSO, DMSO/$CDBr_3$ and DMSO/D_2O. The solvent may affect the absorption spectra in two ways: either by a direct interaction between the carbonyl groups and the solvent, or by inducing a conformational change. The direct interaction usually lowers the vibrational frequency, whereas the second effect can result in a frequency shift in either direction, accompanied by a variation of intensity in the amide I' band.

Even though the peptides are cyclic and conformationally restricted, the solvent can cause conformational changes. The most common way is by breaking the intramolecular hydrogen bond, and forming hydrogen bonds with the solvent. We believe that the shifts toward low frequency of the spectra in DMSO/D_2O are directly attributable to solvent hydrogen bonding of all four carbonyl groups, with a concomitant breaking of the intramolecular hydrogen bond.

Between solution in DMSO/$CDBr_3$ and DMSO, all C=O vibrations (except for $C=O_4$ in *c*CPGC, *cf.* Table 6-2) shift up. We believe that these frequency changes are due to conformational changes induced by breaking the 1 $\rightarrow$ 4 intramolecular hydrogen bond. In a low polarity solvent, such as bromoform, peptides prefer to form an intramolecular hydrogen bond which is manifested by a shift of the tertiary amide I' vibration by at least 6 cm^{-1}, compared to their value in DMSO (Table 6-2). Upon increasing the DMSO concentration, this hydrogen

bond is broken by stronger solvent interactions, and a slight conformational change seems to occur. This change shifts the carbonyl peak to higher frequencies. Since the observed VCD spectra of the peptides in different solvents vary significantly, but the absorption spectra exhibit only minor changes only, we conclude that the conformation changes of the β-turns cannot be detected reliably by monitoring absorption spectra alone.

6.4.2. VCD Spectra

The VCD spectra of the peptides *c*(GPGC), *c*(GPFC) and *c*(GPdFC) show much larger variations when the solvent is varied than the corresponding absorption spectra. A comparison between the VCD spectra of the three peptides in the same solvent reveals that the peptides actually exhibit quite similar VCD spectra. This coarse observation will lead us to believe that the changes in solution conformation caused by the solvent interaction are more severe than those caused by variation of the peptide sequence.

In *c*(GPGC), a VCD spectrum with a positive/positive/negative pattern is observed in DMSO/$CDBr_3$. This pattern is similar to that observed for *c*(GPGC) in pure DMSO. In DMSO/D_2O, a spectral pattern is observed which is devoid of the tertiary amide (low frequency) VCD intensity, and resembles the VCD of a cyclic peptide, *cyclo*-(Cys-Ala-Cys), which may include a γ-turn.[6-8] The peptides with a larger side group in the 3-position, *c*(GPFC) and *c*(GPdFC), exhibit more significant changes in the VCD spectra as the solvent polarity is varied. They both

exhibit large, all-negative VCD patterns in DMSO/D_2O, which we are unable to interpret at the present time. In this solvent, which is the most polar of the solvents studied, the interactions of the peptide with the solvent dominate and influence the conformation profoundly. The changes in the VCD spectra as a function of solvent polarity could correspond to changes in conformation, or a change in equilibrium populations in a mixture of different conformations. This possibility is very likely since the energies for Type I and Type II turns are very similar for *c*(GPGC).

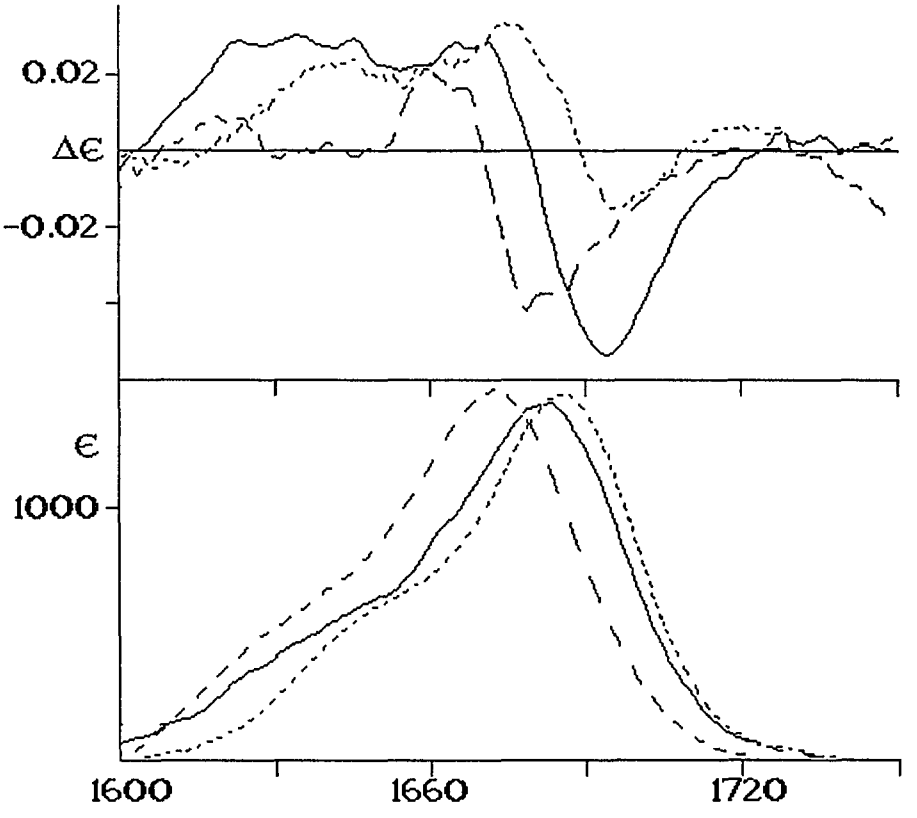

Figure 6-2. Infrared VCD (top) and absorption (bottom) spectra of *cyclo*- (Cys- Pro- Gly -Cys) in DMSO/ $CDBr_3$ (solid trace), DMSO (dotted trace) and DMSO/ D_2O (broken trace)

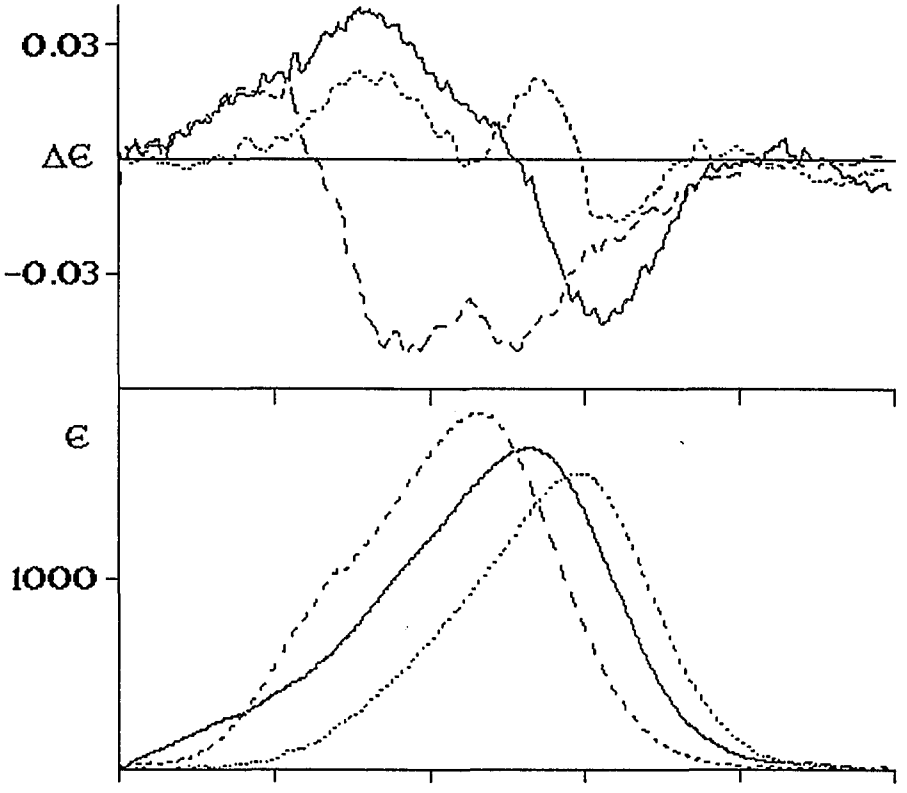

Firgure 6-3. Infrared VCD (top) and absorption (bottom) spectra of *cyclo*- (Cys- Pro- Phe -Cys) in DMSO/ $CDBr_3$ (solid trace), DMSO (dotted trace) and DMSO/ D_2O (broken trace)

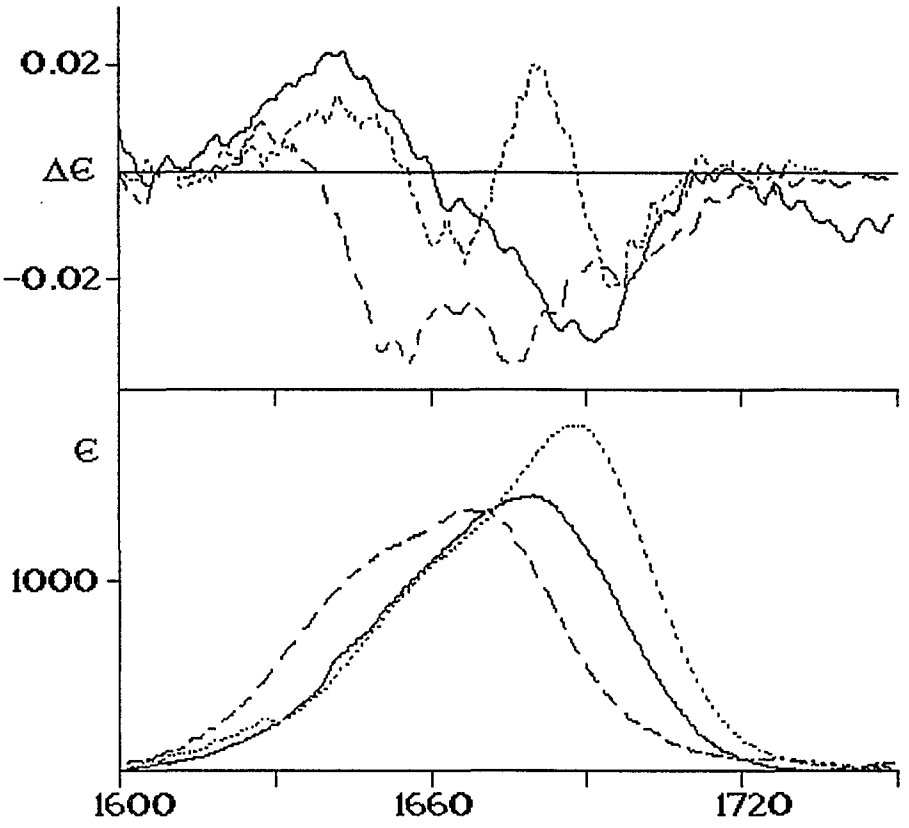

Figure 6-4. Infrared VCD (top) and absorption (bottom) spectra of *cyclo-* (Cys- Pro- DPhe -Cys) in DMSO/ $CDBr_3$ (solid trace), DMSO (dotted trace) and DMSO/ D_2O (broken trace).

Table 6-2 Frequencies [cm^{-1}] of Tertiary and Secondary Amide I' Vibrations

	tert. amide I'	sec. amide I'	$C=O_{i+3}$ amide I'	solvent
cCPGC	1655	1684	1697	DMSO
cCPFC	1664	1688	1703	DMSO
cCPdFC	1661	1687	1700	DMSO
cCPGC	1648	1681	1697	DMSO/$CDBr_3$
cCPFC	1650	1679	1695	DMSO/$CDBr_3$
cCPdFC	1655	1678	1694	DMSO/$CDBr_3$

6.5. DISCUSSION

Because of steric requirements of the individual amino acids in the turns, the Type I β-turns is generally preferred for two L-amino acids in the i+1 and i+2 positions,[6-20] whereas Type II turns are preferred for L-D sequences. A glycyl residue can be accommodated in either a Type I or II turn. Among the molecules studied here, *c*CPFC should prefer a Type I geometry, whereas *c*CPdFC should exist in a Type II β-turn geometry. *c*CPGC can assume either Type I or Type II structures, and most likely exists as an equilibrium mixture of both forms. Previous NMR studied have confirmed these conformational tendencies.[6-21]

Since VCD is a technique which monitors short distance interaction, its conformational sensitivity is particularly pronounced and useful in the studies of small peptides. One of the major advantages of vibrational optical activity is its sensitivity to subtle structural differences of β-turns in slightly different solvent systems. Furthermore, the carbonyl groups of the tetrapeptides introduced above exhibit different amide I' frequencies that are readily distinguishable in infrared absorption and VCD spectroscopies. These different amide I' frequencies are due to the carbonyl group $C=O_i$, adjacent to the tertiary (prolyl) amine, observed at 1655 cm^{-1}, the two carbonyl groups $C=O_{i+1}$ and $C=O_{i+2}$ in the turn which are adjacent to secondary amines (1685 cm^{-1}), and the carboxylic acid $C=O_{i+3}$ group with a frequency of 1697 cm^{-1}. In DMSO/$CDBr_3$, these four peaks could be identified by band decomposition.

The aim of the following discussion is an attempt to interpret the conformational changes observed for the tetrapeptides between pure DMSO and

$DMSO/CDBr_3$, since these spectral changes are far less drastic then the ones observed for $DMSO/D_2O$. Furthermore, we wish to establish whether or not any of the observed spectra represent Type I and Type II β-turn VCD signatures. We shall attempt to determine the effects of the conformational changes induced by the different solvents on the VCD spectra by assuming that the VCD spectra in the amide I' region are determined mostly by the coupling among the carbonyl groups within a given geometry. In the cyclic tetrapeptides that were used to model β-turns, there are only three carbonyls groups involved in the turn itself, while $C=O_{i+3}$hich is outside the ring, is expected to be in an undefined geometry. As pointed out before, one of the remaining three carbonyl groups has a low frequency ($C=O_i$), and two of them have a relatively high frequencies (*cf.* Table 6-2), and it is easily to assign their VCD features based on their frequencies.

We start this attempt to interpret the observed VCD data by presenting, in Figures 6-5 and 6-6, the calculated VCD and absorption spectra for standard Type I and Type II β-turn geometries. These calculations were carried out using the carbonyl coordinates extracted from structural data of the two turns, a constant carbonyl transition moment of 0.29 D, and 1645 and 1685 cm^{-1} transition frequencies for the tertiary ($C=O_1$) and secondary ($C=O_2$ and $C=O_3$) amide frequencies, respectively. Plotted along with the calculated VCD spectra are the observed VCD spectra of *c*(GPFC) in DMSO (Figure 6-5) and *c*CPdFC in $DMSO/CDBr_3$ (Figure 6-6). Similar cyclic dipeptides were found previously to exist in these solvents in Type I and Type II β-turn conformations. [6-21,22]

Next, we shall attempt to quantify the origin of the spectral patterns observed and calculated. Two kinds of VCD patterns were observed and calculated for these model peptides. One pattern (Figure 6-5) consists of a couplet at relatively high frequency that covers a narrow frequency range, and a low frequency positive VCD. The couplet is attributed to interactions between two

high frequency carbonyl groups, $C=O_{i+1}$ and $C=O_{i+2}$ and exhibits a positive/negative pattern with a zero crossing point located at the maximum absorption of the secondary amide I' band. This $C=O_{i+1}$ / $C=O_{i+2}$ interaction indicates a favorable distance/geometry between these groups. The VCD of the $C=O_i$ group is monosignate, and at lower frequency.

The calculated and observed VCD couplet shown in Figure 6-6 is located at lower frequency, and covers a wider frequency range. Therefore, we believe it is due to the interaction of a low frequency and a high frequency carbonyl group, either $C=O_i$ with $C=O_{i+1}$, or $C=O_i$ with $C=O_{i+2}$, or both. Since it involves the coupling between a high and a low frequency carbonyl vibration, the zero crossing of the VCD spectrum is located between the absorption of the secondary and tertiary amide I'. It, too, has a positive/ negative pattern, but the spectrum is much broader. Here, either the $C=O_i$ / $C=O_{i+1}$ or the $C=O_i$ / $C=O_{i+2}$ groups must be in a good coupling geometry.

The dipolar coupling energies V_{ij} between interacting C=O groups, listed in Tables III and IV, may provide a handle to the origin of the observed VCD. The V_{ij} elements depend on the distance and the orientation between the interacting carbonyl groups. To a first approximation, we may assume that a small conformational change in a cyclic molecule will alter the orientation much more than the distance; thus, the coupling energies may provide another sensitive clue to conformation.

According the exciton formalism, large rotational strengths are created for perpendicular geometry between the interacting groups. Such a geometry, however, produces the smallest coupling energy and splitting of the exciton components. On the other hand, a parallel or antiparallel geometry between the interacting groups will produce maximum splitting, but minimal rotational strengths. Thus, one may conclude that large VCD intensities are associated with

intermediate values of V_{ij} if the distance between the carbonyl groups does not change much between the conformers.

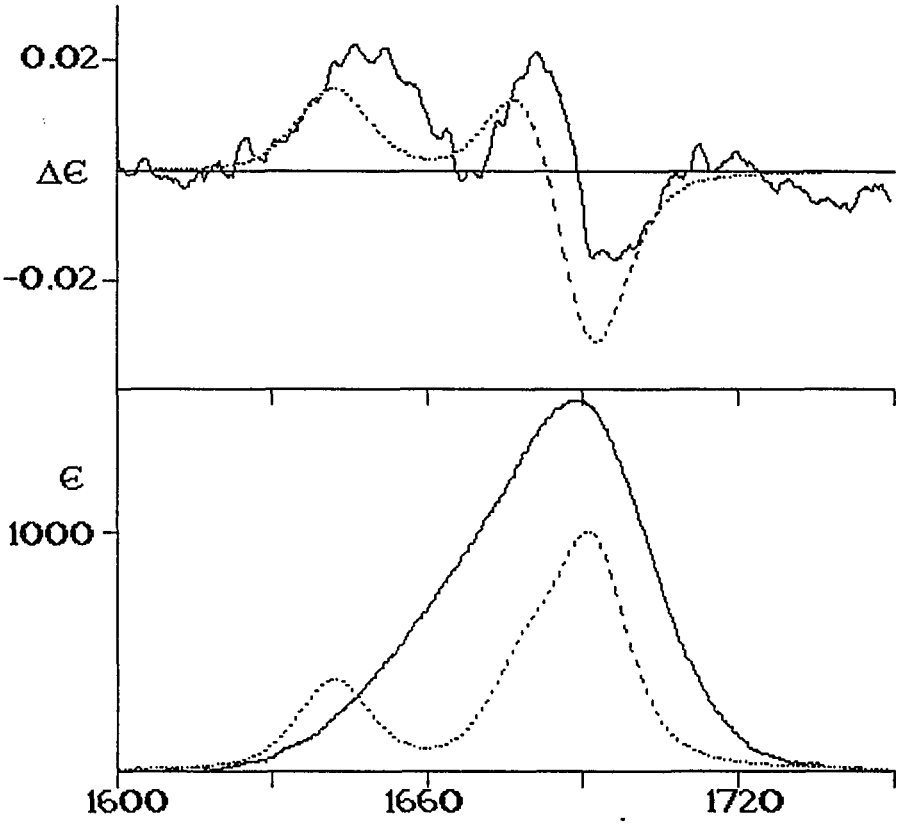

Figure 6-5. Infrared VCD (top) and absorption (bottom) spectra of *cyclo-* (Cys- Pro- Phe- Cys) in DMSO (solid trace), and calculated spectrum Type I β-turn(dotted traces).

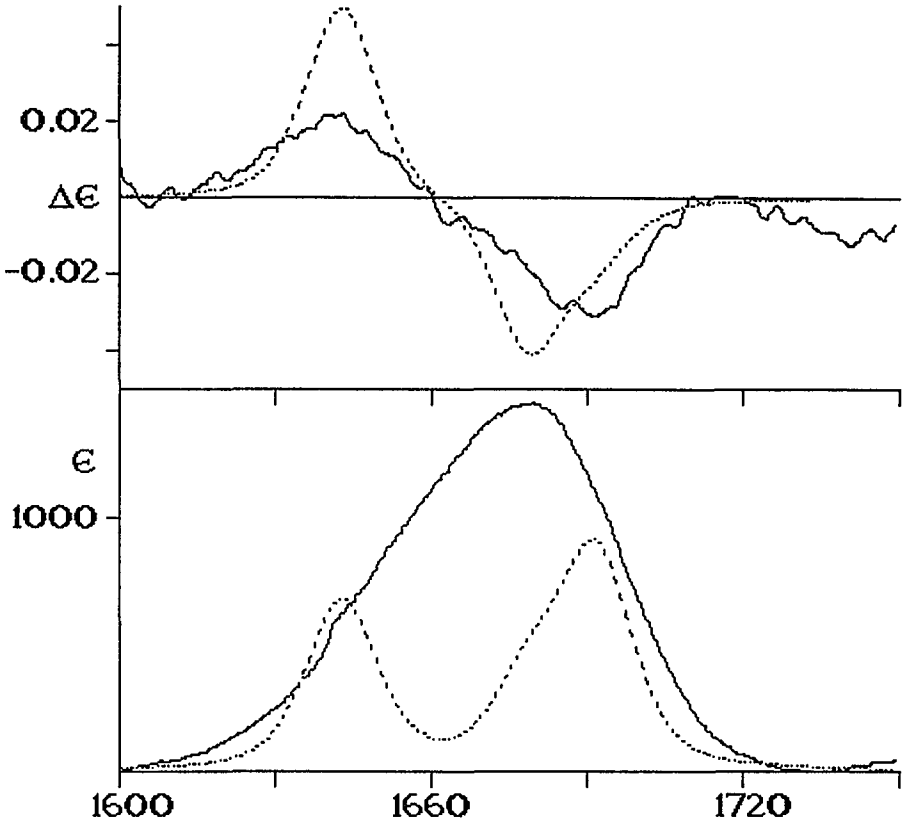

Figure 6-6. Infrared VCD (top) and absorption (bottom) spectra of *cyclo-* (Cys- Pro- D-Phe- Cys) in DMSO /$CDBr_3$ (solid trace), and calculated spectrum Type II β-turn (dotted traces).

For the Type I β-turn, (*cf.* Tables 6-3) V_{23} is responsible for the mixing of the $C=O_2$ / $C=O_3$ coordinates, whereas the large and small coupling energies V_{12} and V_{13}, may prevent the formation of a couplet as discussed above: a large term because of near parallel geometry, and a small term for lack of coupling. In the Type II turn, V_{12}, V_{13} and V_{23} all are similar in magnitude and contribute to the mixing of $C=O_i$ / $C=O_{i+1}$ and the $C=O_i$ / $C=O_{i+2}$. Inspection of Figure 6-1 reveals that in the standard Type I geometry, $C=O_i$ and $C=O_{i+1}$ are close to each other, and both point below the plane of the ring. This near parallel geometry will produce a large coupling energy, but little optical activity. $C=O_{i+1}$ and $C=O_{i+2}$ interact with an energy of about 6 cm^{-1}, which appears the optimum value for generating VCD couplets.

Based on these arguments, the observed VCD spectra of the three tetrapeptides can be categorized by a combination of $C=O_i$ / $C=O_{i+1}$ and $C=O_i$ / $C=O_{i+1}$ interactions (low frequency couplet) and a $C=O_{i+1}$ / $C=O_{i+2}$ interaction (high frequency couplet). *c*(GPFC) in DMSO exists mostly in the Type I conformation (Figure 6-3, short dashes). In the less polar solvent DMSO/$CDBr_3$, the spectrum resembles that of the Type II conformation, but still contains some positive intensity just below the zero crossing frequency. We interpret this to be due to a mixture of Type I and Type II conformation.

In contrast, *c*(GPdFC) exhibits nearly pure Type II conformation in the low polarity solvent DMSO/$CDBr_3$ and a mixture of Type I and Type II structures in pure DMSO. Based on these facts, we conclude that the higher polarity solvent will expose the carbonyl groups to the solvent, so that the $C=O_2$ prefers to stay in position similar to that found in the Type I turn, and secondly, that the disulfide bond certainly makes some contribution to the β-turn conformation. It can either limit the formation of intramolecular hydrogen bond

or constrain the distance between C_i and C_{i+3}. Similar results of interconversion between turn conformations were found using other techniques in cyclic peptides containing Aib at the i+2 position [6-21].

We expect the VCD spectrum of *c*(CPGC) in DMSO/$CDBr_3$ (*cf.* Figure 6-2) to be a mixture of both Type I (or III) and Type II turns, with the former dominating. With increasing solvent polarity, the fraction of Type I conformation becomes more pronounces which is manifested by an increase in the $C{=}O_{i+1}$ / $C{=}O_{i+2}$ couplet.

Another example of a β-turn that was studied by VCD is *c*(GPGdAP) in bromoform. The observed VCD and absorption spectra are shown in Figure 6-7. The absorption spectrum consists of two major peaks with frequencies of 1640 and 1690 cm^{-1}. The VCD spectrum shows two couplets, a strong negative couplet at low frequency (1630-1650 cm^{-1}), and a positive couplet at high frequency (1685-1700 cm^{-1}). NMR[6-23] and X-ray[6-24] studies indicated that this pentapeptide forms a Type II β-turn stabilized by a hydrogen bond between $C{=}O_{Gly(1)}$ and $HN_{D\text{-}Ala}$, and a γ-turn between $C{=}O_{D\text{-}Ala}$ and $HN_{Gly(1)}$. The carbonyls involved in the two turns are both tertiary amide I' groups that form intramolecular hydrogen bonds and are consequently observed at low frequency. Furthermore, the two tertiary C=O groups of *c*(GPGdAP) are located below the ring of the peptide and are very close each other. The three secondary C=O groups are above the peptide ring, but only $C{=}O_{Pro(2)}$ and $C{=}O_{Gly(3)}$ are relatively close to each other, and $C{=}O_{Pro(5)}$ is far away from any other carbonyl group. Thus, one would expected two separate couplets: a low frequency couplet between the tertiary amide vibrations, and a high frequency couplet for the secondary amides. The observed VCD spectrum exhibits this pattern.

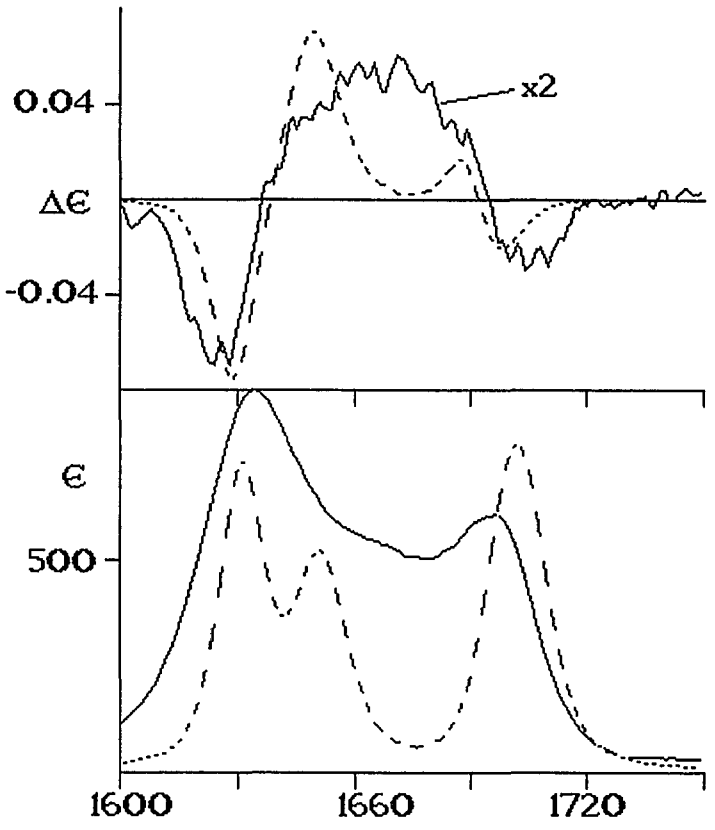

Figure 6-7. Infrared VCD (top) and absorption (bottom) spectra of *cyclo-* (Gly- Pro- Gly- d-Ala- Pro) in $CDCl_3$ (solid trace), and calculated spectrum from NMR structural data (dotted traces).

Table 6-3 Dipole-dipole Coupling Energies (cm^{-1}) for Type I β-turn (between $C=O_i$, $C=O_{i+1}$ and $C=O_{i+2}$)

V_{ij}	i =i	i =i+1	i =i+2
j =1	-	9.26	0.24
j =2		-	6.4
j =3			-

Table 6-4 Dipole-dipole Coupling Energies (cm^{-1}) for Type II β-turn (between $C=O_i$, $C=O_{i+1}$ and $C=O_{i+2}$)

V_{ij}	i =i	i =i+1	i = i+2
j =1	-	-5.60	-6.40
j =2		-	5.5
j =3			-

Table 6-5 Distribution of Conformations in the Cyclic Tetrapeptides

	DMSO	DMSO/$CDBr_3$
c(CPGC)	II, I (III)*	II & I (III)
c(CPFC)	I (III)	II & I (III)
c(CPdFC)	II & I(III)	II

This coupling pattern can be confirmed by NECO computations. Large values of V_{ij} are found to occur between the tertiary amide I' vibrations of $C=O_1$ and $C=O_4$, and the secondary amide I' vibrations $C=O_2$ and $C=O_3$. The weakest coupling occurs with $C=O_5$. Computed VCD spectra, based on the NMR solution structure, are shown in Figure 6-7. The frequency and shapes of the calculated VCD patterns agree reasonably well with the observed VCD results: the couplet at low frequency corresponds to the two tertiary carbonyls of the fused turns, and the positive couplet at higher frequency represents a partial spectrum characteristic of β-turns. The computed VCD spectrum based on the X-ray data shows less

agreement with the observed VCD spectrum. This is understandable in terms of a conformational change the of peptide experiences due to the forces in the crystal. Our data demonstrate how sensitive VCD is to conformational changes of peptides, even if this change is relatively minor. The above results can also be used to draw same direct conclusion about the structure of the peptide, namely the large distance and unfavorable coupling geometry of $C=O_5$. Furthermore, since the VCD pattern of *c*(GPGdAP) is determined by fused β- and γ-turns, and we cannot use it for the interpretation of individual or single β-turn. Finally, the interpretation of the VCD results of *c*(GPGdAP) suggests that the NECO model is a adequate method for the qualitative interpretation of the observed VCD spectra.

6.6 CONCLUSION

After the discussion in the previous section, the question arises of whether or not a VCD pattern for "prototypical turn structures" exists, and what VCD spectrum can be expected for each of the β-turn conformations. Although we have published the VCD spectrum of *c*(GPGdAP) before and had hoped that it may exhibit a "typical" β-turn VCD, we conclude after this more detailed study that *c*(GPGdAP) gives the VCD pattern for fused turn structures only, and not that of a single β-turn. However, it appears that the VCD spectra of *c*(CPFC) in DMSO and that of *c*(CPdFC) in DMSO/$CDBr_3$ represent the VCD patterns of standard Type I and Type II β-turn structures, respectively. We arrive at this conclusion by a comparison of previously derived structures and observed VCD results, and a comparison of the observed VCD patterns with those calculated for standard β-turn geometries. These calculations are based on the ϕ and φ angles of residues i+1 and i+2 in standard Type I (-60, -30; -90, 0) and Type II (-60, 120;

80, 0) β-turns). These four angles determine uniquely the geometry of the three carbonyl groups involved in β-turns.

Experimentally and computationally, we obtain a positive couplets for both Type I and Type II turns. For the Type I turn, an additional positive VCD signal is observed at about 1635 cm^{-1}, followed by the couplet at about 1675/1690 cm^{-1}. For the Type II turn, a broad couplet between 1635/1690 cm^{-1} is observed.

REFERENCES

6-1) Kabsch, W. and Sander, C., (1983) *Biopolymers*, 22, 2577-2637

6-2) Chou, P. Y. and Fasman, G.D., (1977) *J. Mol. Biol.*, 115, 135-175

6-3) Venkatachalam, C. M., (1968) *Biopolymers*, 6, 1425-1436

6-4) Lewis, P. N., Momany, F. A. and Scheraga, H.A., (1971) *Proc.Natl.Acad.Sci.USA*, 68, 2293-2297

6-5) Zimmerman, S. S. and Scheraga, H.A., (1977) *Proc. Natl. Acad. Sci.USA*, 74, 4126-4129

6-6) Xie, P. and Diem, M., (1995) *J.Amer.Chem. Soc.*, 117, 429-437

6-7) Wyssbrod, H. and Diem, M., (1992) *Biopolymers*, 31, 1237 - 1242

6-8) Xie, P., Zhou, Q. and Diem, M., (1994) *Faraday Discussions.*, 99, in press

6-9) Xiang, T., Goss, D.J. and Diem, M., (1993) *Biophysical Journal*, 65, 1255-1261

6-10) Venkatachalapathi, Y.V. and Balaram, P., (1979) *Nature*, 281, 83-84.

6-11) Nair, C.M.K., Vijayan, M., Venkatachalapathi, Y.V. and Balaram, P., (1979) *J. Chem. Soc Chem.Commun.*, 1183-1184.

6-12) Venkatachalapathi, Y.V., Prasad, B.V.V and P. Balaram, (1982) *Biochemistry*, 21, 5502-5509

6-13) Hollosi, M., Kawai, M. K., Fasman, (1985) *Biopolymers*, 24, 211-242

6-14) Perczel, A., Hollosi, M., Foxman, B. M. and Fasman, G. D., (1991) *J.Amer.Chem.Soc.*, 113, 9772-9784

6-15) Hollosi, M., Majer,Z., Ronal, A.Z., Magyar, A., Medzihradsky, K., Holly, S. and Fasman, G.D., (1994) *Biopolymers*, 34, 177-185

6-16) Rose, G.D., Gierasch, L.M. and Smith, J.A., in Adv. Protein Chemistry, Anfinson, C.B., Edsall, J.T. and Richards, F.M., Eds., (1985), Academic Press, NY

6-17) Woody, R.W., in *Peptides, Polypeptides and Proteins,* E.R.Blout, F.A.Bovey, N.Lotan and M.Goodman, Eds., Wiley, New York, (1974) pp 338-350

6-18) Woody, R.W., in "*The Peptides: Analysis, Synthesis , Biology*", V.J. Hruby, Ed., Academic Press, New York, (1985) 15-113

6-19) Diem, M., Roberts, G.M., Barlow, A. and Lee, O., (1988) *Applied Spectrosc.*, 42, 20-28

6-20) Chandrasekaran, R., Lakshminarayana, A.V., Pandya, U.V. and Ramachadran, G.N.,
(1973). *Biochim. Biophys. Acta,* 303, 14-27

6-21) Rao, B.N.N., Kumar, A., Balaram, H., Ravi, A. and Balaram, P., (1983) *J.Am.Chem.Soc.*, 105, 7423-7428.

6-22) Imperiali, B. ,Fisher, S.L. Moats, R.I. and Prins, T. J., (1992). *J.Amer.Chem.Soc.* 114, 3182-3188.

6-23) Pease, L.G. and Watson, C., (1978), *J. Amer.Chem.Soc.*, 100, 1279-1286

6-24) Karle, I., (1978) *J. Amer.Chem.Soc.*, 100, 1286-1289

CHAPTER SEVEN

A CONFORMATIONAL STUDY OF LINEAR TETRAPEPTIDES BY VCD

In this chapter, observed VCD spectra of three linear tetrapeptides are reported. Based on analysis of those spectra, we find that the linear peptide can constructure stable conformations under the same condition as do the cyclic analogs, but their conformations do not resemble those of their cyclic analogs. We conclude that the $\alpha C_{(i)}$ -$\alpha C_{(i+3)}$ distance is a primary factor in forming a β-turn, particularly, in forming a standard type I or type II turns. Under condition of distance constraint, the types of turns formed depend on the sequence of residues at the third position in the turn area.

7.1. INTRODUCTION

Small peptides, particular tetrapeptides, prefer to form β-turn structure in proteins, when proline is at the second position of this peptide. The type of turns depends on the residue after proline.[7-1a,b,c.]

In general, β-turns can be defined as a site at which a polypeptide chain changes direction. There are a couple of characteristics that can be used to examine β-turn structures in proteins. Based on the X-ray data, the $\alpha C_{(i)}$ - $\alpha C_{(i+3)}$

distances of all 4651 tetrapeptides in proteins were computed.[7-2, 3a,b,c.] Those whose distances were below 7Å and not in a helical region were considered as β-turn. Helical regions in proteins are easily recognizable, since at least 3 consecutive tetrapeptides all have $\alpha C_{(i)}$ - $\alpha C_{(i+3)}$ distances below 6 Å. Hence, after omission of consecutive helical tetrapeptides, it is easy to locate the isolated tetrapeptides having $\alpha C_{(i)}$ - $\alpha C_{(i+3))}$ distances below 7 Å as candidates of β-turns.

The second characteristic for recognition of a β-turn is the dihedral angles, ϕ and φ, of the backbone polypeptide chain. The ϕ, φ angles of β-turns are mainly characterized by the angles of the middle 2 residues (i+1 and i+2) of which 3 types, I, II, III and their conformational mirror images I', II' and III', were descried by Venkatachalam. The angles of each turn are listed on Table 6-1. One turn in right-handed α-helix will be presented by 4 consecutive residues having approximate ϕ, φ angles (-57.4° and -47.5°) for each residue.

The $O_{(i)}$ - $N_{(i+3)}$ distances were counted as a third characteristic of β-turn, because 1 → 4 hydrogen bonds were formed very often in regions of β-turns. In sum, it is desirable to find out what is a primary importance for forming and stabilizing β-turn structure and how does the sequence in peptides deduce specific β-turns in both cyclic and linear tetrapeptides?

Reviewing data about the conformation of β-turns in proteins, it is hard to define a specific or unique conformation for β-turns. Several types of β-turn were found in proteins. The formation of such β-turns depends on the sequence in position i+1 and i+2 of turn region and the environment outside the turns, for example, the sequences of the peptide chain front and behind of the turn core and solvent effects on hydrogen bonding.

Because of the diversity of the φ and ϕ angles in various turn structures, several research groups have studied on the conformation of β-turns by using small, linear peptides as model peptide.[7-4,5,6.] These model peptides being used

have same properties, which can form either an extra intra-molecular-hydrogen bond beside the 1 → 4 hydrogen bond or a linkage between head and tail of β-turn core . It does seem to provide a same effect as a disulfide bond between $\alpha C_{(1)}$ and $\alpha C_{(4)}$. The basic idea in those studies of model peptide is to limit the distance between $\alpha C_{(1)}$ and $\alpha C_{(4)}$ in a peptide. Under such a constraint, the influence of residues at position i+1 and i+2 of turn becomes a primary factor, which decides what kind of turns can be formed.

Attempts have been made previously to identify β-turns in cyclic peptides, because they may be considered to have a rigid conformation. Actually, the conformations of such cyclic peptides can be varied by the nature of the chemical environment. As a follow up studies of the conformations of cyclic model tetrapeptide, we report here the VCD data of linear tetrapeptides with sequences identical with the cyclic ones, and under the same condition used in the case of cyclic peptides. The goal of this study was trying to determine the key characteristics which contribute to the formation and stabilization of turn, and the behavior of peptide sequence in forming turns. Since the VCD spectrum detects a short range interactions between carbonyls of peptide, we can focus on a locally coupling interaction among three carbonyls (i, i+1 and i+2) in β-turns.

7.2. MATERIALS AND METHODS

All data presented in this section were collected on the dispersive VCD spectrometer at Hunter college. The details of instrumentation and preparation of samples are given in the previous chapter. The concentration dependence of conformation was tested by diluting the concentration of peptide to 10mM. At this concentration, no conformational change in those peptides were observed.

7.3. RESULTS

The observed IR and VCD spectra of three linear tetrapeptides, *l*(CPGC), *l*(CPFC) and *l*(CPdFC) in different solvents, are shown in Figures 7-1, 2, 3 and 4. The solvents were DMSO:$CDBr_3$ (1:2); DMSO; DMSO/D_2O (1:2) and TFE, which represent different polarities and have various hydrogen bonding ability. In general, a less polar solvent promotes intra-molecular-hydrogen bonds in peptide and a polar solvent that is a hydrogen bond donor or acceptor destroys intra-molecular-hydrogen bonds and release constraints on the peptide chain.

7.3.1. Absorption spectra

The IR spectra show a broad peak with a low frequency shoulder in the amide I' region. These features indicate that two amide I' absorptions, tertiary and secondary ones are involved. The tertiary amide I' is located at a lower frequency region compared with the secondary one. Shifts in IR spectra with changes of solvents can be interpreted that such a change on frequency and intensity reflects either variation on intra-molecular-hydrogen bonds or a change of peptide conformation in peptides, such as polar groups in the peptide being exposed to the solvent. The three tetrapeptides exhibit very similar IR spectra in each solvent. A summery of the spectral data is listed in Table 7-1.

Table 7-1. Freuqency (cm-1) of amude I' vibration of linear tetrapeptides

Solvent	Tertairy Amide I' cm^{-1}	Secondary Amide I' cm^{-1}
Bromoform:DMSO (2 : 1)	1660	1680
DMSO	1665	1685
D2O : DMSO (2 : 1)	1645	1670
TFE	1655	1670

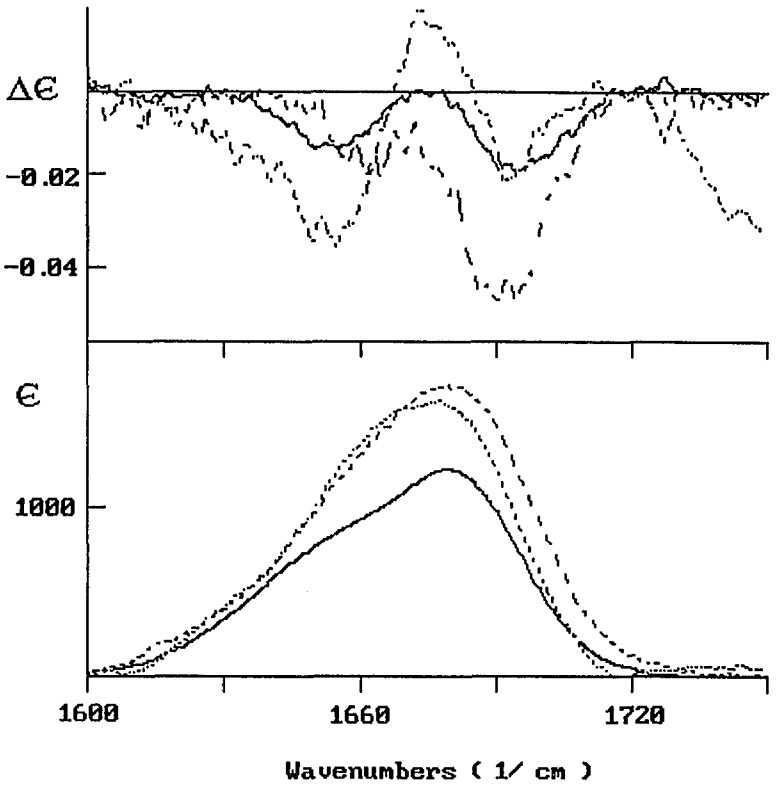

Figure 7-1 Infrared absorption (bottom) and VCD spectra (top) of *l*(CPGC) (solid line); *l*(CPFC) (dotted line) and *l*(CPdFC) (broken line) in DMSO: Bromoform (1:2 by volume).

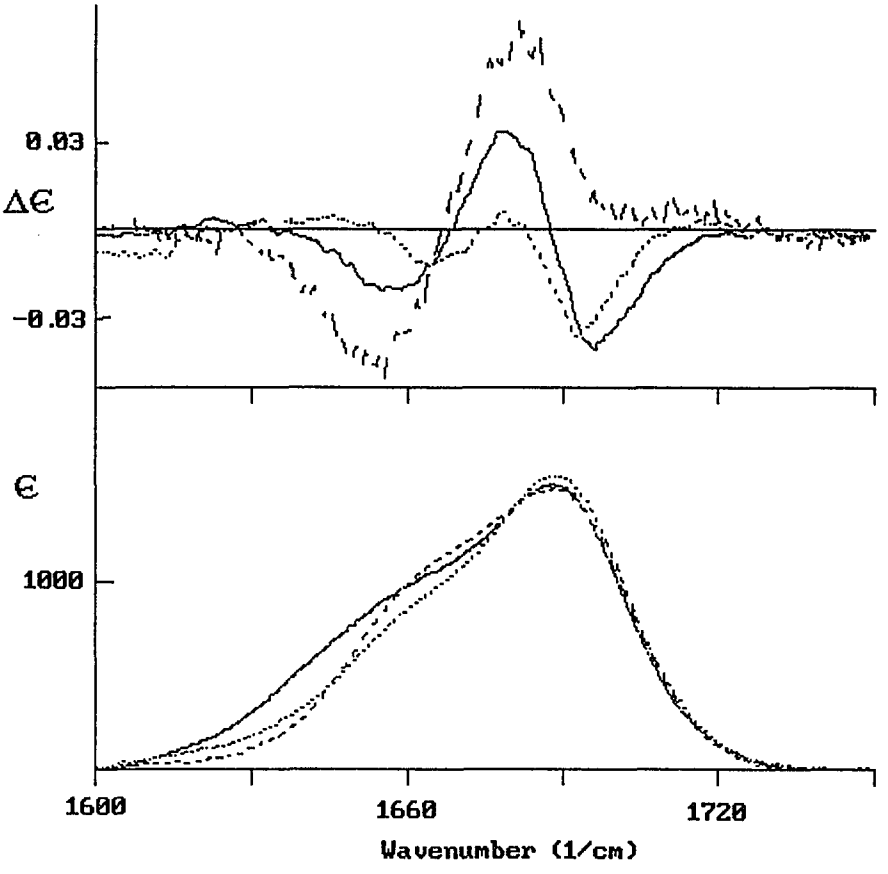

Figure 7-2 The Infrared absorption (bottom) and VCD spectra (top) of *l*(CPGC) (solid line); *l*(CPFC) (dotted line) and *l*(CPdFC) (broken line) in DMSO.

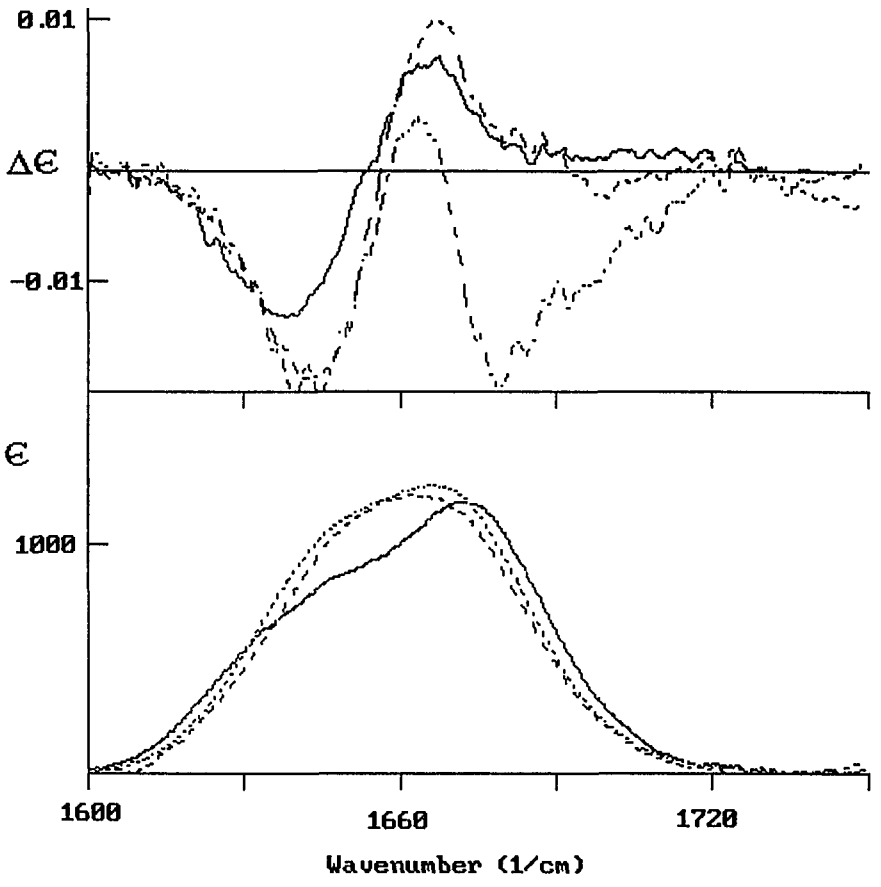

Figure 7-3 The Infrared absorption (bottom) and VCD spectra (top) of *l*(CPGC) (solid line); *l*(CPFC) (dotted line) and *l*(CPdFC) (broken line) in DMSO:D_2O (1:2by volume).

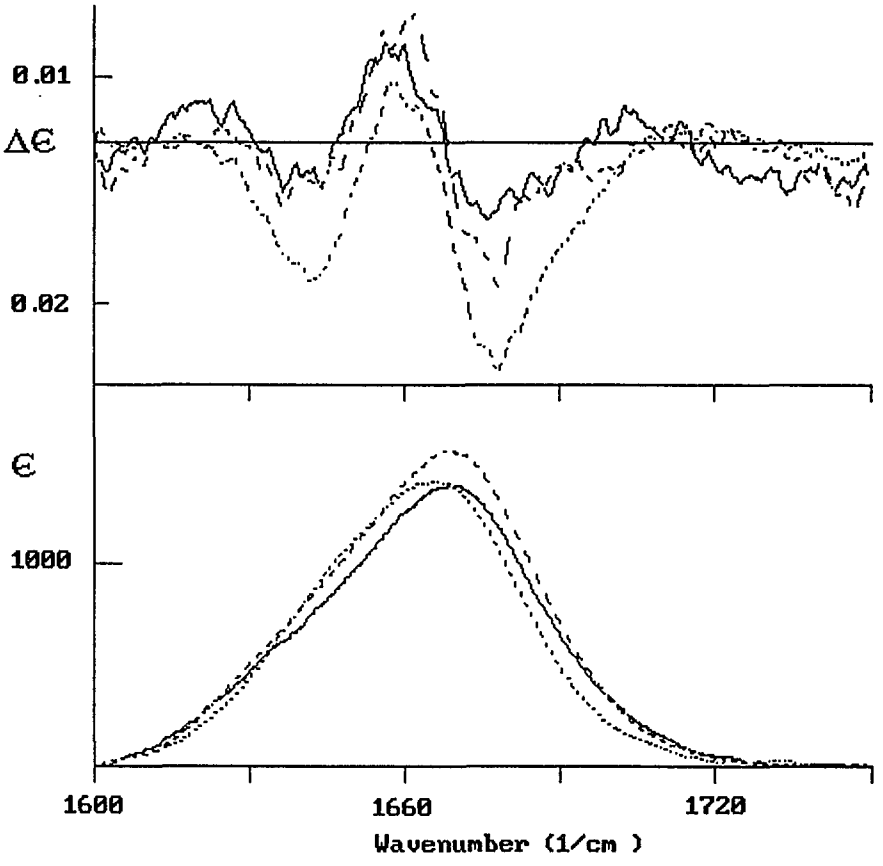

Figure 7-4 The Infrared absorption (bottom) and VCD spectra (top) of *l*(CPGC) (solid line); *l*(CPFC) (dotted line) and *l*(CPdFC) (broken line) in TFE.

In a low polarity solvent, bromoform, the IR spectra of the three peptides exhibit a broad and asymmetric peak. The absorbance of the tertiary amide I', $C=O_{(i)}$, of the three peptide occurs at 1655-1660 cm^{-1} reflecting the formation of a hydrogen bond between $C=O_{(i)}$ and $NH_{(i+3)}$. The higher frequency peak in absorption spectra is composed of two kinds of carbonyls: $C=O_{(i+1)}$ and $C=O_{(i+2)}$ both are secondary amide I' and non-hydrogen bonded carbonyl groups with maximum at 1675-1680 cm^{-1}. Their geometry would be fixed in certain conformations of the peptides. Therefore, they might couple with each other , if their orientation is suitable. $C=O_{(i+3)}$ is free and independent one (far away from others). It has an amide I' peak in about 1690 cm^{-1}.

The polar, hydrogen bond acceptor solvent, DMSO, broadens the IR peaks and shifts them up by about 5-10 cm^{-1}. In principle, DMSO should break intra-molecular-hydrogen bonds of $NH_{(i+3)}$, since S=O group of the DMSO forms hydrogen bonds with NHs in the peptide. This effect, however, can not explain why all peaks become broad and shift to higher wavenumber. An alternative interpretation of the DMSO effect is: it is due to the high dielectric constant of DMSO.

TFE is a hydrogen bond donor. It shifts the frequency of amide I' to lower wavenumber region, and the IR spectra in TFE become more symmetric. Water can form hydrogen bonds with C=O and NH groups. The frequency of all C=O are down shifted, and the peak shape of IR spectra become symmetric. TFE and D_2O seem to cause a similar conformational changes in these peptide.

In general, the kind of β-turns that can be formed depends on the residues at the third position in a turn, where proline is at the second position. Review of these IR spectra of the three peptides with various residues in the third position does not show a pattern that can distinguish the conformational differences of

three peptides, even though there is some solvent dependence observed. Structural differences in these peptide has been confirmed by other techniques. [7-4,5]

The correspondence between spectra and structure is best understood for proteins in D_2O.[7-6] For example, bands centered between 1650-1658 cm^{-1} are associated with α-helical segments, whereas the random coil segments are associated with an IR band around 1640-1648 cm^{-1}. The IR bands between 1620-1640 cm^{-1} have been assigned by many authors to β-pleated sheets. The amide I vibration at higher frequencies is considered to β-turn conformation. However, these frequency region for amide I vibration, which may relate to the structure of protein, actually should be shifted, when the protein is in a different solvent or chemical environment, even though their conformation may not change at all. Consequently, the examination of polypeptide conformation, through the analysis of their IR spectra, is somehow limited by the lack of correlation between specific backbone conformations and individual component bands.[7-7] Furthermore, because of the diversity of turn conformation and broad band shapes in the IR spectra from proteins, the interpretation of the conformation of β-turns in protein is curiously difficult by the analysis of their IR spectra alone.

7.3.2. VCD Spectra

The observed VCD spectra of the peptides produce entirely different features as the solvent is varied. For *l*(CPFC), a VCD spectrum with a larger negative / positive / a smaller negative (n / p / *s*n.) pattern is observed in non-polar solvent, whereas in TFE, its VCD spectrum shows a pattern with a *s*n / p / n. couplet. These spectra form approximate mirror images pairs.(Figure 7-5) VCD spectra of *l*(CPFC) in pure DMSO and a DMSO /D_2O area similar with n. / p. pattern. A minor difference occurs in that the ratio between the negative part

and the positive part of VCD spectra.(Figure 7-6.) That implies that a polarity change from pure DMSO to DMSO/D_2O does not alter conformation of *l*(CPFC).

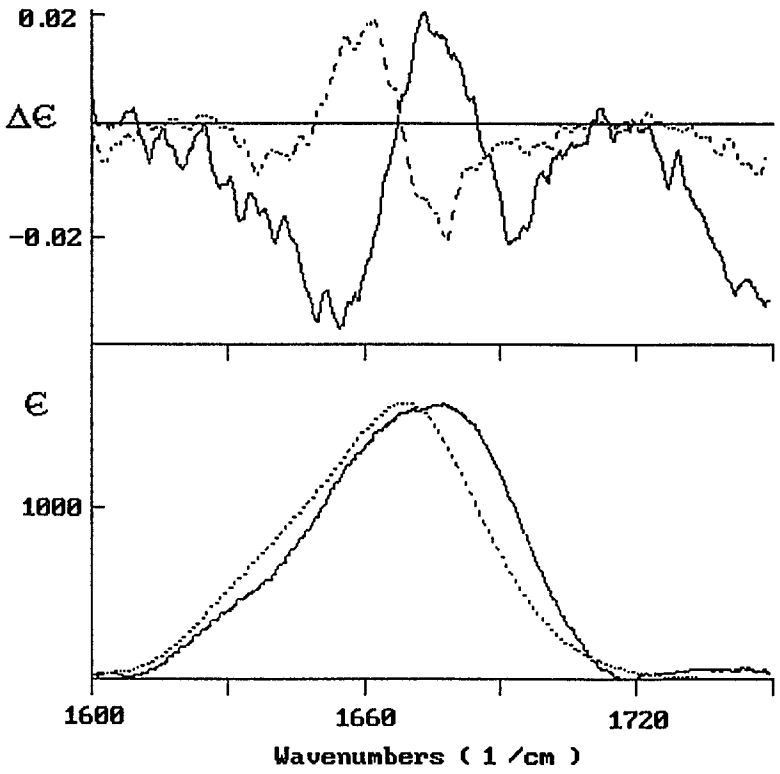

Figure 7-5 The absorptional (bottom) and VCD spectra (top) of *l*(CPFC) in DMSO : Bromoform = 1:2 (solid line) and in TFE (dotted line), respectively.

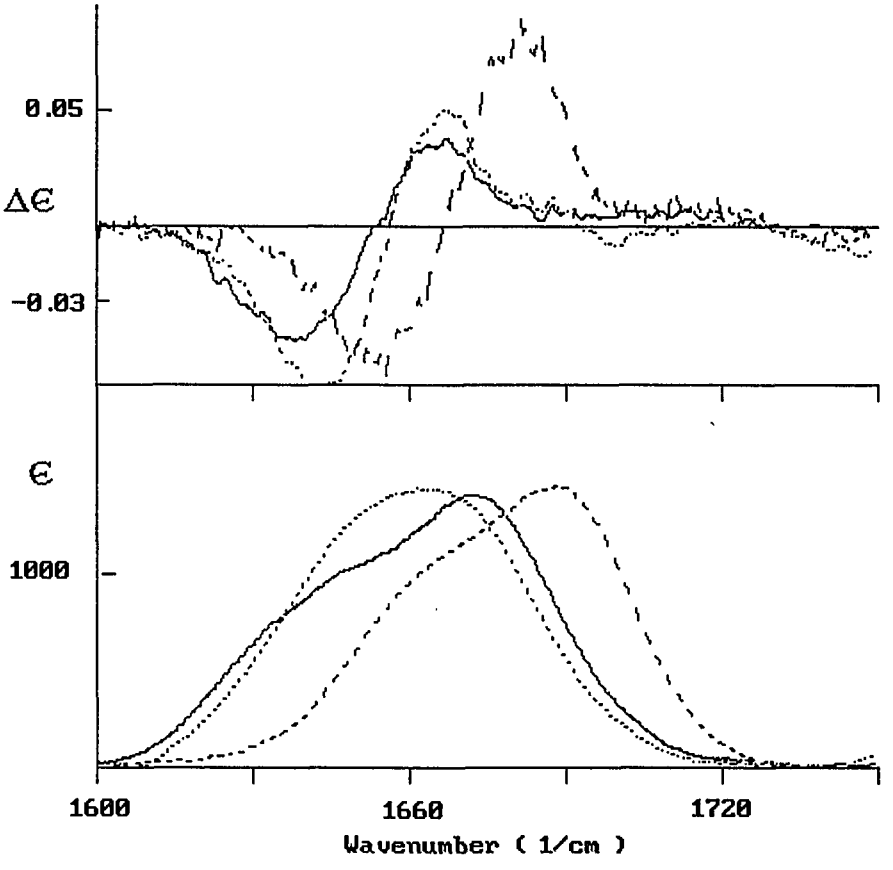

Figure 7-6. The infrared absorptions (bottom) and VCD spectra of *l*(CPGC) in D_2O/DMSO(solid line); and *l*(CPFC) in D_2O/DMSO (dotted line) as well as DMSO (Broken line), which exhibit same patterns, respectively.

In *l*(CPGC), the spectrum from DMSO / D_2O has an identical pattern as that of *l*(CPFC) in the same solvent. But in pure DMSO, the pattern of *l*(CPGC) matches the shape of pattern (n / p / n) of *l*(CPFC) in TFE and is similar to the spectrum of *l*(CPFC) in bromoform/DMSO. (Figure 7-7). When it is in less polar solvent, two negative peaks were observed in its VCD spectrum. That spectrum resembles the spectrum of *l*(CPdFC) in D_2O/ DMSO. TFE brings about a similar pattern of *l*(CPGC) as it in case of *l*(CPFC), but with weak signal level. So we conclude that conformation of *l*(CPGC) in polar solvent is same as that of *l*(CPFC) in less polar solvent, whereas its conformation in less polar solvent resembles that of *l*(CPdFC) in more polar solvent. The behavior of *l*(CPGC) in various solvents is expected and has been confirmed by other techniques.

The VCD spectra of *l*(CPdFC) in solvents of various polarity are quite different from those of other peptides. The common part of the VCD pattern of *l*(CPdFC) is the negative bias of the couplet produced by secondary carbonyls at high frequency.(Figure 7-8)

7.4. DISCUSSION

Based on analysis of these VCD spectra from the three linear peptides, their conformations seem to have no features in common with their cyclic analogs, even though they have the same sequences and data we acquired under same conditions. This finding suggests two possibilities: One is that linear peptides are so flexible in those solvents that they may not form a stable conformation at all. Or they may create conformations other than a regular type I or type II β-turn, which were formed by their cyclic analogs. The strong VCD

spectra of those peptides support the second interpretation, since lack of conformational stability will manifest itself by a lack of VCD.

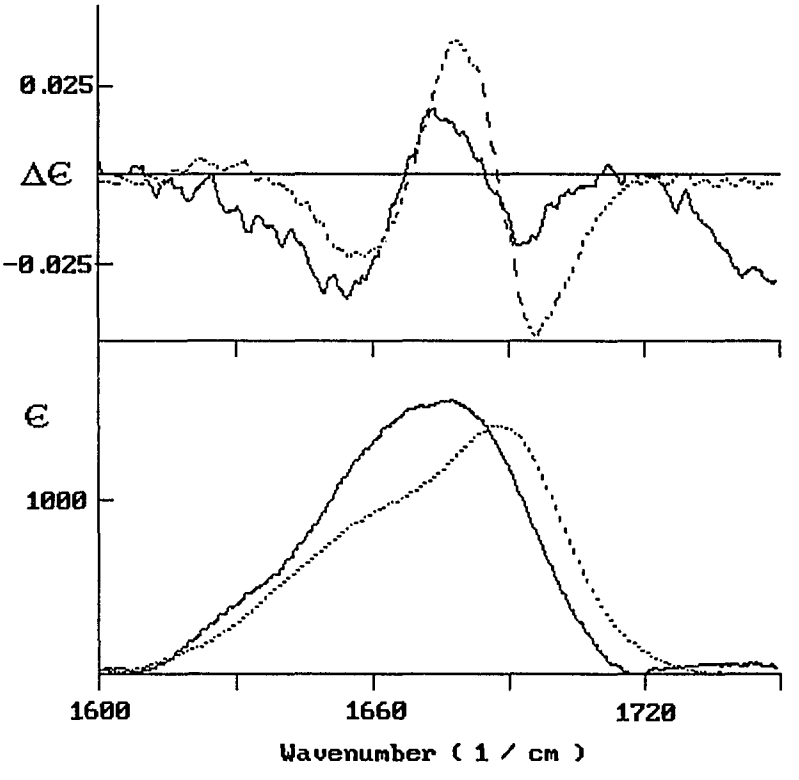

Figure 7-7. The infrared absorption (bottom) and VCD spectra (top) of *l*(CPFC) in DMSO/Bromoform (solid line) and *l*(CPGC) in DMSO (dotted line), respectively.

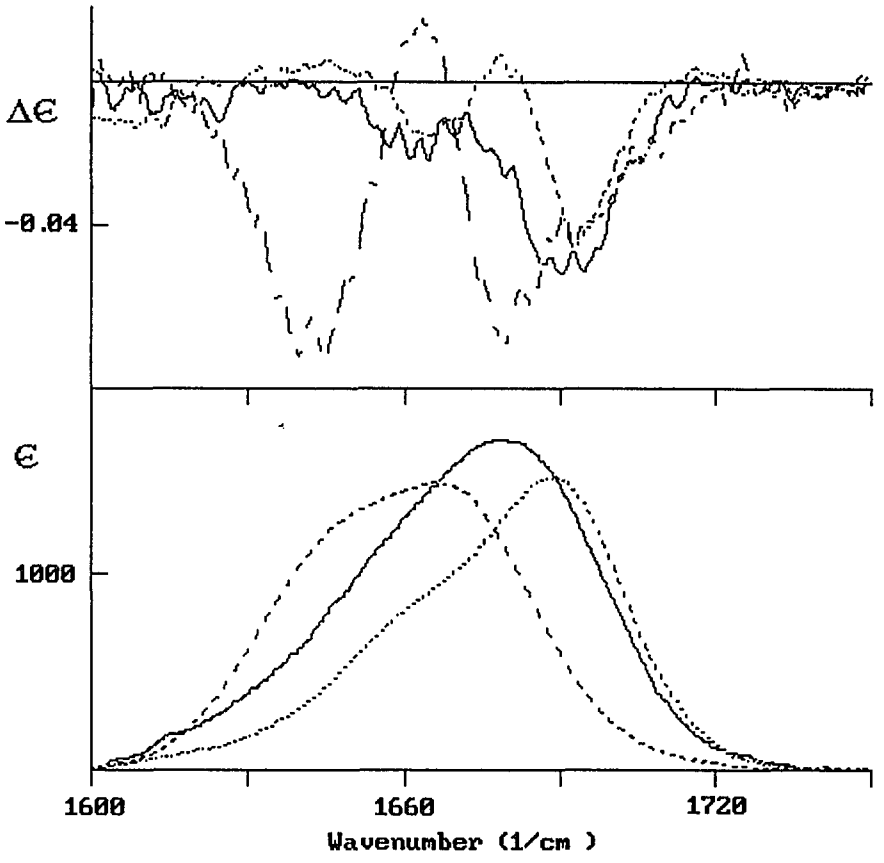

Figure 7-8. The absorption (bottom) and VCD spectra (top) of *l*(CPdFC) in DMSO: Bromoform =1: 2 (solid line); in DMSO (dotted line)and in DMSO: D_2O = 1 : 2 (broken line), respectively.

The aim of the following discussion is to attempt to qualitatively or intuitively interpret the changes in VCD spectra observed from linear tetrapeptides. In general, since there are three carbonyls with different vibrational frequencies (one at low frequency region and two at high frequency) in β-turn, which are fixed in geometry, coupling between carbonyls can occur in two ways: a low(tert.)- high (sec.) and a high (sec.) - high (sec.) coupling. We like to call the proposed interpretation " frequency strategy". It interprets the couplets between $C=O_{(i)}$ and $C=O_{(i+1)}$ or $C=O_{(i)}$ and $C=O_{(i+2)}$ as well as between $C=O_{(i+1)}$ and $C=O_{(i+2)}$, respectively. The typical pattern shown in those VCD spectra from 3 linear peptides are a n / p for low- high couplet and a p / n for high -high couplet with various ratios of negative and positive parts. Those patterns correspond to a certain geometry of carbonyls.

According to the exciton formalism, the dipolar coupling energy between interacting C=O groups depends on the distance and direction between dipoles of C=O. The large rotational strengths are created for perpendicular geometry between the interacting groups. Such a geometry, however, produces the smallest coupling energy and splitting of the exciton components. Parallel or antiparallel geometry present maximum splitting, but minimal rotational strengths.

In *l*(CPFC), a simple n / p couplet pattern in polar solvents (DMSO and DMSO/D_2O) covers the lower wavenumber region of absorption and can be classified as a low -high couplet. The zero-crossing of this VCD spectrum, located between the tertiary and secondary amide I', (1655 cm^{-1} in D_2O and 1668 cm^{-1} in DMSO, respectively) further supports this interpretation. In such a polar solvent, the $1 \rightarrow 4$ intra-hydrogen bond will be broken by solvent and the $NH_{(i+3)}$ would prefer H-bonding with solvent. $C=O_{(i+2)}$ will be situated at the position, at which it may be parallel or antiparallel to $C=O_{(i+1)}$. Since there is a L

side-chain group at the third position, we believe that $C=O_{(i+1)}$ and $C=O_{(i+2)}$ are close to each other, and it is more reasonable to assume they may align parallel rather than anitiparallel. Consequently, they may not have any contributions to rotational strength. Therefore, the coupling of structure is between $C=O_{(i)}$ and $C=O_{(i+1)}$ or $C=O_{(i)}$ and $C=O_{(i+2)}$. The shape of couplet depends on the orientation of these dipoles.

In a less polar solvent, the driving force of folding is intra-molecular-hydrogen bonding. So the $C=O_{(i+2)}$ may turn to a position at which $C=O_{(i)}$ can hydrogen-bond with $NH_{(i+3)}$ and the orientation of $C=O_{(i+1)}$ and $C=O_{(i+2)}$ is no longer parallel any more. These two dipoles now can couple with each other. Therefore, a high-high couplet appears in the VCD spectrum of *l*(CPFC) in the high frequency region. Therefore, two couplets exist in this geometry of *l*(CPFC): A n / p couplet at lower frequency (zero-crossing at 1665 cm^{-1}) for the low- high interaction between $C=O_{(i)}$ and $C=O_{(i+1)}$ or between $C=O_{(i)}$ and $C=O_{(i+2)}$, and a p / n couplet in the high frequency (zero-crossing at 1685 cm^{-1}), for high-high coupling interaction between $C=O_{(i+1)}$ and $C=O_{(i+2)}$. To produce a $1 \rightarrow 4$ intra-hydrogen bonds in that conformation, it must form a different turn than type I and II β-turns, whose spectra were observed by previously VCD. Reviewing the three VCD spectra of *l*(CPFC) in various solvents, the low-high couplet shows up in each of the spectra with the same pattern (n / p) in frequency region between tert. and sec. amide I linkage. It suggests that the conformation changes of *l*(CPFC) with solvent polarities is due to rotation of $C=O_{(i+2)}$.

Due to the absence of a side group in the third position of *l*(CPGC), it may assume structures similar to one of *l*(CPFC) and *l*(CPdFC) in various solvents. In fact, in D_2O/DMSO, the VCD spectrum of *l*(CPGC) is identical to that for *l*(CPFC) in the same solvent. We believe it has the same conformation as *l*(CPFC). We expect that the C=O groups in *l*(CPGC) are forming inter molecular

H-bond with D_2O is a major driving force. In other words, hydrogen and the L side-chain group on $\alpha C_{(i+2)}$ would cause the same influence on peptide folding under this given condition.

It is not surprising that *l*(CPGC) in pure DMSO behaves like *l*(CPFC) in a less polar solvent and exhibits two couplets in the low and high frequency regions, respectively. The best description of those spectra of *l*(CPGC) in pure DMSO and *l*(CPFC) in a less polar solvent is that they are mirror images. The VCD spectrum of *l*(CPGC) contains a stronger couplet in the high frequency range than in the low frequency range. This indicates that $C=O_{(i+2)}$ of *l*(CPGC) can turn easily in less hydrogen bonded solvent than $C=O_{(i+2)}$ of *l*(CPFC) does in same solvent, because there are lower steric barriers at $\alpha C_{(i+2)}$ of *l*(CPGC), but L-side-chain group on $\alpha C_{(i+2)}$ of *l*(CPFC) blocks the motion of $C=O_{(i+2)}$. In other words, DMSO can not cause a movement of $C=O_{(i+2)}$ to the position where it was in D_2O in that case.

In bromoform, the VCD spectrum of *l*(CPGC) exhibits a same spectrum as *l*(CPdFC) in D_2O. Two negative peaks present in both low and high frequency. This spectrum can be considered a combination of negatively biased n / p / n couplet. The negative pattern corresponds to an unstable or ill-defined conformation of the peptide.

The couplet between $C=O_{(i+1)}$ and $C=O_{(i+2)}$ at higher frequency exists unchanged in spectra of *l*(CPdFC) in all three solvents. Based on the shapes of these couplets and their frequencies in *l*(CPdFC), we are assuming, that the D-side-chain group in the third position can more efficiently either limits the movement of the $C=O_{(i+2)}$ group or block the movement of both $C=O_{(i+2)}$ and $C=O_{(i+2)}$, keeping the distance and orientation of $C=O_{(i+1)}$ and $C=O_{(i+2)}$ constant. These two carbonyls can couple with each other in all conformations. With the changes of polarity of solvent, we believe that their conformational changes must

exclusively relate to the variation of geometry of $C=O_{(i)}$. Actually, changes in VCD spectra of *l*(CPdFC) in the three solvents do only occur on the low frequency region. Reducing the polarity of solvent minimizes the a portion of the low- high coupling between $C=O_{(i)}$ and $C=O_{(i+1)}$ or $C=O_{(i+2)}$.

Another way to recognize that conformations of *l*(CPGC) are an intermediate state between states of *l*(CPFC) and *l*(CPdFC) in each solvent is the comparison of the VCD spectra of those peptides in the three solvents. we found, that a conformational state of *l*(CPGC) in the same solvent is a transition between the conformation of *l*(CPFC) and *l*(CPdFC).

Inspection of VCD spectra from all three peptide in TFE reveals that they present similar spectrum with weaker signal than in other solvents. This is consistent with results from other techniques, which suggests that TFE can promote peptide to form α-helix structure in regardless of their sequences.

In order to interpret the differences of VCD spectra between cyclic and linear tetrapeptides and among linear peptides, we refer to the structure of standard β-turns, which are confirmed by other techniques. (Figure 6-1)

Virtually, there exist three peptide linkages in β-turn conformations, which determine types of structure formed. The movement or rotation of such planes of peptide linkage depends on the nature of side-chains on each α-carbon, particularly, on situation of its adjacent α-carbon. Since $C=O_{(i)}$ is a tertiary peptide linkage, the proline ring fixed the angle of N- $\alpha C_{(i+1)}$. But the $C=O_{(i)}$ can easily form a cis peptide linkage with a small energy difference. The formation of a cis linkage in $C=O_{(i)}$ plane will largely depend on the movability of $\alpha C_{(i)}$. In order to transform to the cis conformer, $\alpha C_{(i)}$ has to turn into β-turn core with a $C=O_{(i)}$ turning out. In cyclic peptide discussed in chapter 6, the distance between $\alpha C_{(i)}$ and $\alpha C_{(i+3)}$ is fixed by the S-S bond. In other words, the position of $\alpha C_{(i)}$ is

fixed. Consequently, it is difficult to form a cis conformer in the cyclic tetrapeptides.

Movements of $C{=}O_{(i+2)}$ in the cyclic peptide are still possible, event though $\alpha C_{(i+3)}$ is less movable. It can be seen in cases of *c*(CPFC) and *c*(CPdFC). Such a movement depends on the size and location of the side-chain on $\alpha C_{(i+2)}$. Since $C{=}O_{(i)}$ can not move too much, the rotation of $C{=}O_{(i+2)}$'s plane also is affected by $NH_{(i+3)}$, which attempts to form an intra $1 \rightarrow 4$ H-bond with $C{=}O_{(i)}$.

The movement of $C{=}O_{(i+1)}$ plane is restricted by the size and the position of side-chain on both $\alpha C_{(i+1)}$ and $\alpha C_{(i+2)}$. Since the L- proline is at second position, the effects of side-chain on $\alpha C_{(i+2)}$ become a sole factor in determining the types of turns formed in a cyclic peptide. Furthermore, since each C=O is closer to its own α-carbon, the steric effect from a side-chain on this α-carbon has a more influence on the movement of C=O instead other factors. Therefore, the geometry of $C{=}O_{(i+1)}$, in general, should be mainly terminated by the side-chain on $\alpha C_{(i+1)}$ rather than on $\alpha C_{(i+2)}$ except other primary constraints involved on forming a structure. In comparison each cyclic peptide with their linear analogs, the main difference between their structure is the limitation of distance between $\alpha C_{(i)}$ and $\alpha C_{(i+3)}$. In cyclic peptides, it is limited by the disulfide bond. Therefore, the variation of movement of $C{=}O_{(i)}$ and $C{=}O_{(i+2)}$ planes in cyclic peptides should be much smaller than in acyclic one.

There are two kinds of influences on folding of cyclic tetrapeptides, which arise from limitation of $\alpha C_{(i)}$ - $\alpha C_{(i+3)}$ distance. First, S-S bond brings two "arms" of turn together. Possibly, they are parallel to each other. This constraint on peptide chain might make that the side-chain's influence becomes a major factor in forming certain types of turn. Second, a fixed distance between $\alpha C_{(i)}$ and $\alpha C_{(i+3)}$ would efficiently limit rotations of $C{=}O_{(i)}$ and $C{=}O_{(i+2)}$ planes, particularly, for preventing $C{=}O_{(i)}$ into cis conformer.

In linear peptide, a limitation on $\alpha C_{(i)}$ - $\alpha C_{(i+3)}$ distance does not exist. The C=O planes have more freedom to rotate. For example, the cis conformer can be easily formed regardless of the position of $\alpha C_{(i)}$. Accordingly, the pattern of couplets between $C=O_{(i)}$ and $C=O_{(i+1)}$ or $C=O_{(i)}$ and $C=O_{(i+2)}$ must be different than cyclic analogs. So there exist more suitable geometries for $C=O_{(i)}$ in linear tetrapeptides.

Based on arguments above, the observed VCD spectra of three linear tetrapeptide can be interpreted in following way. According to the sequence strategy of β-turn[7-3a], the $C=O_{(i+1)}$ in *l*(CPFC) should prefer a position as it in the type I turn, since its energy would be lower. Therefore, the differences between the observed VCD spectra of *l*(CPFC) in various solvents must be due to movements of both $C=O_{(i)}$ and $C=O_{(i+2)}$. Since there is no limitation on the $\alpha C_{(i)}$ - $\alpha C_{(i+3)}$ distance , one can expect some reasonable structures other than type I structure for *l*(CPFC).

In the case of *l*(CPdFC), $C=O_{(i+1)}$ may be located in a position similar to a type II turn like *c*(CPdFC), because of the effect on D-side-chain in $\alpha C_{(i+2)}$. Without other constraints on peptide chains, this may not be a favorable position with respect to the L-side chain from proline residue. Such a higher energy geometry may not stable for linear peptide, particularly, in the case there is no limitation on the $\alpha C_{(i)}$ - $\alpha C_{(i+3)}$ distance. Therefore, some adjustment of its conformation have to be made with polarity of solvent. Following a same idea, the D-side chain on $\alpha C_{(i+2)}$ is an important factor for the movement of $C=O_{(i+2)}$ with various polarity of solvent.

Additionally, since the high-high couplet shows up in all case of *l*(CPdFC), the orientation between $C=O_{(i+1)}$ and $C=O_{(i+2)}$ seems to be fixed. Consequently, the possibility of cis conformer of $C=O_{(i)}$ is another reason for that *l*(CPdFC) will not form the structure as those in case of cyclic peptide.

7.5. CONCLUSION

The discussion above suggests that the various polarities of solvents can be used as a probe to detect constraints on peptide structures and to understand the driving force for structural formation of peptide. By using such a technique, the conformations of three linear tetrapeptides in various solvents, which were monitored by VCD, have not shown any features in common with those of their cyclic analogs. A number of conclusions may be drawn:

By comparing results of conformational studies of acyclic with that of cyclic peptides under the same chemical composition, it appears that a primary characteristic for forming certain types of turns, particularly for standard type I and type II of β-turns, is the $\alpha C_{(i)}$ - $\alpha C_{(i+3)}$ distance in the turns. That effect was called by other researchers the distance -dependent strategy. In practice, under such restriction of the $\alpha C_{(i)}$ -$\alpha C_{(i+3)}$ distance (less than 6 or 7A) the suitable type of turns can be built up by certain sequence of residues in peptide, whether or not it form 1 → 4 hydrogen bond in the turn core. The facts observed by VCD support an intuitive idea about β-turn, which was mentioned by Kunz[7-8]: for linear peptide, the considered β-turn structure should have more than four residues involved.

Secondly, the sequence effects on the conformation can be seen from the three linear peptides. *l*(CPFC) has a opposite behavior as *l*(CPdFC), and *l*(CPGC) has a structural intermediate to them.

Regardless of limitation on $\alpha C_{(i)}$ -$\alpha C_{(i+3)}$ distance in linear tetrapeptide, the sequence effect and movement of α-carbon on forming a specific β-turn becomes more clear and important. If proline is at second position of turn core,

the position of side-chain on $\alpha C_{(i+2)}$ can restricts both movements of $C{=}O_{(i+1)}$ and $C{=}O_{(i+2)}$. To consider short distance, it may have a more influence on geometry of $C{=}O_{(i+2)}$.

REFERENCES

7-1a) B. N. Narrating Rae. (1983) *J. Am. Chem. Soc.*, 105,7423-28.

7-1b) M.Hollosi and G.D.Fasman (1985), *Biopolymers* 24,211-241.

7-1c) B. N. Rae,(1983), *J. Am. Chem. Soc.* 105,7423-7428.

7-2)Peter Y. Chou and G. D. Fasman. (1977) *J. Mol. Biol.* 115,135-175.

7-3a)George D. Rose; Lila M. Gierash and John A Smith. *Adv. in Protein Chem.* (1985) 37,1-109.

7-3b) K. Ramnarayam. (1994) *peptide reseach* 7, 270-278.

7-3c) C.M. Wilmot and J. M. Thornton (1988) *J. Mol. Biol.* 203, 221-232.

7-3d) H. J. Dyson. (1988) *J. Mol. Biol.* 201,161-200.

7-4) B. Imperiali. (1992) *J. Am. Chem. Soc.* 114, 3182-3188.

7-5) Andras Perczel. (1991) *J. Am. Chem. Soc.* 113,9772-9784.

7-6) M. Hollosi. G.D. Fasman. (1994) *Biopolymers* 34, 177-185.

7-7) Byler, M. and Susi, H. Biopolymers. (1986) 25, 269-287.

7-8) Kuntz, I. D. (1972) *J. Am. Chem. Soc.* 94, 4009-4012.

BIBLIOGRAPHY

1-1a) Pauling, L. (1951), *Proc. Natl. Acad. Sci.* 37, 205.

1-1b). Zimmerman, S. S. and Scheraga, H.A., (1977) *Proc.Natl.Acad.Sci.USA*, 74, 4126-4129.

1-1c) Guzzo, A. V. (1965) *Biophys. J.* 5, 809-822.

1-2) G.D. Fasman, (1989) in "Prodiction of Protein Structure and The Principle of Protein Conformation"; Edited by G.D. Fasman. Plenum Press, New York. 193-316.

1-3) L. M. and Sternhell, S. (1969) " *Applications of Nuclear Magnetic Resonance Spectroscopy in Organic Chemistry.*" Pergamon, Oxford.

1-4) Jardetzky,O. (1980) *Biochim. Biophys. Acta* 621, 227-232.

1-5) Kopple, K. D. (1983) . *Int. J. Pept. Protein Res.* 21, 43-48.

1-6) Kopple, K. D. and Zhu, P. P. (1983). *J. Am. Chem. Soc.* 105, 7742-7746.

1-7) Williamson, M. P. & Wuthrich, K. (1985). *J. Mol. Biol.* 182, 295-315.

1-8a) J. Bandekar, (1992) *Biochim. et. Biophys. Acta.* 1120, 123-143.

1-8b) R. W. Sarver Jr. & W.C. Krueger (1991), *Anal. Biochem.* 194, 89-100..

1-9) Kopple, K. D., Go, A., and Pilipauskas, D. R. (1975). J. Am. Chem. Soc. 97, 6830-6838.

1-10) Pease, L. G., and Watson, C. (1978). *J. Am. Chem. Soc.* 100, 1279-1286.

1-11) Aubry, A., and Marraud, M. (1983). *Biopolymers* 22, 341-345.

1-12) Bandekar, J., and Krimm, S. (1979). *Proc. Natl. Acad. Sci.* U.S.A. 76, 774-777.

1-13) Bandekar, J., and Krimm, S. (1980). *Biopolymers* 19, 31-39.

1-14) F. U. P. Leutert and Burger, M.M. (1986) *Pro. Natl. Acta. Sci.* 83, 1315-1319.

1-15) Susi,H. and Byler, D. M. (1983) *Bichem. Biophys. Res. Commun.* 115, 391-397.

1-16) W. K. Surewicz and H. H. Mantsch (1988), *Biochim, Biophys. Acta.* 952, 115-130.

1-17) Cantor, C. R., and Schimmel, P. R. (1980). " *Biophysical Chemistry*," Parts I, II. Freeman, San Francisco.

1-18) Woody, R. W. (1985), *The Peptides*, 7, 15.

1-19) Yang. Y. T., Wu, C.S.C. and Martinez, H. M. (1986). *Methods Enzymol.* 130, 208.

1-20) Johnson, W. C. (1985). *Methods Biochem. Anal.* 31, 61.

1-21) Greenfield, N. J., and Fasman, G. D. (1969). *Biochemistry* 8, 4108.

1-22) Woody, R. W. (1974). In " *Peptides, Polypeptides, and Proteins*". 338-350. Wiley John and Sons, New York.

1-23) Madison, V., and Schellman, J. (1970). *Biopolymers* 9, 569-588.

1-24) Bush, C. A. Sarkar, S. K., and Kopple, K. D. (1978). *Biochemistry* 17, 4951-4954.

1-25) Madison, V., and Kopple, K. D. (1980). *J. Am. Chem. Soc.* 102. 4855-4863.

1-26) Keiderling, T. A. (1990) in "Practical Fourier Transform Infrared Spectroscopy", 203-284. Acad. Press. Inc.

1-27) P. P. Sritana and T.A. Keiderling (1989) *Biochem.* 28, 5917-23.

1-28) P.Pancoska and T. A. Keiderling (1991), *J. Am. Chem. Soc.* 30, 6885-6895.

2-1) Kuhn, W. (1958) *Ann. Rev. Phys Chem.* 9, 417.

2-2) L.Rosenfeld, (1929), *Z. Physik*, 52,161

2-3) E. U. Condon, (1937), *Rev. mod. Physics* 9, 432.

2-4) W. Moffitt and A. Moscowitz, (1959), *J. Chem. Physics* 30, 648

2-5) Moffit, W., (1956) *J. Chem. Phys.*, 25, 467- 78.

2-6)C. W. Duetsche, (1969) *Ann. Rev. Phys. Chem.* 20 407-448.

2-7) Tinoco, I. (1963), *Radiation Research*, 20, 133-39.

2-8) Holzwarth, G. and Chabay, I. (1972), *J. Chem. Phys.* 57, 1632-1635.

2-9) T. R. Fraulkner (1977) *J. Chem. Chem. Soc.* 99, 8160-8168.

2-10) C. Marcott (1977) *J. Am. Chem. Soc.* 99, 8169-8175.

2-11) Birke, S. S. and Diem, M. (1992) *Biochemstry* 31, 450-455.

3-1.L. A. Nafie (1976), *J. Am. Chem. Soc.* 98 2715.

3-2) L.A. Nafie and M. Diem (1979), *Accts. Chem. Res.* 12, 296.

3-3) L. A. Nafie and M. Diem (1979) *J. Am. Chem. Soc.* 101, 496.

3-4) G. Holzwearth (1974) *J. Am. Chem. Soc.* 96, 252.

3-5) M. Diem,. (1988), *Appl. Spectr.* 42, (1) 20-27.

3-6) O. Lee and M. Diem, (1992) *Analy. Instr.* 20(1) 23-43.

3-7) M. Diem, (1992), *SPIE Proceedings* 1681, 67-78.

4-1). L.F. Mollehauer, D. Downie, H. Engstrom, and W. B. Grant. (1969). *Appl. Opt.* 8. 661.

4-2) S.N. Jasperson and S.E. schnatterly. (1969) *Rev. Sci. Instrum.* 40, 761.

4-3) J. C. Cheng, L. A. Nafie, and P. J. Stephens. (1975) *J. Opt. Soc. AM.* 65, 1031-35.

4-4) L. F. Mollehauer, D. Downie, H.Engstrom, and W. B. Grant,(1969), *Appl. Opt.* 8. 661.

4-5) S, N, Jasperson and S. E. Schnatterly, (1969), *Rev. Sci. Instrum.* 40, 761.

4-6) J . C. Cheng, L. A. Nafie, and P. J. Stephens, (1975) *J. Opt. Soc. Am.* 65, 1031-35.

4-7) E. D. Lipp, and L. Nafie (1984), *Appl. Spectr.* 38, 20-26.

4-8) P. Malon and T. A. Keiderling (1988), *Appl. Spectr.* 42, 32-38.

5-1) Diem, M., (1994), *Volume 14. Analytical Applications of Circular Dichroism"*, Purdie, N. and Brittain, H.G., Editors, Elsevier Science Publishers, Amsterdam, The Netherlands, pp. 91 - 130

5-2) Keiderling, T.A., (1990), *"Practical Fourier Transform Infrared Spectroscopy: Industrial and Laboratory Chemical Analyses"*, Ferraro, J.R. & Krishnan,K., Eds, Academic Press, NY, pp. 203-283

5-3) Baur, P. and Keiderling, T.A., (1992) *J. Amer. Chem. Soc.*, 114, 9100 - 9105

5-4) Madison, V., Atreyi, M., Deber, C.M. and Blout, E.R., (1974) *J. Amer. Chem. Soc.*, 96, 6725 - 6734

5-5) Deber, C.M., Madison, V. and Blout, E.R., (1976) *Acc.Chem.Res.*, 9, 106-113

5-6) Kartha, G., Varughese, K.I. and Aimoto, S., (1982) *Proc. Natl. Acad. Sci. USA*, 79, 4519-4522

5-7) Krishna, K. and Kartha, G., (1985) "*Peptides: Structure and Function. Proceedings of the Ninth American Peptide Symposium*", Deber, C.M., Hruby, V.J and Kopple, K.D., Editors, Pierce Chem.Comp., USA, p. 163-166

5-8) Diem, M., Roberts, G.M., Lee, O. and Barlow, A., (1988) *Appl.Spectrosc.* 42, 20 - 27

5-9) Lee, O., Roberts, G.M. and Diem, M., (1989) *Biopolymers*, 28, 1759-1770

5-10) Birke, S.S., Agbaje, I. and Diem, M., (1992) *Biochemistry*, 31, 450-455

5-11) Baur, P. and Keiderling, T.A., (1994) *J.Amer.Chem.Soc.*, in press

5-12) Xiang, T., Goss, D.J. and Diem, M., (1993) *Biophysical Journal*, 65(3), 1255-1261

5-13) Xie, P., Zhou, Q., and Diem, M, (1994) *Proc. Faraday Soc.*, submitted

6-1) Kabsch, W. and Sander, C., (1983) *Biopolymers*, 22, 2577-2637

6-2) Chou, P. Y. and Fasman, G.D., (1977) *J. Mol. Biol.*, 115, 135-175

6-3) Venkatachalam, C. M., (1968) *Biopolymers*, 6, 1425-1436

6-4) Lewis, P. N., Momany, F. A. and Scheraga, H.A., (1971) *Proc. Natl. Acad. Sci. USA,* 68, 2293-2297

6-5) Zimmerman, S. S. and Scheraga, H.A., (1977) *Proc. Natl. Acad. Sci.USA,* 74, 4126-4129

6-6) Xie, P. and Diem, M., (1995) *J.Amer.Chem. Soc.*, 117, 429-437

6-7) Wyssbrod, H. and Diem, M., (1992) *Bio-polymers,* 31, 1237 - 1242

6-8) Xie, P., Zhou, Q. and Diem, M., (1994) *Faraday Discussions.*, 99, in press

6-9) Xiang, T., Goss, D.J. and Diem, M., (1993) *Biophysical Journal,* 65, 1255-1261

6-10) Venkatachalapathi, Y.V. and Balaram, P., (1979) *Nature,* 281, 83-84.

6-11) Nair, C.M.K., Vijayan, M., Venkatachalapathi, Y.V. and Balaram, P., (1979) *J.Chem. Soc Chem.Commun.,* 1183-1184.

6-12) Venkatachalapathi, Y.V., Prasad, B.V.V and P. Balaram, (1982) *Biochemistry,* 21, 5502-5509

6-13) Hollosi, M., Kawai, M. K., Fasman, (1985) *Biopolymers,* 24, 211-242

6-14) Perczel, A., Hollosi, M., Foxman, B. M. and Fasman, G. D., (1991) *J.Amer.Chem.Soc.*, 113, 9772-9784

6-15) Hollosi, M., Majer,Z., Ronal, A.Z., Magyar, A., Medzihradsky, K., Holly, S. and Fasman, G.D., (1994) *Biopolymers,* 34, 177-185

6-16) Rose, G.D., Gierasch, L.M. and Smith, J.A., in Adv. Protein Chemistry, Anfinson, C.B., Edsall, J.T. and Richards, F.M., Eds., (1985), Academic Press, NY

6-17) Woody, R.W., in *Peptides, Polypeptides and Proteins,* E.R.Blout, F.A.Bovey, N.Lotan and M.Goodman, Eds., Wiley, New York, (1974) pp 338-350

6-18) Woody, R.W., in "*The Peptides: Analysis, Synthesis , Biology*", V.J. Hruby, Ed., Academic Press, New York, (1985) 15-113

6-19) Diem, M., Roberts, G.M., Barlow, A. and Lee, O., (1988) *Applied Spectrosc.*, 42, 20-28

6-20) Chandrasekaran, R., Lakshminarayana, A.V., Pandya, U.V. and Ramachadran, G.N.,
(1973). *Biochim. Biophys. Acta,* 303, 14-27

6-21) Rao, B.N.N., Kumar, A., Balaram, H., Ravi, A. and Balaram, P., (1983) *J.Am.Chem.Soc.,* 105, 7423-7428.

6-22) Imperiali, B. ,Fisher, S.L. Moats, R.I. and Prins, T. J., (1992). *J.Amer.Chem.Soc.* 114, 3182-3188.

6-23) Pease, L.G. and Watson, C., (1978), *J. Amer.Chem.Soc.*, 100, 1279-1286

6-24) Karle, I., (1978) *J. Amer.Chem.Soc.*, 100, 1286-1289

7-1a) B. N. Narrating Rae. (1983) *J. Am. Chem. Soc.*, 105,7423-28.

7-1b) M.Hollosi and G.D.Fasman (1985), *Biopolymers* 24,211-241.

7-1c) B. N. Rae,(1983), *J. Am. Chem. Soc.* 105,7423-7428.

7-2)Peter Y. Chou and G. D. Fasman. (1977) *J. Mol. Biol.* 115,135-175.

7-3a)George D. Rose; Lila M. Gierash & John A Smith. *Adv. in Protein Chem.* (1985) 37,1-109.

7-3b) K. Ramnarayam. (1994) *peptide reseach* 7, 270-278.

7-3c) C.M. Wilmot and J. M. Thornton (1988) *J. Mol. Biol.* 203, 221-232.

7-3d) H. J. Dyson. (1988) *J. Mol. Biol.* 201,161-200.

7-4) B. Imperiali. (1992) *J. Am. Chem. Soc.* 114, 3182-3188.

7-5) Andras Perczel. (1991) *J. Am. Chem. Soc.* 113,9772-9784.

7-6) M. Hollosi. G.D. Fasman. (1994) *Biopolymers* 34, 177-185.

7-7) Byler, M. and Susi, H. Biopolymers. (1986) 25, 269-287.

7-8) Kuntz, I. D. (1972) *J. Am. Chem. Soc.* 94, 4009-4012.